VANESSA ALVES MANTOVANI

HYDROLOGICAL CYCLE OF A NEOTROPICAL FOREST:

CARBON AND NITROGEN INPUTS AND DYNAMICS

LAVRAS-MG
2022

VANESSA ALVES MANTOVANI

HYDROLOGICAL CYCLE OF A NEOTROPICAL FOREST: CARBON AND NITROGEN INPUTS AND DYNAMICS

Tese apresentada à Universidade Federal de Lavras, como parte das exigências do Programa de Pós-Graduação em Recursos Hídricos, área de concentração em Hidrologia, para obtenção do título de Doutor.

Dr. Carlos Rogério de Mello
Orientador

Dra. Marcela de Castro Nunes Santos Terra
Orientadora

LAVRAS-MG
2022

Ficha catalográfica elaborada pelo Sistema de Geração de Ficha Catalográfica da Biblioteca Universitária da UFLA, com dados informados pelo(a) próprio(a) autor(a).

Mantovani, Vanessa Alves.
Hydrological cycle of a neotropical forest: carbon and nitrogen inputs and dynamics. / Vanessa Alves Mantovani. - 2022.
146 p.

Orientadores: Carlos Rogério de Mello; Marcela de Castro Nunes Santos Terra.
Tese (doutorado) - Universidade Federal de Lavras, 2022.
Bibliografia.

1. Hidrologia florestal. 2. Entrada de nutrientes. 3. Armazenamento de carbono no solo. I. de Mello, Carlos Rogério. II. Terra, Marcela de Castro Nunes Santos. III. Título.

VANESSA ALVES MANTOVANI

CICLO HIDROLÓGICO DE UMA FLORESTA NEOTROPICAL: AS ENTRADAS E A DINÂMICA DO CARBONO E DO NITROGÊNIO

HYDROLOGICAL CYCLE OF A NEOTROPICAL FOREST: CARBON AND NITROGEN INPUTS AND DYNAMICS

Tese apresentada à Universidade Federal de Lavras, como parte das exigências do Programa de Pós-Graduação em Recursos Hídricos, área de concentração em Hidrologia, para obtenção do título de Doutor.

APROVADA em 25 de fevereiro de 2022.

Dra. Lívia Alves Alvarenga	DRH/UFLA
Dra. Marcela de Castro Nunes Santos Terra	DCF/UFLA
Dr. Carlos Alberto Silva	DCS/UFLA
Dra. Kelly Cristina Tonello	DCA/UFSCar

Dr. Carlos Rogério de Mello
Orientador

Dra. Marcela de Castro Nunes Santos Terra
Orientadora

LAVRAS-MG
2022

AGRADECIMENTOS

À Coordenação de Aperfeiçoamento de Pessoal do Nível Superior (CAPES), pela concessão da bolsa que possibilitou a execução de todo o trabalho.

À Coordenação de Aperfeiçoamento de Pessoal do Nível Superior (CAPES), ao Conselho Nacional de Desenvolvimento Científico e Tecnológico (CNPq) e à Fundação de Amparo à Pesquisa do estado de Minas Gerais (FAPEMIG), pelo apoio e financiamento deste trabalho.

Ao Laboratório de Gestão de Resíduos Químicos (DMA-UFLA), ao Laboratório de Estudo da Matéria Orgânica do Solo (LEMOS-UFLA), ao Laboratório de Análises de Água (LAADEG-UFLA), ao Laboratório de Análises Químicas (DRH-UFLA), ao Laboratório de Hidrologia Ambiental (DRH-UFLA), pelas facilitações e execução das análises.

Ao Laboratório de Hidrologia Florestal (DRH-UFLA), o foco principal deste estudo.

Ao Programa de Pós-Graduação em Recursos Hídricos que me recebeu de braços abertos.

À Universidade Federal de Lavras (UFLA), pelo suporte, e por ser um lugar tão agradável.

Ao Professor Carlos Rogério, pelas oportunidades, pelos inúmeros ensinamentos e pelo apoio.

À Marcela pela ajuda incondicional, em todas as partes do processo, desde a concepção do estudo, às idas a campo e auxílio nas análises estatísticas e escrita científica.

Ao técnico Renato que não mediu esforços ao nos auxiliar na organização, estrutura da amostragem, nas idas à campo, medições e coletas, e também pelas piadas e conversas que deixaram nossos dias mais leves.

À toda equipe do Laboratório de Hidrologia Florestal que, durante todo o período de medições, coletas e análises me ajudaram imensamente a conduzir este trabalho.

Aos colaboradores que possibilitaram a execução desta tese, dedicando tempo no auxílio da construção dos artigos.

Aos meus colegas do Programa de Pós-Graduação, pela amizade e por todo o apoio, conselhos, desabafos e pelas maratonas de café, trabalhos e estudos.

Aos professores da UFLA, pelos ensinamentos que possibilitaram meu desenvolvimento acadêmico e profissional.

Ao meu marido Júnior que esteve ao meu lado em todos os momentos, sempre me apoiando, me motivando e acreditando na minha capacidade. Por topar mudar a vida para Lavras e recomeçar em busca dos meus sonhos. Te Amo!

Aos meus pais, Leila e Nelson e minha irmã Fabiana que em toda a minha vida me apoiaram, acreditaram em mim, e permitiram que eu estudasse e me desenvolvesse como profissional.

As minhas avós Laila (*in memoriam*) e Geni que, desde pequena, me ensinaram a importância da educação.

À toda minha família que sempre está presente em todos os momentos da minha vida.

Aos novos amigos que Lavras me proporcionou.

Às minhas amigas da UNESP, por serem a família que eu escolhi, por serem fontes de inspiração de profissionalismo e de sucesso na carreira ambiental, pelo apoio diário, pelas trocas, pelo desabafo e pelos momentos de descontração.

A todos os meus amigos que, por sorte, não são poucos, que fizeram e fazem parte da minha vida e da minha construção como pessoa e profissional.

O presente trabalho foi realizado com o apoio da Coordenação de Aperfeiçoamento de Pessoal de Nível Superior – Brasil (CAPES) – Código de Financiamento 001.

Obrigada!

RESUMO GERAL

As florestas são essenciais para a manutenção da disponibilidade de água, nutrientes, reservas de carbono e do clima global, sendo sua conservação indispensável do ponto de vista social, econômico e ambiental. Os aspectos relacionados à partição da precipitação, assim como o comportamento dos nutrientes, em florestas, constituem um campo em constante desenvolvimento. Nesse contexto, na presente tese, objetivou-se avaliar a dinâmica dos fluxos de carbono e nitrogênio, via precipitação, em um remanescente de Mata Atlântica (Floresta Estacional Semidecidual Montana), em Lavras-MG. E analisar os fatores bióticos e abióticos que influenciam o enriquecimento do carbono no escoamento pelo tronco; e o comportamento do armazenamento do carbono, no solo, até 1 metro de profundidade, nas estações seca e chuvosa, identificando os fatores que afetam esse armazenamento. Foram coletadas amostras, entre maio de 2018 e abril de 2019, da precipitação bruta (externa), em 3 locais, e da precipitação interna e do escoamento pelo tronco, em 10 locais selecionados no interior do remanescente florestal, considerando as espécies mais abundantes e a distribuição espacial. As variáveis físicas e químicas avaliadas incluíram pH, condutividade elétrica, carbono total dissolvido, nitrato, nitrito e nitrogênio total Kjeldahl. Para a análise do teor de carbono e cálculo do estoque de carbono, a serapilheira foi mensalmente coletada, seca e pesada, e o solo coletado em sete profundidades (0-5, 5-10, 10-20, 20-30, 30-40, 40-60, 60-100 cm), em 4 meses selecionados no período (maio, agosto e dezembro de 2018 e abril de 2019). O teor de carbono foi analisado nas amostras de serapilheira e solo, correspondentes aos meses selecionados. Como resultado identificou-se que a chuva é enriquecida com carbono e nitrogênio ao atravessar a floresta; 75%b das entradas de carbono e nitrogênio, no solo, via precipitação efetiva, ocorreram na estação chuvosa; e os mesmos locais tiveram as entradas mais altas, independentemente do período analisado. A concentração de carbono, no escoamento pelo tronco, foi maior que na precipitação interna e bruta, e maior na estação seca do que na chuvosa. Além disso, as razões de enriquecimento de carbono foram sensíveis às características estruturais das árvores e às condições meteorológicas, destacando a estrutura da casca, área da copa, intensidade máxima da precipitação e a sazonalidade. O teor de carbono no solo diminuiu com a profundidade e, na camada superficial (0-10 cm), foi maior na estação chuvosa. A análise multivariada identificou que as variáveis selecionadas como significativas para o armazenamento do carbono, no solo, foram temperatura do solo, teor de carbono na serrapilheira, condutividade hidráulica e coeficiente de variação do diâmetro das árvores na parcela. O modelo de correlação foi capaz de explicar 80% do carbono armazenado no solo. Assim, os resultados obtidos melhoram nossa compreensão dos processos de deposição, lixiviação e absorção de nutrientes pelas copas, além de destacar a importância da floresta tropical no ciclo hidrológico e de nutrientes, com destaque para o ciclo do carbono que guarda estreita relação com as mudanças climáticas. Tal compreensão pode fundamentar melhores estratégias de manejo e conservação de florestas e bacias hidrográficas.

Palavras-chave: Hidrologia florestal. Entrada de nutrientes. Características estruturais das árvores. Armazenamento de carbono no solo.

GENERAL ABSTRACT

Forests are essential for maintaining water and nutrients availability, carbon stocks, and the global climate, and their preservation is crucial from a social, economic, and environmental viewpoint. Aspects related to the rainfall partitioning, and the nutrients cycling in forests are a field in constant development. In this context, this thesis aimed to evaluate the dynamics of carbon and nitrogen fluxes via rainfall, in an Atlantic Forest Fragment (Montana Seasonal Semideciduous Forest), in Lavras-MG. And to analyze the main biotic and abiotic factors that influence the stemflow carbon enrichment; and the soil carbon stock behavior up to 1-meter depth in the dry and wet seasons, identifying the factors that affect this storage. Samples were collected between May 2018 and April 2019 of gross rainfall (external) in 3 locations, and throughfall, and stemflow in 10 locations selected inside the forest fragment, considering the most abundant tree species, and the sampling spatial distribution. The physical and chemical variables evaluated included pH, electrical conductivity, total dissolved carbon, nitrate, nitrite, and total Kjeldahl nitrogen. To analyze the carbon concentration and calculate the carbon stock, the litterfall was collected, dried, and weighed monthly and the soil was sample in 7 depths (0-5 cm, 5-10 cm, 10-20 cm, 20-30 cm, 30-40 cm, 40-60 cm, 60-100 cm), in 4 months selected in the period (May, August, December 2018 and April 2019). The carbon concentration was analyzed in the litter and soil samples, corresponding to the selected months. As outcomes, it was identified that rainfall is enriched with carbon and nitrogen when crossing the forest; 75% of the carbon and nitrogen inputs in soil, via net precipitation, was in the wet season; and the same locations had the greatest inputs, regardless of the analyzed period. The stemflow carbon concentration was higher than in the throughfall and gross precipitation, and higher in the dry season than in the wet season. In addition, the carbon enrichment ratios were sensitive to the tree's structural features and to the meteorological conditions, mainly the bark structure, crown area, maximum rainfall intensity, and seasonality. Soil carbon concentration decreases with depth, and in the surface layer (0-10 cm) it was higher in the wet season. The multivariate analysis identified that the variables selected as significant for soil carbon storage were soil temperature, litter carbon content, hydraulic conductivity, and coefficient of variation in the diameter of trees in the plot. The correlation model was able to explain 80% of the carbon stored in the soil. Thus, the results obtained improve our understanding of nutrient deposition, leaching, and absorption processes by canopies and the importance of the tropical forest in the hydrological and nutrient cycle, with emphasis on the carbon cycle, which is closely related to climate change. Such understanding can support better management and conservation strategies for forests and watersheds.

Key-words: Forest hydrology. Nutrients inputs. Trees structural features. Soil carbon stock.

SUMÁRIO

PRIMEIRA PARTE

1 INTRODUÇÃO

A Mata Atlântica possui alta biodiversidade, uma quantidade elevada de espécies endêmicas, e grande importância para a regulação do clima, o abastecimento de água e a manutenção das encostas. A Mata Atlântica está altamente degradada e fragmentada, em razão do crescimento das cidades, e das atividades agropecuárias.

As florestas são responsáveis por diversos serviços ecossistêmicos, como a preservação dos recursos hídricos, regulação do clima, moderação de eventos extremos e ciclagem de nutrientes, e sua conservação é indispensável do ponto de vista social, econômico e ambiental. A interação chuva-floresta é complexa, e a precipitação que atravessa o dossel é responsável pela entrada constante de água e nutrientes no solo da floresta. Os processos que condicionam as entradas de nutrientes, na floresta via precipitação constituem um campo em constante desenvolvimento para a hidrologia florestal.

Os ciclos de importantes nutrientes como carbono e nitrogênio estão sendo alterados, nos últimos séculos, em razão das mudanças no uso e ocupação do solo, com a intensa contribuição de fontes antrópicas. O monitoramento da deposição atmosférica é obtido em iniciativas isoladas, limitadas a regiões e períodos específicos, o que empobrece a ampla análise dos impactos da entrada de nitrogênio, via precipitação, nos ecossistemas terrestres. A importância das florestas como sumidouro de carbono e as alterações ocasionadas pelo incremento do nitrogênio proveniente de fontes antrópicas vêm sendo intensamente discutidas recentemente. Assim, as florestas são mundialmente reconhecidas por seu papel na captura e armazenamento de carbono. Entretanto, um maior detalhamento acerca da distribuição desse estoque nos diversos "compartimentos" da floresta, bem como no solo, é necessário. Nesse sentido, a utilização de técnicas de amostragem e análises laboratoriais adequadas – frequentemente laboriosas e onerosas – são fundamentais na geração de dados confiáveis sobre a dinâmica desses nutrientes em ambiente florestal.

Apesar do aumento considerável de estudos relacionados às entradas de nutrientes em florestas tropicais, apenas alguns abordam a variabilidade espacial e temporal na precipitação que atravessa o dossel das florestas. E os processos que condicionam os fluxos de nutrientes no escoamento pelo tronco são ainda mais desconhecidos, bem como sua real contribuição no processo de ciclagem dos nutrientes. Estudar essa dinâmica pode ampliar o conhecimento a

respeito da sustentabilidade e do funcionamento dos remanescentes florestais mediante as alterações ocasionadas.

Nesta pesquisa, contou-se com um extenso e oneroso banco de dados, abrangendo 61 eventos de precipitação, ao longo de um ano de coleta, representando mais de 1200 amostras de água da chuva. Concomitantemente, foram coletadas 280 amostras de solo e 120 amostras de serrapilheira. E tem como objetivo geral avaliar a dinâmica das entradas de carbono e nitrogênio, via precipitação, em remanescente de Mata Atlântica (Floresta Estacional Semidecidual Montana) e analisar o armazenamento do carbono, no solo, até a profundidade de 1 metro.

Nesse contexto, buscou-se:

a) comparar as concentrações e as entradas de carbono e nitrogênio, via precipitação, à medida que a chuva atravessa o dossel da floresta;
b) avaliar o comportamento temporal das entradas de carbono e nitrogênio, via precipitação efetiva: sazonalmente (considerando as estações seca e chuvosa), e mensalmente;
c) avaliar o comportamento espacial das entradas de carbono e nitrogênio, via precipitação efetiva, no remanescente florestal;
d) descrever as taxas de enriquecimento do carbono, no escoamento pelo tronco, em relação à precipitação bruta e à precipitação interna;
e) avaliar o efeito de fatores bióticos e abióticos no enriquecimento do carbono no escoamento pelo tronco;
f) determinar o armazenamento do carbono nas camadas do solo, até 1 m de profundidade, e descrever a variabilidade considerando a sazonalidade; e
g) identificar as variáveis bióticas e abióticas significativas para o armazenamento do carbono no solo.

2 REFERENCIAL TEÓRICO

2.1 Hidrologia florestal

Clima é um fator importante na distribuição dos diferentes tipos de floresta em escala global (PAN *et al.*, 2013). A Mata Atlântica, a segunda maior floresta tropical da América do Sul, possui elevada biodiversidade e endemismo, e ocupa regiões tropicais e subtropicais do Brasil (RIBEIRO *et al.*, 2009; OLIVEIRA-FILHO; FONTES, 2000). Originalmente, a Mata Atlântica cobria 17% da área total do país, o que corresponde a mais de 1 milhão de km² (JOLY; METZGER; TABARELLI, 2014). Entretanto, a degradação da floresta, principalmente para a agropecuária e expansão urbana, reduziu a área de cobertura para 12,4% da área original (SOS MATA ATLÂNTICA, 2020; RIBEIRO *et al.*, 2009; MORELLATO; HADDAD, 2000; OLIVEIRA-FILHO; FONTES, 2000). A Mata Atlântica possui alta fragmentação, com 80% dos fragmentos menores que 50 hectares, entretanto, o impacto da fragmentação na estrutura, diversidade e no funcionamento das florestas tropicais ainda foi pouco estudado (RIBEIRO *et al.*, 2009; TERRA *et al.*, 2018b).

A Mata Atlântica é composta por florestas ombrófilas (densa, aberta e mista), florestas semidecíduas e decíduas (JOLY; METZGER; TABARELLI, 2014). A disposição dos tipos de floretas é influenciada pela temperatura, altitude e, principalmente, pela sazonalidade da precipitação e umidade do solo (OLIVEIRA-FILHO; FONTES, 2000; TERRA *et al.*, 2018b). Florestas ombrófilas são restritas às regiões montanhosas e costeiras do Brasil, com precipitação bem distribuída, ao longo do ano, e as florestas semidecíduas se estendem pelo sudeste e centro-oeste do país, em regiões com a estação seca bem definida (MORELLATO; HADDAD, 2000; OLIVEIRA-FILHO; FONTES, 2000). As florestas semidecíduas são compostas de 20 a 50% por árvores que perdem suas folhas como estratégia para suportar a estação seca de até seis meses (MORELLATO; HADDAD, 2000; VELOSO; RANGEL FILHO; LIMA, 1991; IBGE, 2012).

Apesar dos diversos serviços ecossistêmicos prestados pelas florestas, a Mata Atlântica está altamente ameaçada pelo processo de fragmentação e antropização (RIBEIRO *et al.*, 2009), reforçando, ainda mais, a importância de pesquisas que viabilizem o gerenciamento e a proteção das florestas. Nesse sentido, a Mata Atlântica é considerada um *hotspot* global (MYERS *et al.*, 2000), e requer constantes esforços para sua conservação.

Dentre os serviços ecossistêmicos de maior relevância, associados à Mata Atlântica, estão: o fornecimento de água para mais de 120 milhões de brasileiros (abastecimento e geração

de energia elétrica), a manutenção da estabilidade de encostas, e a regulação da distribuição das chuvas (JOLY; METZGER; TABARELLI, 2014). Os processos ecológicos e a biodiversidade das floretas que compõem esse bioma influenciam diretamente nos serviços, como a disponibilidade de água, o ciclo dos nutrientes e o estoque de carbono (JOLY; METZGER; TABARELLI, 2014; CARMO *et al.*, 2012; ALVES *et al.*, 2010).

A partição da precipitação nas florestas vem sendo objeto de estudo de diversas pesquisas recentemente, e é um tema complexo, em decorrência da sua interdisciplinaridade. A interceptação da chuva, pelas florestas, é responsável pelo armazenamento de água na copa e influencia a entrada de água no solo (AUBREY, 2020). A precipitação interna é composta pela parcela que atinge o solo por gotejamento das copas e pela chuva que atravessa a floresta sem ser interceptada pela vegetação (SU *et al.*, 2019; VAN STAN *et al.*, 2020). O escoamento pelo tronco é a parcela da chuva que drena no tronco das árvores. Portanto, a precipitação efetiva (precipitação interna + escoamento pelo tronco) é a chuva que atinge o chão da floresta (SADEGHI; GORDON; VAN STAN, 2020).

A precipitação efetiva, resultante do processo de interação chuva-floresta (VAN STAN; FRIESEN, 2020), é influenciada pelas condições meteorológicas e pelas características da vegetação (KLAMERUS-IWAN *et al.*, 2020). A intensidade das chuvas, velocidade do vento, estrutura das copas, altura das árvores, angulação dos galhos, espessura da casca, presença de musgo, índice de área foliar e senescência são fatores determinantes para a precipitação interna e o escoamento pelo tronco (SADEGHI; GORDON; VAN STAN, 2020; TERRA *et al.*, 2018a).

A heterogeneidade do dossel influencia a interceptação e o processo de redistribuição da água pelas copas das árvores, contribuindo, de forma expressiva, para a variabilidade espacial da precipitação efetiva (VAN STAN *et al.*, 2020; TERRA *et al.*, 2018a; RODRIGUES *et al.*, 2022). Nesse sentido, os estudos desenvolvidos na área da hidrologia florestal, por meio do monitoramento das variáveis hidrológicas e florestais, são fundamentais para o avanço do entendimento do papel das florestas, na conservação da água e na manutenção de serviços ecossistêmicos.

2.2 Entrada de carbono e nitrogênio, via precipitação, nas florestas

O processo de interação chuva-floresta é complexo e marca o ponto inicial da ciclagem de nutrientes. A precipitação efetiva é responsável pela entrada constante de nutrientes no solo da floresta e desempenha um papel importante nos ciclos biogeoquímicos (SADEGHI;

GORDON; VAN STAN, 2020; HAAG, 1985). A compreensão completa dos processos que condicionam a entrada de nutrientes na floresta, por meio da precipitação ainda é um desafio para a hidrologia florestal.

Apesar de o escoamento pelo tronco ser uma parcela pequena da precipitação efetiva, essa fração compreende um fluxo concentrado que é responsável pela entrada de água e nutrientes nas proximidades das árvores. Sendo assim, esse fluxo pode afetar, diretamente, as características físico-químicas e biológicas das raízes e acelerar a redistribuição de nutrientes nos ecossistemas florestais (GERMER *et al.*, 2012; VAN STAN; VAN STAN; LEVIA, 2014; TERRA *et al.*, 2018a; SU *et al.*, 2019). A entrada de nutrientes nas florestas depende das características morfológicas da vegetação, dos processos de deposição atmosférica, dos materiais derivados das copas, troncos e folhas das árvores e dos processos de retenção e lixiviação, durante a passagem da chuva pela floresta (TERRA *et al.*, 2018a; SADEGHI; GORDON; VAN STAN, 2020; HOFHANSL *et al.*, 2012; MARQUES *et al.*, 2019; SU *et al.*, 2019).

No dossel das árvores, são depositados temporariamente partículas provenientes da atmosfera (deposição seca), que podem ser retidas pelas árvores e/ou transferidas para o solo via precipitação efetiva (SU *et al.*, 2019; PONETTE-GONZÁLEZ; VAN STAN; MAGYAR, 2020; AUBREY, 2020). A estrutura do dossel influencia na quantidade de precipitação que é capturada, localmente, e a química da atmosfera influencia na composição da deposição seca (VAN STAN *et al.*, 2020). A passagem da chuva pela floresta também lixivia materiais produzidos nas superfícies das árvores e materiais produzidos por organismos que habitam as árvores (PONETTE-GONZÁLEZ; VAN STAN; MAGYAR, 2020). Nesse sentido, as características dos tecidos das árvores e o ciclo de vida da fauna são determinantes nos processos de lixiviação e retenção de nutrientes na floresta (VAN STAN *et al.*, 2020).

A variabilidade sazonal dos solutos é mais significativa em florestas decíduas e semidecíduas do que em florestas ombrófilas (VAN STAN; STUBBINS, 2018), e alguns fatores, descritos a seguir, condicionam esse comportamento. Durante o período seco, material particulado e aerossol são acumulados, na atmosfera, nas copas das florestas e em outras superfícies como em edificações e no solo (deposição seca). Os primeiros eventos de precipitação, no início da estação chuvosa, são responsáveis por "lavar" a atmosfera e o dossel da floresta, proporcionando altas concentrações de solutos na precipitação(NEU *et al.*, 2016; YOU *et al.*, 2020). Na estação chuvosa, há um decréscimo no acúmulo da deposição seca em função da maior frequência e intensidade de chuva, sendo essas responsáveis por diluir os

compostos e reduzir as concentrações dos solutos (YOU *et al.*, 2020, MICHALZIK; MATZNER, 1999; ZHANG *et al.*, 2016).

Atividades agrícolas e queimadas são fontes importantes de carbono na precipitação bruta (NEU *et al.*, 2016). Regiões fortemente influenciadas por incêndios possuem consideráveis concentrações de carbono na precipitação, indicando que a presença do carbono pode estar diretamente relacionada à queima da biomassa (MARKEWITZ *et al.*, 2004; GERMER *et al.*, 2007; NEU *et al.*, 2016). O metabolismo florestal e os processos de decomposição da matéria orgânica nas florestas são as principais fontes do carbono orgânico na precipitação efetiva (PARKER 1983; NEU *et al.*, 2016; SCHRUMPF *et al.*, 2006; MELLEC; MEESENBURG; MICHALZIK, 2010; STUBBINS; GUILLEMETTE; VAN STAN, 2020). Nesse sentido, a precipitação que atinge a floresta transfere o carbono dos dosséis para o solo em fluxos significativos e constantes, que podem contribuir com o estoque de carbono no solo (STUBBINS; GUILLEMETTE; VAN STAN, 2020). Portanto, é necessário avançar no entendimento dessa dinâmica, principalmente em longo prazo.

O nitrogênio pode se comportar de diferentes formas nas florestas, podendo ser retido pelo dossel ou lixiviado junto com a água da chuva que percola no solo. Nas florestas tropicais, como a Amazônia, o Cerrado e a Mata Atlântica, foram observados um aumento na concentração do nitrogênio na precipitação após a passagem pelo dossel da floresta (SCHROTH *et al*. 2001; LILIENFEIN; WILCKE 2004; SOUZA *et al.* 2015). Os processos de absorção e a qualidade do ar condicionam a quantidade de nitrogênio que é depositado nas florestas e, posteriormente, lixiviado, para o solo, via precipitação efetiva (QUALLS, 2020; AUBREY, 2020). A produção de alimento e a utilização de combustíveis fósseis, são consideradas as fontes mais importantes de aporte de nitrogênio antropogênico na atmosfera (GALLOWAY *et al.*, 2004), e, cada vez, esse processo tem mais peso como contribuinte para o nitrogênio depositado nas florestas. A presença do nitrogênio na atmosfera também é condicionada pela emissão de gases por automóveis, incêndios, emissões de atividades agropecuárias e industriais. As formas reativas (NO_3^- e NH_4^+) são as principais entradas de nitrogênio nas florestas, via precipitação efetiva, e o nitrogênio orgânico é principalmente fornecido pelos processos biológicos (MELLEC; MEESENBURG; MICHALZIK, 2010). Embora o sistema florestal também contribua com o aumento da concentração de nitrogênio na precipitação efetiva, a deposição de aerossóis e gases atmosféricos é considerável (PARKER, 1983; SCHROTH *et al.*, 2001). Nesse sentido, a variabilidade espacial das entradas de nutrientes depende das características da floresta e da

localização em relação às fontes de emissões atmosféricas (VAN STAN *et al.,* 2020; MARQUES *et al.*, 2019).

A dinâmica da entrada de nutrientes, nas florestas, via precipitação é um desafio para o desenvolvimento de novos estudos na área da hidrologia florestal, considerando a necessidade de aprimorar o entendimento dos condicionantes dos padrões espaciais e temporais (SU *et al*., 2019).

2.3 Enriquecimento do carbono no escoamento pelo tronco

Nas florestas, o escoamento pelo tronco é a parcela da precipitação que fica temporariamente retida na copa das árvores e escoa pelos galhos e troncos, atingindo o solo. O escoamento pelo tronco foi negligenciado nos estudos da hidrologia florestal, pois na maioria dos casos, representa uma pequena porcentagem (0,17 a 14%) da precipitação bruta (TERRA *et al.*, 2018a; LEVIA; GERMER, 2015). Entretanto, compreende um fluxo concentrado de água e nutrientes, no entorno das árvores, com um papel relevante nos processos biogeoquímicos, na infiltração e redistribuição de água e nutrientes nas florestas e no funcionamento dos ecossistemas (GERMER *et al*., 2012; SU *et al.*, 2019).

Os cálculos das taxas de afunilamento e de enriquecimento possibilitam aprimorar o entendimento da contribuição do escoamento pelo tronco como ponto de entrada de água e nutrientes nas florestas (LEVIA; GERMER, 2015). A taxa de afunilamento é a relação entre a quantidade de água que atinge o solo da floresta pelo escoamento e a quantidade que atingiria em uma área equivalente a área basal da árvore, sem a presença da vegetação (HERWITZ 1986). A taxa de enriquecimento do escoamento pelo tronco é semelhante e representa a relação entre a concentração do nutriente que atinge o solo pelo escoamento e a quantidade que atingiria em uma área equivalente a área basal da árvore, sem a presença da vegetação (LEVIA; HERWITZ, 2000).

Nesse sentido, considerando o efeito do afunilamento, as copas das árvores são capazes de canalizar até 100 vezes mais água para o solo próximo ao caule, quando comparados com a precipitação bruta, em uma área equivalente (GERMER; WERTHER; ELSENBEER, 2010; SU *et al*., 2016; SIEGERT; LEVIA, 2014). E o solo, próximo às árvores, pode receber uma quantidade significativa de carbono, que pode atingir 70 vezes mais que em uma área sem vegetação (DUVAL, 2019; VAN STAN; STUBBINS, 2018).

As taxas de afunilamento e enriquecimento possibilitam comparar os solutos em diferentes florestas, localidades, espécies de árvores, e estações do ano e auxiliam na identificação de fatores bióticos e abióticos que influenciam a dinâmica do transporte do dossel para a base das árvores, (LEVIA; GERMER, 2015; LEVIA *et al.*, 2011; LEVIA; HERWITZ, 2000; ANDRÉ; JONARD; PONETTE, 2008).

O volume do escoamento e a razão de afunilamento apresentam comportamentos diferentes, considerando-se as diferentes classes de diâmetro das árvores (SU *et al*., 2016). Árvores maiores tendem a drenar um maior fluxo de água da chuva e nutrientes. No entanto, árvores menores (com diâmetro menor) foram mais eficazes no processo de afunilamento da chuva (SU *et al*., 2016; SIEGERT; LEVIA, 2014), e o mesmo ocorreu com a razão de enriquecimento dos solutos, árvores com diâmetro menor foram capazes de fornecer maiores concentrações (CHEN *et al*., 2019; SCHOOLING *et al*., 2017, LIU *et al*., 2019; SU. *et al*., 2016). Reforçando a importância do escoamento pelo tronco, mesmo em árvores pequenas, para ciclagem de nutrientes em ecossistemas florestais (GERMER *et al.*, 2012).

Nesse sentido, Dowtin; Siegert; Levia (2020) indicam a possibilidade de a diversidade das espécies ser determinante para as diferenças significativas dos aportes de nutrientes nas florestas, tendo em vista, que foram encontradas diferenças nas taxas de enriquecimento entre as espécies estudadas. A concentração de carbono orgânico dissolvido no escoamento pelo tronco foi influenciada pelo período de seca antecedente, na Floresta Amazônica (TOBÓN; SEVINK; VERSTRATEN, 2004). No bioma Cerrado, a espécie, a geometria do dossel e a textura da casca tiveram contribuições específicas nas concentrações de nutrientes do escoamento pelo tronco (TONELLO *et al.*, 2021b). E o escoamento pelo tronco foi influenciado pela textura da casca, pelo diâmetro da árvore, pela razão altura e largura da copa, por características da casca como molhabilidade, absorvibilidade e teor de lignina (TONELLO *et al.*, 2021c; TONELLO *et al.*, 2021a).

O desenvolvimento de modelos que possibilitem identificar as características da vegetação e variáveis meteorológicas que influenciam no transporte do carbono para o solo da floresta, via escoamento pelo tronco pode melhorar a compreensão da importância dessa via de transporte.

2.4 Armazenamento de carbono no solo da floresta

As mudanças climáticas, o aumento das temperaturas e as alterações nos regimes das chuvas têm fortes consequências na manutenção das florestas (SU *et al.*, 2019; VIEIRA *et al.*, 2011). Essas alterações podem ser responsáveis pelo aumento da mortalidade das árvores, impactando diretamente o armazenamento de carbono em todo o ecossistema, (ANDEREGG *et al.*, 2020; BRANDO *et al.*, 2019). As secas severas podem aumentar a queda de serrapilheira, resultando em alterações nos fluxos de carbono e nutrientes (MACINNIS-NG; SCHWENDENMANN, 2014). O entendimento das consequências para o armazenamento do carbono, no solo e nas florestas, em virtude das mudanças climáticas e das alterações no uso e ocupação do solo, é fundamental (STUBBINS; GUILLEMETTE; VAN STAN, 2020).

A precipitação é uma via importante de entrada de nutrientes, nas florestas, em razão de sua constância e à rapidez com que os solutos atingem o solo. A heterogeneidade das entradas de água, via precipitação efetiva, tanto na quantidade quanto na composição química, influencia os processos de decomposição da serrapilheira, a disponibilidade de nutrientes e a reincorporação dos elementos ao sistema (QUALLS, 2020; AUBREY, 2020). Sendo assim, a maioria dos elementos retorna ao solo via decomposição da serrapilheira (TOBÓN; SEVINK; VERSTRATEN, 2004; AUBREY, 2020). A serrapilheira compreende a biomassa morta, ou seja, a camada de folhas, galhos, casca, material reprodutivo, fungos e fauna que é depositada acima do solo (QUALLS, 2020). A queda da serrapilheira é um dos principais fluxos do carbono nas florestas (MACINNIS-NG; SCHWENDENMANN, 2014).

Florestas tropicais são consideradas importantes para o estoque, o sequestro do carbono proveniente de fontes antrópicas e a regulação do clima global, sendo um campo de estudo em constante desenvolvimento (HUBAU *et al.*, 2020; TIAN *et al.*, 2015). Sanderman *et al*. (2018) identificaram que a principal causa para a perda de carbono armazenado no solo, em áreas de mangue, foi o desmatamento.

O mapeamento em grande escala do armazenamento do carbono no solo, realizado no Cerrado, identificou temperatura, precipitação, altitude, teor de silte e argila como variáveis que influenciam na dinâmica do armazenamento (MORAIS *et al.*, 2020). Doetterl *et al.* (2015) identificaram que as variáveis geoquímicas do solo têm mais poder de previsão do armazenamento do carbono do que as variáveis climáticas.

Os estoques de carbono quantificados no Cerrado, em Minas Gerais, foram aproximadamente 53% maiores que as médias reportadas anteriormente para todo o bioma, sugerindo que, possivelmente, tenha-se mais carbono armazenado nos solos do que o estimado

anteriormente (MORAIS *et al.*, 2020). Provavelmente, em decorrência da utilização de métodos mais precisos de quantificação do teor de carbono e da determinação da densidade dos solos, cobrindo todos os pontos analisados e todas as profundidades, ferramentas cruciais, para melhorar o cálculo do carbono armazenado nos solos (FERNANDES *et al.*, 2015; GOMES *et al.*, 2019). Assim, reforça-se a necessidade da realização de estudos de quantificação de carbono no solo, em escala regional e em solos sob vegetação nativa.

As florestas como sumidouros de carbono só tiveram destaque no Acordo de Paris, em 2015, com ênfase na necessidade de proteção e de barrar o desmatamento como objetivo para reduzir as emissões (UNFCCC 2015). O armazenamento do carbono, na vegetação e no solo, mostram-se importantes para o cumprimento das metas de redução das emissões, reafirmando a importância da quantificação precisa em escala regional e local (MOOMAW; LAW; GOETZ, 2020).

REFERÊNCIAS

ALVES, L. F. *et al.* Forest structure and live aboveground biomass variation along an elevational gradient of tropical Atlantic moist forest (Brazil). *Forest Ecology and Management*, v. 260, n. 5, p. 679–691, 2010.

ANDEREGG, W. R. L. *et al.* Climate-driven risks to the climate mitigation potential of forests. *Science*, v. 368, n. 6497, 2020.

ANDRÉ, F.; JONARD, M.; PONETTE, Q. Effects of biological and meteorological factors on stemflow chemistry within a temperate mixed oak–beech stand. *Science of The Total Environment*, v. 393, n. 1, p. 72–83, abr. 2008. Disponível em: <https://linkinghub.elsevier.com/retrieve/pii/S0048969707012752>.

AUBREY, D. P. Relevance of Precipitation Partitioning to the Tree Water and Nutrient Balance. *In*: VAN STAN, II, J. T.; GUTMANN, E.; FRIESEN, J. (org.). **Precipitation Partitioning by Vegetation**. Cham, Switzerland: Springer International Publishing, 2020.

BRANDO, P. M. *et al.* Droughts, Wildfires, and Forest Carbon Cycling: A Pantropical Synthesis. *Annual Review of Earth and Planetary Sciences*, leitura de partes importantes já foram realizadas, v. 47, n. 1, p. 555–581, 2019.

CARMO, J. B. DO *et al.* Conversion of the coastal Atlantic forest to pasture: Consequences for the nitrogen cycle and soil greenhouse gas emissions. *Agriculture, Ecosystems and Environment*, v. 148, p. 37–43, 2012.

CHEN, S. *et al.* Stemflow hydrology and DOM flux in relation to tree size and rainfall event characteristics. *Agricultural and Forest Meteorology*, v. 279, n. September, p. 107753, dez. 2019. Disponível em: <https://linkinghub.elsevier.com/retrieve/pii/S0168192319303697>.

DOETTERL, S. *et al.* Soil carbon storage controlled by interactions between geochemistry and climate. *Nature Geoscience*, v. 8, n. 10, p. 780–783, 2015.

DOWTIN, A. L.; SIEGERT, C. M.; LEVIA, D. F. Comparisons of flux-based stemflow enrichment ratios for two Quercus spp. within the megalopolis of the eastern USA. *Urban Ecosystems*, 2020.

DUVAL, T. P. Rainfall partitioning through a mixed cedar swamp and associated C and N fluxes in Southern Ontario, Canada. *Hydrological Processes*, v. 33, n. 11, p. 1510–1524, 30 maio 2019. Disponível em: <https://onlinelibrary.wiley.com/doi/10.1002/hyp.13414>.

FERNANDES, R. B. A. et al. Comparison of different methods for the determination of total organic carbon and humic substances in Brazilian soils. Revista Ceres, v. 62, n. 5, p. 496–501, 2015.

GALLOWAY, J. N. et al. Nitrogen Cycles: Past, Present, and Future. Biogeochemistry, v. 70, n. 2, p. 153–226, set. 2004.

GERMER, S. *et al.* Disproportionate single-species contribution to canopy-soil nutrient flux in

an Amazonian rainforest. *Forest Ecology and Management*, v. 267, p. 40–49, 2012.

GERMER, S. *et al.* Seasonal and within-event dynamics of rainfall and throughfall chemistry in an open tropical rainforest in Rondônia, Brazil. *Biogeochemistry*, v. 86, n. 2, p. 155–174, 2007.

GERMER, S.; WERTHER, L.; ELSENBEER, H. Have we underestimated stemflow? Lessons from an open tropical rainforest. *Journal of Hydrology*, v. 395, n. 3–4, p. 169–179, 2010. Disponível em: <http://dx.doi.org/10.1016/j.jhydrol.2010.10.022>.

GOMES, L. C. et al. Modelling and mapping soil organic carbon stocks in Brazil. Geoderma, v. 340, n. January, p. 337–350, 2019.

HAAG H.P., 1985. Ciclagem de nutrientes em florestas tropicais. Fundação Cargill, Campinas

HERWITZ, S. R. Infiltration-excess caused by Stemflow in a cyclone-prone tropical rainforest. Earth Surface Processes and Landforms, v. 11, n. 4, p. 401–412, 1986.

HOFHANSL, F. et al. Controls of hydrochemical fluxes via stemflow in tropical lowland rainforests: Effects of meteorology and vegetation characteristics. *Journal of Hydrology*, v. 452–453, p. 247–258, 2012.

HUBAU, W. *et al.* Asynchronous carbon sink saturation in African and Amazonian tropical forests. *Nature*, v. 579, n. 7797, p. 80–87, 2020.

IBGE - Instituto Brasileiro de Geografia e Estatística. Manual Técnico da Vegetação Brasileira. Rio de Janeiro, 2012.

JOLY, C. A.; METZGER, J. P.; TABARELLI, M. Experiences from the Brazilian Atlantic Forest: Ecological findings and conservation initiatives. *New Phytologist*, v. 204, n. 3, p. 459–473, 2014.

KLAMERUS-IWAN, A. *et al.* Storage and Routing of Precipitation Through Canopies. *In*: VAN STAN, II, J. T.; GUTMANN, E.; FRIESEN, J. (org.). **Precipitation Partitioning by Vegetation**. Cham, Switzerland: Springer International Publishing, 2020.

LEVIA, D. F. *et al.* Atmospheric deposition and corresponding variability of stemflow chemistry across temporal scales in a mid-Atlantic broadleaved deciduous forest. *Atmospheric Environment*, v. 45, n. 18, p. 3046–3054, 2011.

LEVIA, D. F.; GERMER, S. A review of stemflow generation dynamics and stemflow-environment interactions in forests and shrublands. *Reviews of Geophysics*, v. 53, n. 3, p. 673–714, set. 2015.

LEVIA, D. F; HERWITZ, S. R.. Physical properties of water in relation to stemflow leachate dynamics: implications for nutrient cycling. *Canadian Journal of Forest Research*, v. 30, n. 4, p: 662-66, 2000.

LILIENFEIN, J.; WILCKE, W. Erratum: Water and element input into native, agri- And silvicultural ecosystems of the Brazilian savanna (Biogeochemistry 67 (183-212)).

Biogeochemistry, v. 68, n. 1, p. 131–133, 2004.

LIU, Y. *et al.* Base Cation Fluxes from the Stemflow in Three Mixed Plantations in the Rainy Zone of Western China. *Forests*, v. 10, n. 12, p. 1101, 2 dez. 2019. Disponível em: <https://www.mdpi.com/1999-4907/10/12/1101>.

MACINNIS-NG, C.; SCHWENDENMANN, L. Litterfall, carbon and nitrogen cycling in a southern hemisphere conifer forest dominated by kauri (Agathis australis) during drought. *Plant Ecology*, v. 216, n. 2, p. 247–262, 2014.

MARKEWITZ, D. *et al.* Nutrient loss and redistribution after forest clearing on a highly weathered soil in Amazonia. *Ecological Applications*, v. 14, n. 4 SUPPL., p. 177–199, 2004.

MARQUES, R. F. DE P. V. *et al.* Rainfall water quality under different forest stands. *CERNE*, v. 25, n. 1, p. 8–17, mar. 2019.

MELLEC, A.; MEESENBURG, H.; MICHALZIK, B. The importance of canopy-derived dissolved and particulate organic matter (DOM and POM) — comparing throughfall solution from broadleaved and coniferous forests. *Annals of Forest Science*, v. 67, n. 4, p. 411–411, 2010.

MOOMAW, W. R.; LAW, B. E.; GOETZ, S. J. Focus on the role of forests and soils in meeting climate change mitigation goals: Summary. *Environmental Research Letters*, v. 15, n. 4, 2020.

MORAIS, V. A. *et al.* Spatial distribution of soil carbon stocks in the Cerrado biome of Minas Gerais, Brazil. *CATENA*, v. 185, p. 104285, fev. 2020.

MORELLATO, P. C.; HADDAD, C. F. B. Introduction: the Brazilian Atlantic Forest. *Biotropica*, v. 32, n. 4b, p. 786–792, 2000.

MICHALZIK, B.; MATZNER, E. Dynamics of dissolved organic nitrogen and carbon in a Central European Norway spruce ecosystem. *European Journal of Soil Science*, v. 50, n. 4, p. 579–590, 1999.

MYERS, N. *et al.* Biodiversity hotspots for conservation priorities. *Nature*, v. 403, n. 6772, p. 853–858, fev. 2000.

NEU, V. *et al.* Dissolved organic and inorganic carbon flow paths in an amazonian transitional forest. *Frontiers in Marine Science*, v. 3, n. JUN, p. 1–15, 2016.

OLIVEIRA-FILHO, A. T.; FONTES, M. A. L. Patterns of floristic differentiation among atlantic forests in southeastern Brazil and the influence of climate. *Biotropica*, v. 32, n. 4 B, p. 793–810, 2000.

PAN, Y. *et al.* The Structure, Distribution, and Biomass of the World's Forests. *Annual Review of Ecology, Evolution, and Systematics*, v. 44, n. 1, p. 593–622, 23 nov. 2013.

PARKER, G. G. **Throughfall and Stemflow in the Forest Nutrient Cycle**. 1983. ISSN 00652504.v. 13

PONETTE-GONZÁLEZ, A. G.; VAN STAN, J. T.; MAGYAR, D. Things Seen and Unseen in Throughfall and Stemflow. *In*: VAN STAN, II, J. T.; GUTMANN, E.; FRIESEN, J. (org.). **Precipitation Partitioning by Vegetation**. Cham, Switzerland: Springer International Publishing, 2020.

QUALLS, R. G. Role of Precipitation Partitioning in Litter Biogeochemistry. *In*: VAN STAN, II, J. T.; GUTMANN, E.; FRIESEN, J. (org.). **Precipitation Partitioning by Vegetation**. Cham, Switzerland: Springer International Publishing, 2020.

RIBEIRO, M. C. *et al.* The Brazilian Atlantic Forest: How much is left, and how is the remaining forest distributed? Implications for conservation. *Biological Conservation*, v. 142, n. 6, p. 1141–1153, 2009.

RODRIGUES, A. F. *et al.* Throughfall spatial variability in a neotropical forest: Have we correctly accounted for time stability? *Journal of Hydrology*, [*s. l.*], v. 608, p. 127632, 2022. Available at: https://doi.org/10.1016/j.jhydrol.2022.127632

SADEGHI, S. M. M.; GORDON, D. A.; VAN STAN, J. T. A Global Synthesis of Throughfall and Stemflow Hydrometeorology. *In*: VAN STAN, II, J. T.; GUTMANN, E.;

FRIESEN, J. (org.). **Precipitation Partitioning by Vegetation**. Cham, Switzerland: Springer International Publishing, 2020.

SANDERMAN, J. *et al.* A global map of mangrove forest soil carbon at 30 m spatial resolution. *Environmental Research Letters*, v. 13, n. 5, 2018.

SCHOOLING, J. T. *et al.* Stemflow chemistry in relation to tree size: A preliminary investigation of eleven urban park trees in British Columbia, Canada. *Urban Forestry and Urban Greening*, v. 21, n. November, p. 129–133, 2017.

SCHROTH, G. *et al.* Nutrient fluxes in rainfall, throughfall and stemflow in tree-based land use systems and spontaneous tree vegetation of central Amazonia. *Agriculture, Ecosystems and Environment*, v. 87, n. 1, p. 37–49, 2001.

SCHRUMPF, M. *et al.* TOC, TON, TOS and TOP in rainfall, throughfall, litter percolate and soil solution of a montane rainforest succession at Mt. Kilimanjaro, Tanzania. *Biogeochemistry*, v. 78, n. 3, p. 361–387, 2006.

SIEGERT, C. M.; LEVIA, D. F. Seasonal and meteorological effects on differential stemflow funneling ratios for two deciduous tree species. *Journal of Hydrology*, v. 519, n. , p. 446–454, 2014. Disponível em: <http://dx.doi.org/10.1016/j.jhydrol.2014.07.038>.

SOUZA, P.A.; PONETTE-GONZÁLEZ, A.G.; de MELLO, W.Z.; WEATHERS, K.C.; SANTOS, I.A. Atmospheric organic and inorganic nitrogen inputs to coastal urban and montane Atlantic Forest sites in southeastern Brazil. *Atmos. Res.* 160:126–137, 2015.

SOS MATA ATLÂNTICA. Relatório Anual 2020. Disponível em: < https://www.sosma.org.br/sobre/relatorios-e-balancos/> Acessado em 18 de março de 2022.

STUBBINS, A.; GUILLEMETTE, F.; VAN STAN, J. T. Throughfall and Stemflow: The

Crowning Headwaters of the Aquatic Carbon Cycle. *In*: VAN STAN, II, J. T.; GUTMANN, E.; FRIESEN, J. (org.). **Precipitation Partitioning by Vegetation**. Cham, Switzerland: Springer International Publishing, 2020.

SU, L. *et al.* Inter- and intra-specific variation in stemflow for evergreen species and deciduous tree species in a subtropical forest. *Journal of Hydrology*, v. 537, p. 1–9, 2016. Disponível em: <http://dx.doi.org/10.1016/j.jhydrol.2016.03.028>.

SU, L. *et al.* Hydrochemical Fluxes in Bulk Precipitation, Throughfall, and Stemflow in a Mixed Evergreen and Deciduous Broadleaved Forest. *Forests*, v. 10, n. 6, p. 507, 14 jun. 2019.

TERRA, M. DE C. N. S.; DE MELLO, C. R.; *et al.* Stemflow in a neotropical forest remnant: vegetative determinants, spatial distribution and correlation with soil moisture. *Trees*, v. 32, n. 1, p. 323–335, 8 fev. 2018a. Disponível em: <http://dx.doi.org/10.1007/s00468-017-1634-3>.

TERRA, M. DE C. N. S.; SANTOS, R. M. DOS; *et al.* Water availability drives gradients of tree diversity, structure and functional traits in the Atlantic–Cerrado–Caatinga transition, Brazil. *Journal of Plant Ecology*, v. 11, n. 6, p. 803–814, 22 dez. 2018b. Disponível em: <https://academic.oup.com/jpe/article/11/6/803/5032688>.

TIAN, H. *et al.* Global patterns and controls of soil organic carbon dynamics as simulated by multiple terrestrial biosphere models: Current status and future directions. *Global Biogeochemical Cycles*, v. 29, n. 6, p. 775–792, 5 jun. 2015.

TOBÓN, C.; SEVINK, J.; VERSTRATEN, J. M. Solute fluxes in throughfall and stemflow in four forest ecosystems in northwest Amazonia. *Biogeochemistry*, v. 70, n. 1, p. 1–25, 2004.

TONELLO, K. C.; CAMPOS, S. D.; *et al.* How Is Bark Absorbability and Wettability Related to Stemflow Yield? Observations From Isolated Trees in the Brazilian Cerrado. *Frontiers in Forests and Global Change*, v. 4, n. May, p. 1–15, 12 maio 2021a. Disponível em: <https://www.frontiersin.org/articles/10.3389/ffgc.2021.650665/full>.

TONELLO, K. C.; ROSA, A. G.; *et al.* Rainfall partitioning in the Cerrado and its influence on net rainfall nutrient fluxes. *Agricultural and Forest Meteorology*, v. 303, n. June, 2021b. Disponível em: < https://www.sciencedirect.com/science/article/abs/pii/S0168192321000551>.

TONELLO, K. C.; VAN STAN, J. T.; *et al.* Stemflow variability across tree stem and canopy traits in the Brazilian Cerrado. *Agricultural and Forest Meteorology*, v. 308–309, p. 108551, out. 2021c. Disponível em: <https://linkinghub.elsevier.com/retrieve/pii/S0168192321002355>.

UNFCCC. 2015. Paris Agreement - Article 5. Disponível em: (https://unfccc.int/process-and-meetings/the-paris-agreement/the-paris-agreement)

VAN STAN, J. T. *et al.* Spatial Variability and Temporal Stability of Local Net Precipitation Patterns. *In*: VAN STAN, II, J. T.; GUTMANN, E.; FRIESEN, J. (org.). **Precipitation Partitioning by Vegetation**. Cham, Switzerland: Springer International Publishing, 2020.

VAN STAN, J. T.; FRIESEN, J. Precipitation Partitioning, or to the Surface and Back Again: Historical Overview of the First Process in the Terrestrial Hydrologic Pathway. *In*: VAN

STAN, II, J. T.; GUTMANN, E.; FRIESEN, J. (org.). **Precipitation Partitioning by Vegetation**. Cham, Switzerland: Springer International Publishing, 2020.

VAN STAN, II, J. T.; STUBBINS, A. 2018. Tree-DOM: Dissolved organic matter in throughfall and stemflow. *Limnol. Oceanogr. Lett.* 3(3):199–214.

VAN STAN, J. T.; VAN STAN, J. H.; LEVIA, D. F. Meteorological influences on stemflow generation across diameter size classes of two morphologically distinct deciduous species. *International Journal of Biometeorology*, v. 58, n. 10, p. 2059–2069, 2014.

VELOSO, H. P.; RANGEL FILHO, A. L. R.; LIMA, J. C. A. *Classificação da Vegetação Brasileira, Adaptada a um Sistema Universal*. Rio de Janeiro: IBGE, Departamento de Recursos Naturais e Estudos Ambientais, 1991.

VIEIRA, S. A. *et al.* Stocks of carbon and nitrogen and partitioning between above-and belowground pools in the Brazilian coastal Atlantic Forest elevation range. *Ecology and Evolution*, v. 1, n. 3, p. 421–434, 2011.

YANG, X. *et al.* Dynamic rainfall-partitioning relationships among throughfall , stemflow , and interception loss by Caragana intermedia. *Journal of Hydrology*, v. 574, n. October 2018, p. 980–989, 2019. Disponível em: <https://doi.org/10.1016/j.jhydrol.2019.04.083>

YOU, Y. *et al.* Hydrological fluxes of dissolved organic carbon and total dissolved nitrogen in subtropical forests at three restoration stages in southern China. *Journal of Hydrology*, v. 583, n. 498, 2020.

ZHANG, Y. FENG *et al.* Variations of Nutrients in Gross Rainfall, Stemflow, and Throughfall Within Revegetated Desert Ecosystems. *Water, Air, and Soil Pollution*, v. 227, n. 6, 2016.

SEGUNDA PARTE – ARTIGOS

ARTIGO 1 - SPATIAL AND TEMPORAL PATTERNS IN CARBON AND NITROGEN INPUTS BY NET PRECIPITATION IN ATLANTIC FOREST, BRAZIL

Vanessa Alves Mantovani[1*], Marcela de Castro Nunes Santos Terra[2], Carlos Rogério de Mello[1], André Ferreira Rodrigues[1], Vinicius Augusto de Oliveira[1], Luiz Otávio Rodrigues Pinto[2]

[1]Water Resources Department, Federal University of Lavras, C.P. 3037, 37200-900, Lavras MG, Brazil

[2]Forest Science Department, Federal University of Lavras, C.P. 3037, 37200-000, Lavras MG, Brazil

vanismantovani@hotmail.com*, marcelacns@gmail.com, crmello@ufla.br, afrodrigues09@gmail.com, aovinicius@gmail.com, luizorp@outlook.com

*correspondence

Artigo publicado no periódico “Forest Science” – ISSN 1938-3738, sendo apresentado segundo as normas de publicação.

Versão final disponível em: https://academic.oup.com/forestscience/advance-article-abstract/doi/10.1093/forsci/fxab056/6472766

Abstract

Understanding both carbon and nitrogen temporal and spatial inputs by rainfall in tropical forests is critical for proper forest conservation and management and might ultimately elucidate how climate change might affect nutrient dynamics in forest ecosystems. This study aimed to quantify the net precipitation contribution to the Atlantic Forest’s total carbon (C) and total nitrogen (N), identifying potential differences between these inputs regarding temporal (seasonal and monthly) and spatial scales. Rainfall samples were collected before and after interacting with the forest canopy from May 2018 to April 2019. The rainfall was enriched after crossing the forest

canopy. Significant differences were found for gross rainfall and net precipitation between annual carbon (104.13 kg ha^{-1} and 193.18 kg ha^{-1}) and nitrogen (16.81 kg ha^{-1} and 36.95 kg ha^{-1}) inputs, respectively. Moreover, there was seasonal variability in the C and N inputs with 75% occurring in the wet season. Overall, the spatial patterns revealed that the same locations had the highest inputs regardless of the analyzed period. The forest-rainfall interactions provide constant C and N inputs, especially in the wet season, and are fundamental for the maintenance of ecological processes.

Study Implications: The hydrological and nutrient cycles are tied together. There was significant nutrient enrichment after rainfall interacts with the forest canopy. Rainfall seasonality and canopy deciduousness and heterogeneity drive the temporal and spatial variabilities of carbon and nitrogen. The wet season represented an average of 75% of the total annual carbon and nitrogen contribution, via net precipitation. Such findings enhance our understanding of nutrient deposition, leaching, and absorption processes by canopies and the importance of the tropical forest in the hydrological and nutrient cycle. This knowledge might serve as a guide to improve management practices and justify conservation initiatives.

Keywords: forest hydrology, semideciduous forest, throughfall, stemflow, nutrient inputs

Introdution

Tropical forests are indispensable from both socioeconomic and environmental points of view as they provide several ecosystem services, such as water resource preservation, climate regulation, extreme event buffering, and nutrient cycling, which together guarantee people's welfare and livelihood. Tropical forests have been under intense degradation and fragmentation for centuries, which has resulted in forest remnants with different recovering stages (Nunes et

al. 2021, Souza et al. 2021). These forest fragments are still capable of providing ecosystem services, such as biodiversity maintenance, carbon storage, and water yield (Mello et al. 2019, Souza et al. 2021), and therefore they must be properly managed. However, little is known about the water-nutrient interactions in these fragments. Understanding both water and nutrient cycles in tropical forests is mandatory to shed more light on the importance of conservation. Rainfall partitioning in the forest canopy drives most of the water-nutrient interactions in forest ecosystems (Van Stan and Stubbins 2018). Thus, canopy interception has received special attention because of its importance in the subsequent biogeochemical processes such as soil erosion, streamflow, nutrient cycling, groundwater recharge, evapotranspiration, and biological activity (Zheng and Jia 2020, Rodrigues et al. 2021). The water and nutrient redistribution within a forest is driven by the rainfall-canopy interactions because forest canopy is responsible to intercept both rainfall and dry depositions (Terra et al. 2018a, Aubrey et al. 2020, Zhu et al. 2021). Rainfall redistribution can be split into throughfall (Tf), stemflow (Sf), and canopy evaporation. Tf encompasses both the water dripping from the crowns and the portion that crosses the forest without touching the canopy (Parker et al.1983). Sf channels on the trunks and is deposited near tree bases, influencing the local soil moisture variability (Terra et al. 2018a). Net precipitation (NP) integrates Tf and Sf and represents the rainfall portion that effectively reaches the forest floor.

Nutrient inputs also rely on the canopy-rainfall interactions (Terra et al. 2018a, Sadeghi et al. 2020), which are driven by both weather and forest characteristics (Zheng and Jia 2020). Therefore, NP chemistry is generally affected by vegetation type, morphological traits, atmospheric deposition, and materials derived from canopy and trunks (Hofhansl et al. 2012, Marques et al. 2019, Su et al. 2019, Tonello et al. 2021). Such interactions drive the nutrient pathways in forest systems, highlighting NP as one of the main input ways (Haag 1985, Sadeghi

et al. 2020). Although Sf is a small portion of NP (ranging from 0.02% to 11.9%), Sf is a concentrated flux responsible for water and nutrient inputs near trees (Lilienfein and Wilcke 2004, Dezzeo and Chacón 2006, Hofhansl et al. 2012, Diniz et al. 2013, Tu et al. 2013, Terra et al. 2018a, Limpert and Siegert 2019). Sf importance relies on changing the roots' physical, chemical, and biological properties, which in turn accelerates nutrient redistribution (Germer et al. 2012, Terra et al. 2018a, Su et al. 2019).

Nitrogen and carbon cycles are essential for living organisms and for sustaining a number of ecological processes. For instance, the carbon storage in tropical forests is crucial for mitigating climate-change impacts (Silveira et al. 2019, Sullivan et al. 2020). However, forests are sensitive to extreme events (i.e., droughts and wildfires), which could affect the carbon balance, reduce productivity, and increase tree mortality (Phillips et al. 2010, Reichstein et al. 2013, Anderegg et al. 2020). In this regard, the nitrogen cycle has been changed in the last centuries due to the contribution of anthropogenic sources (Jaffe and Weiss-Penzias 2003). Food production and fossil fuels are considered the most important sources of nitrogen release into the atmosphere (Galloway et al. 2004). Because emissions from agricultural and industrial activities continue to increase, as well as the frequency of wildfires, more nitrogen is released into the atmosphere every year (Jaffe and Weiss-Penzias 2003), which affects nitrogen cycling. Reactive forms of nitrogen (NO_3^- and NH_4^+) are the main nitrogen inputs in forests via NP, whereas organic nitrogen is mainly supplied by biological processes (Mellec et al. 2010). The impacts of increasing nitrogen inputs are still uncertain because it may improve (by fertilization) or decrease (by acidification, eutrophication, and unbalance) ecosystem productivity (Galloway et al. 2004).

Most of the uncertainties regarding tropical forest response to changes in carbon and nitrogen inputs are due to knowledge gaps in the storing and redistributing processes. Carbon and nitrogen atmospheric deposition monitoring come from isolated initiatives, limited to specific regions and

periods, which impairs a broad analysis of nutrient inputs via NP on forest ecosystems and, ultimately, the understanding of the role played by forests in these biogeochemical cycles (Schroth et al. 2001, Lilienfein and Wilcke 2004, Markewitz et al. 2004, Germer et al. 2007, Souza et al. 2015, Neu et al. 2016, Tonello et al. 2021). Despite the considerable increase in interest, only a few studies have addressed the spatial and temporal variability of nutrient concentration in Tf and Sf in tropical areas (Filoso et al. 1999, Zimmermann et al. 2007, Zimmermann et al. 2008).

The main difficulties to tackle these knowledge gaps are logistics and costs, because continuous data collection and lab analysis are necessary (Levia and Frost 2006). The few initiatives have usually taken into account single rainfall events or selected events within specific time periods (Schroth et al. 2001, Tobón et al. 2004, Germer et al. 2007, Hofhansl et al. 2011, Hofhansl et al. 2012), such as wet seasons (Ciglasch et al. 2004, Möller et al. 2005, Oziegbe et al. 2011) and/or weekly or biweekly samplings (Lilienfein and Wilcke 2004, Schwendenmann and Veldkamp 2005, Dezzeo and Chacón 2006, Goller et al. 2006, Fujii et al. 2009, Souza et al. 2015, Neu et al. 2016). However, sampling that covers the entire hydrological year allows complete understanding of the nutrient cycle because changes in rainfall pattern, temperature, and vegetation characteristics can be tracked. Moreover, studies regarding total carbon (C) and total nitrogen (N) for highly threatened tropical forests are scarce.

The Brazilian Atlantic Forest is a world biodiversity hotspot (Myers et al. 2000) and the second-largest South American rainforest, encompassing tropical and subtropical regions with different elevations and rainfall amounts (Oliveira-Filho and Fontes 2000, Ribeiro et al. 2009). The Atlantic Forest is composed of two types of forest, rainforests and semi-deciduous forests, which have idiosyncrasies related to seasonality. Rainfall, temperature, and elevation are the main distribution drivers of the vegetation types (Oliveira-Filho and Fontes 2000, Terra et al. 2018b).

Atlantic rainforests are restricted to Brazilian coasts and mountain range regions, whereas the semi-deciduous forests extend across the southeastern Brazil hinterlands. The semi-deciduous forests are composed of tree species that cope with the dry climatic conditions of winter (Morellato and Haddad 2000), in which up to 50% of the trees lose their leaves during the dry season (Veloso et al. 1991, IBGE 2012). The Atlantic Forest, like other tropical forests, have high stocks of carbon and nitrogen above and below ground (Trumbore et al. 1995, Villela et al. 2012). The carbon stocks differ in neotropical forests, linked to heterogeneity of size of trees and terrain topography (Alves et al. 2010). Ongoing climate change (increase in temperature and decrease in rainfall) may affect carbon and nitrogen dynamics in Atlantic forests, increasing soil carbon and nitrogen losses, because of accelerating organic matter decomposition (Vieira et al. 2011; Villela et al. 2012). Additionally, the Atlantic forests have been threatened by anthropic activities, which contribute to the decrease in carbon and nitrogen stocks (Ribeiro et al. 2009). Understanding both carbon and nitrogen temporal and spatial dynamics in tropical forests can aid in understanding the source, path, and role of these elements in the forest soil (Stubbins 2020). In addition, it can elucidate the nutrient patterns between seasons and how climate change and rainfall regimes influence these inputs. Thus, highlighting the role of water and nutrient cycles in Atlantic forests might alert decision-makers to the importance of improving protection programs and management strategies.

Thus, this research aimed to assess the NP contribution to carbon and nitrogen inputs in an Atlantic Forest remnant (AFR), relying on data collected throughout one hydrological year. In this context, we sought to: (1) compare carbon and nitrogen concentration and inputs between gross precipitation and the rainfall partitioned by forest canopy, (2) identify the impacts of seasonality on carbon and nitrogen inputs on seasonal (dry and wet) and monthly bases, and (3) assess the spatial behavior of C and N inputs across the forest stand.

Material and Methods

Site description

The study site is a 6.35 ha AFR located in southeastern Brazil (21°13′40″ S, 44°57′50″ W) with an average elevation of 925 m. This forest remnant is classified as montane seasonal semi-deciduous forest (Oliveira-Filho et al. 1996). This forest type is widespread throughout the more inland portion of the Atlantic Forest biome in southeastern Brazil, where up to 50% of the trees lose their leaves in the dry season (Scolforo and Carvalho 2006). The relief is gently undulating and the soil is classified as Dystrophic Red Latosol (Junqueira Junior et al. 2017). The well-defined seasons with rainfall concentration in the summer (December to March) characterizes the climate as Cwa according to the Köppen classification (Junqueira Junior et al. 2019). Long-term average annual precipitation (1981–2010) is 1461.8 mm, in which 85% falls during the wet period (October to March) (INMET 2018). The mean annual temperature is 20.3°C, ranging from 16.9°C (June and July) to 22.5°C in February (INMET 2018).

Gross rainfall (GR), Throughfall (Tf), and Stemflow (Sf) measurements

Gross rainfall (GR; rainfall above the forest canopy), Tf, and Sf were monitored from May 2018 to April 2019, encompassing 86 rainfall events. The monitoring was performed either four hours after the rainfall had ceased or the next morning (for events that occurred in late afternoon) to avoid events overlapping. Ten trees were selected from the most abundant species to better frame the Sf characteristics in the AFR. According to Junqueira Junior (2019), the most abundant species are *Copaifera langsdorffii* Desf. (Fabaceae), *Xylopia brasiliensis* Spreng (Annonaceae), and *Miconia willdenowii Klotzsch ex Naudin*. (Melastomataceae) (Table 1). These tree species represent 30% of the AFR cover value index (Souza et al. 2021). Moreover, the selected trees were well distributed across the site (Figure 1) and properly represented the size range of the study site (DBH; diameter at breast height, 1.3 m above ground; see Table 1). Sf collectors were built with a hose slit open along the length and nailed in a spiral fashion around

the tree trunk. The Sf drained into a bin and was measured with graduated cylinders of volume capacities ranging from 0.1 L to 1.0 L (Figure 2A). GR was measured in three storage rain gauges (Ville de Paris-type) placed around the forest remnant (Figures 1 and 2B). Thereafter, GR over the AFR was assessed by the Thiessen Polygon approach. In addition, 10 storage rain gauges were installed near the selected trees to monitor Tf. These gauges have an open area of 0.038 m² and were placed 1.5 m above the forest floor to avoid splash-in (Figure 2A). GR and Tf were converted to depth by dividing the collected volume (liters) by the rain-gauge catchment area (meters squared). For Sf, the volume stored in the bin (liters) was divided by the total projected crown area (meters squared). This projected area was determined according to Shinzato et al. (2011), in which eight vertical projections with 45° spacing were set in the ground. The canopy area for each was calculated as follows:

$$\text{A } (m^2) = \Sigma \frac{(a * b * sen\ 45^{\circ})}{2} \qquad (1)$$

in which A is the projected crown area and a and b are the vertical 45° projections. This measurement was performed twice to consider the projected crown areas in the dry (July 2018) and wet (March 2019) periods.

Table 1. Identification of trees species in the Atlantic Forest remnant, and DBH measurement (once time in period May 2018 to April 2019).

Tree code	Scientific name	DBH (cm)	Canopy area (m) in wet season	Canopy area (m) in dry season	Height (m)
1	*Xylopia brasiliensis* Spreng. *(Annonaceae)*	27.37	54.70	30.59	18
2	*Copaifera langsdorffii* Desf. *(Fabaceae)*	32.15	38.96	91.59	16
3	*Copaifera langsdorffii* Desf. *(Fabaceae)*	14.96	9.91	22.16	15
4	*Copaifera langsdorffii* Desf. *(Fabaceae)*	31.83	110.37	81.58	21
5	*Miconia willdenowii* Klotzsch ex Naudin *(Melastomataceae)*	21.65	22.26	15.04	13.5
6	*Miconia willdenowii* Klotzsch ex Naudin *(Melastomataceae)*	12.1	14.40	13.64	15
7	*Xylopia brasiliensis* Spreng. *(Annonaceae)*	50.29	96.42	129.06	26
8	*Xylopia brasiliensis* Spreng. *(Annonaceae)*	11.46	10.62	18.04	14
9	*Miconia willdenowii* Klotzsch ex Naudin *(Melastomataceae)*	24.19	17.06	23.88	14
10	*Xylopia brasiliensis* Spreng. *(Annonaceae)*	8.91	4.18	4.65	13

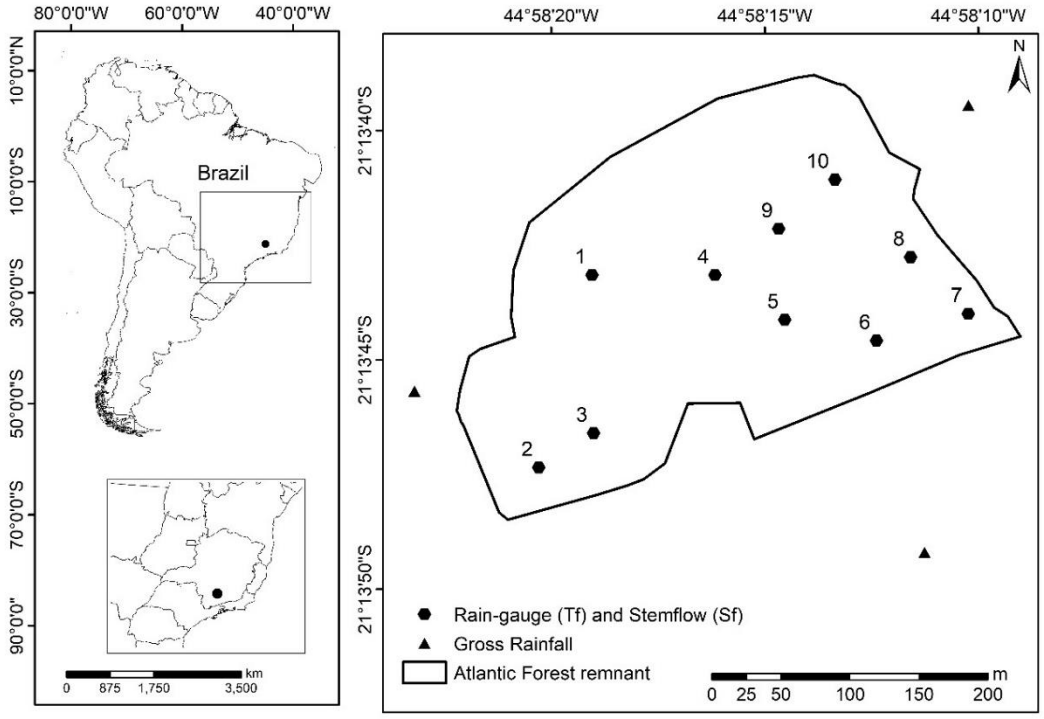

Figure 1. The geographical location of the AFR in Brazil and the positions of the measuring points (Tf and Sf, are represented with the same points, rain gauges and stemflow buckets are on average 1.5m apart from each other).

Figure 2. Rain gauge and stemflow apparatus for, respectively, throughfall and stemflow measurements (a) and external rain gauge for gross rainfall measurements (b).

Chemical analysis

Water samples from GR, Tf, and Sf were collected for events >5 mm due to analysis requirements, summing up sixty-one (out of 86) rainfall events. The GR samples from the three external rain gauges were aggregated before performing the analyses (Figure 1). The following physical and chemical parameters were analyzed: pH, electric conductivity (EC), C, nitrate (NO_3^-), nitrite (NO_2^-), and total Kjeldahl nitrogen (TKN, which refers to ammoniacal and organic nitrogen). The samples were analyzed for pH, EC, and carbon after every rainfall event (i.e., single samples). The samples were first accumulated on a monthly scale (i.e., composite samples) before the analysis of NO_3^-, NO_2^-, and TKN were carried out. All procedures concerning the samples (collecting, preserving, and analyzing) followed the Standard Methods (APHA 2014) criteria (Table A1—Supplementary Material), which ensured that the nitrogen was not lost during storage.

The carbon concentration analyses were performed with a Shimadzu total carbon analyzer (TOC-VCPH) (Table A1— Supplementary Material) (Shimadzu 2003). The procedure consisted of inserting the samples in a combustion tube, which was filled with an oxidation catalyst, and burning them at a temperature of 680°C. The C was converted to carbon dioxide and quantified in a nondispersive infrared sensor. The procedure for TKN analysis consisted of converting organic nitrogen to ammoniacal nitrogen by acid digestion. Then, the sample pH was raised to convert all ammoniacal nitrogen to ammonium. After distillation, nitrogen was quantified by the titrimetric method (ABNT 1997). The NO_2^- analysis was performed by the colorimetric method, which consists of quantifying NO_2^- through the formation of a reddish-purple color. Absorbances at 543 nm were measured in a Quimis UV-VIS Spectrophotometer for NO_2^- (APHA 2014), whereas absorbances at 410 nm were read for NO_3^- after the formation of a yellow color (Yang et al. 1998). The NO_2^- and NO_3^- concentrations were calculated from the standard calibration curve (APHA 2014). The analyses were performed in triplicate and a sample blank was prepared in each set of analyses for quality control.

Data analysis

Rain gauges remained open and/or Sf collectors were knocked over by animals, making it impossible to collect Tf and Sf for some events. Thus, linear regressions were fitted with GR data to overcome these issues and to fill the unavoidable gaps in the measuring points. The regressions were performed for each point separately, resulting in R^2 greater than 0.78 and 0.54 for Tf and Sf, respectively.

Next, the mean monthly concentrations in GR, Tf, and Sf were estimated by the volume-weighted mean (VWM) for pH, EC, and C as follows:

$$VWM = \frac{\sum_{n=1}^{i} C_{i,e} \ . V_{i,e}}{\sum_{n=1}^{i} V_{i,e}} \quad (2)$$

in which C represents the parameter concentration (pH, EC, and C) and V represents the total volume at collector *i* for event *e*. It was possible to estimate the monthly N ($kg.ha^{-1}$) and C ($kg.ha^{-1}$) inputs with the total nitrogen ($N = TKN + NO_3^- + NO_2^-$) and carbon (C) concentration:

$$I = \frac{C \,.\, D}{100} \quad (3)$$

in which I represents the nitrogen or carbon input ($kg\ ha^{-1}$), C is the monthly average N and C concentration ($mg\ L^{-1}$), and D is the monthly GR, Tf, and Sf (mm).

Temporal analysis

The temporal variability was assessed through the monthly inputs of GR and NP. To do so, NP was first averaged across the area. Then, statistical differences in C and N inputs ($kg\ ha^{-1}$) between GR and NP (objective 1) as well as the differences between inputs of the dry and wet season and throughout the months (objective 2) were assessed by paired *t*-tests. All statistical analyses were performed in the R language (version 3.6.2) software program (R Development Core Team 2018).

Spatial analysis

Spatial analysis was performed to assess the C and N input ($kg.ha^{-1}$) patterns in the AFR. Thus, the samples were accumulated to account for three periods: annual; dry season; and wet season (objective iii). Spatial variability was assessed by coefficient of variation (CV). Moreover, the spatial patterns of C and N inputs ($kg.ha^{-1}$) were shown considering the dry and wet seasons and the entire period, thus enabling visualization of the C and N contribution at every single point. The spatialization was performed using bubble graphs in the Quantun GIS software program (QGIS Version 3.14.0).

Results

Hydrological monitoring

A total of 86 rainfall events were monitored from May 2018 to April 2019, adding up to 1,601.6 mm. Rainfall was 1,535.3 mm for the same period in a meteorological station located 1 km from the forest (INMET 2019). Considering that the long-term annual average rainfall (1981–2010) is 1,461.8 mm, the sampling year represented a typical year in terms of rainfall, almost 10% above average (Figure 3; Table A2—Supplementary Material). Approximately 85% of GF occurred in the wet season in the AFR (October to March), which is in accordance with the expected pattern of the region (Table A2). The GR extremes were observed in December (328.4 mm) and July (0.0 mm), respectively. Tf was the main portion of GR across the monitoring period with 1,278.6 mm (79.8%), ranging from 70.78% (June) to 85.72% (December). Interception loss accounted for 319.7 mm (20.0% of GR), with a maximum ratio in June (29.17%) and a minimum in December (14.05%). Sf accumulated 3.2 mm (0.20% of GR), with a maximum contribution in August (0.42 %) and a minimum in June (0.04%). These contributions are in accordance with Rodrigues et al. (2021) and properly represent the canopy water balance of an AFR.

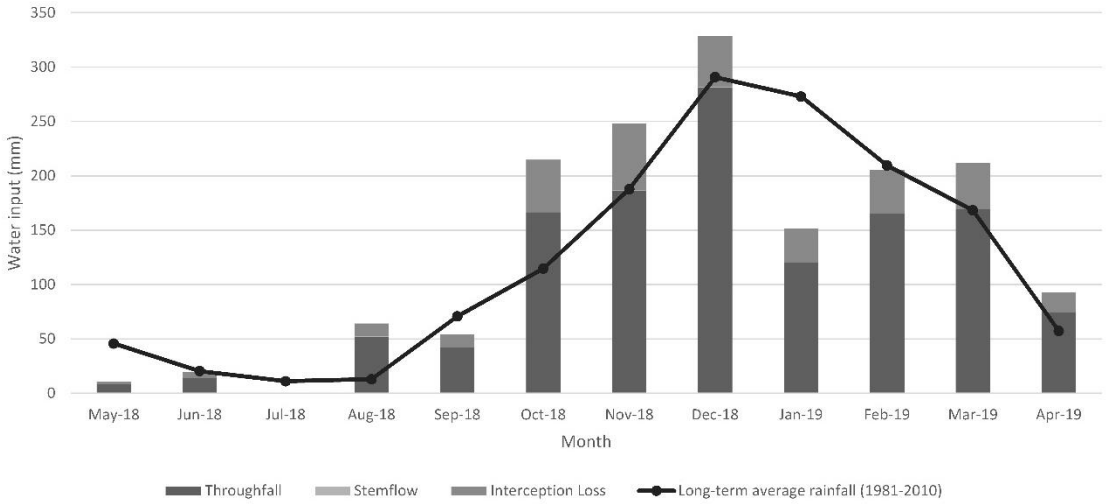

Figure 3. Monthly inputs of water in the Atlantic Forest remnant through throughfall, stemflow, and interception loss, and long-term average rainfall (1981–2010).

Chemical analysis

Rainfall samples were collected from sixty-one events (only those with more than 5 mm), summing up 1,536.5 mm, 1,236.7 mm, and 3.1 mm for GR, Tf, and Sf, respectively. This represents ~96% of the study period (Table A3— Supplementary Material). The annual average pH was 7.14, 6.96, and 5.66 in GR, Tf, and Sf, respectively. The average EC for GR was 22.41 μS cm^{-1}, whereas it was 72.42 μS cm^{-1} and 91.16 μS cm^{-1} for Tf and Sf, respectively. These values are 3.2 and 4.1 times greater than GR, respectively (Table 2). C and N concentrations were higher in Sf, followed by Tf and GR (Table A4—Supplementary Material). The N concentration in Sf was higher than in Tf for all months except May (Figure 4A, B). Considering annual average concentration (mg L^{-1}), C was almost three times higher in Tf and more than five times higher in Sf, whereas N was more than twice as high in Tf and four times higher in Sf regarding GR concentrations.

Considering N forms separately, NO_3^- mean concentrations in GR, Tf, and Sf were 0.25, 0.75, and 1.68 mg L^{-1}, respectively. NO_2^- mean concentrations in GR, Tf, and Sf were 0.04, 0.11, and 0.05 mg L^{-1}, respectively, and TKN mean concentrations in GR, Tf, and Sf were 1.5, 3.3, and 5.9 mg L^{-1}, respectively.

Table 2. pH and electric conductivity (EC) of gross rainfall (GR), average throughfall (Tf) and average stemflow (Sf) with their respective standard deviations and coefficients of variation (CV).

	GR		Tf		Sf	
Months	pH	EC (µS cm^{-1})	pH	EC (µS cm^{-1})	pH	EC (µS cm^{-1})
May 2018	7.44	32.00	7.18 ± 0.37 (5.2%)	182.10 ± 47.36 (26%)	7.47 ± 0.44 (6%)	301.20 ± 278.12 (92%)
Jun 2018	7.29	58.00	7.30 ± 0.31 (4.2%)	206.00 ± 271.08 (132%)	7.15 ± 0.51 (7%)	117.44 ± 54.60 (46%)
Jul 2018	0.00	0.00	0.00 ± 0.00 (0%)	0.00 ± 0.00 (0%)	0.00 ± 0.00 (0%)	0.00 ± 0.00 (0%)
Aug 2018	5.56	15.57	5.40 ± 1.31 (24.3%)	81.24 ± 30.46 (37%)	5.05 ± 0.48 (10%)	138.25 ± 48.44 (35%)
Sep 2018	7.35	34.30	7.17 ± 0.05 (0.7%)	78.92 ± 15.59 (20%)	5.51 ± 0.34 (6%)	153.88 ± 48.88 (32%)
Oct 2018	7.26	19.22	7.04 ± 0.08 (1.1%)	56.24 ± 16.93 (30%)	5.37 ± 0.47 (9%)	69.73 ± 31.36 (45%)
Nov 2018	7.13	17.22	6.93 ± 0.07 (1.0%)	40.83 ± 14.24 (35%)	5.09 ± 0.66 (13%)	43.88 ± 19.85 (45%)
Dec 2018	6.86	15.23	6.71 ± 0.09 (1.3%)	33.88 ± 7.71 (23%)	5.11 ± 0.44 (9%)	29.50 ± 17.40 (59%)
Jan 2019	7.61	21.48	7.40 ± 0.15 (2.0%)	43.56 ± 10.03 (23%)	5.56 ± 0.31 (6%)	31.52 ± 17.18 (55%)
Feb 2019	7.48	10.26	7.17 ± 0.08 (1.1%)	42.45 ± 6.58 (16%)	5.24 ± 0.62 (12%)	45.86 ± 28.17 (61%)
Mar 2019	7.24	8.88	7.06 ± 0.05 (0.7%)	37.75 ± 8.66 (23%)	5.19 ± 0.85 (16%)	35.55 ± 18.56 (52%)
Apr 2019	7.37	14.31	7.20 ± 0.05 (0.7%)	48.61 ± 10.88 (22%)	5.57 ± 0.36 (6%)	35.96 ± 12.48 (35%)
Mean annual	7.14 ± 0.56 (33%)	22.41 ± 14.26 (73%)	6.96 ± 0.55 (33%)	77.42 ± 59.97 (87%)	5.66 ± 0.84 (35%)	91.16 ± 83.19 (100%)

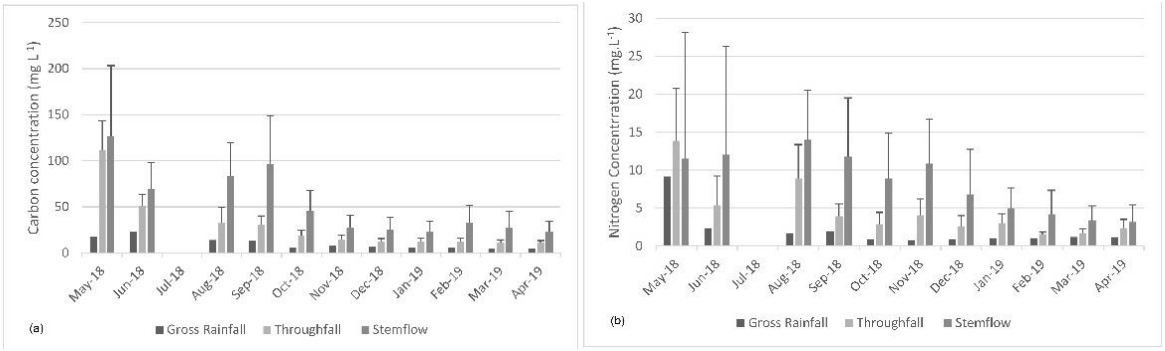

Figure 4. (a) Carbon and (b) nitrogen concentrations in gross rainfall, throughfall, and stemflow with their respective standard deviations.

Temporal analyses

The total annual C input in GR was 104.13 kg ha^{-1}, whereas in NP, it was 193.18 kg ha^{-1} (191.97 kg ha^{-1} in Tf and 1.21 kg ha^{-1} in Sf) (Table A5—Supplementary Material). The total annual flux of C in NP (Tf + Sf) in relation to GR increased by 86%. In the wet season, C input was 143.52 kg ha^{-1}, 74.3% of the total annual. Significant differences were found between GR and NP (P-value < 0.05), and NP between dry and wet season C inputs (P-value < 0.05).

The total annual N input in GR was 16.81 kg ha^{-1} whereas in NP, it was 36.96 kg ha^{-1} (36.69 kg ha^{-1} in Tf, and 0.27 kg ha^{-1} in Sf) (Table A5—Supplementary Material). The total annual flux of N in NP (Tf + Sf) in relation to GR increased by 120%. In the wet season, N input was 27.76 kg ha^{-1}, 75.1% of the total annual. Significant differences were found between GR and NP (*P*-value < 0.05), and, considering NP, between dry and wet season N inputs (*P*-value < 0.05). These results highlight the seasonality of C and N input via rainfall.

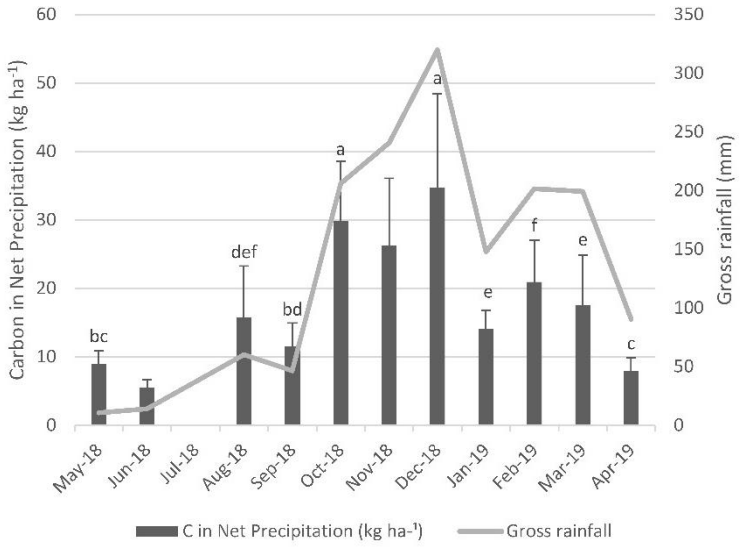

Figure 5. Monthly average carbon (C) inputs in net precipitation (kg ha^{-1}) and monthly gross rainfall (mm). Different letters above bars mean statistical differences (*P* < 0.05) between months.

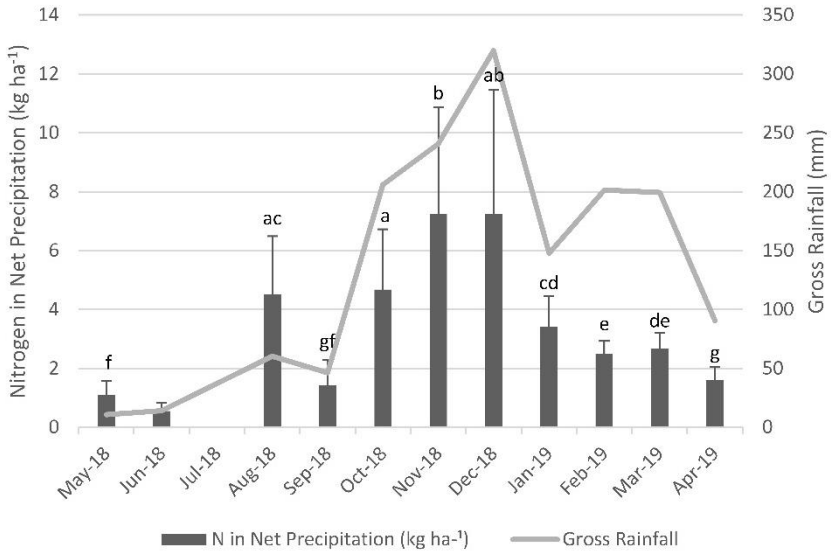

Figure 6. Monthly average nitrogen (N) inputs in net precipitation (kg ha−1) and monthly gross rainfall (mm). Different letters above bars mean statistical differences (*P < 0.05*) between months.

The months with the highest C inputs in NP were December, October, and November, whereas the lowest contributions were in September, May, and June. C inputs follow rainfall seasonality (i.e., the higher the rainfall amount, the higher the C inputs) (Figure 5). The highest N inputs were in November and December, whereas August and October were statistically similar. The same was observed in January, February, and March. Apart from August, N inputs were greater throughout the wet season (October to May). Thus, the months with the lowest inputs were April, May, June, and September, with no statistical differences among them (Figure 6).

Spatial analyses

The spatial variability of N and C inputs (kg ha^{-1}) was assessed with the CV for monthly, seasonal (dry and wet seasons), and annual scales (Table A6—Supplementary Material). C and N inputs generally had the same variability in both the annual and the wet season. However, the spatial variability of N (26%) was higher than that of C (18%) in the dry season. The variability for seasonality was higher in the wet than the dry season for both inputs. The CV of C throughout the year ranged from 19% (January) to 47% (August), and N varied from 17% (February) to 60% (September). The distribution of C and N inputs (kg ha^{-1}) for the seasons and the entire period (total annual) are shown considering individual points (Figure 7). Overall, there was similarity between N and C inputs in the dry season. However, C and N inputs presented remarkable differences in the wet season, especially in the southwestern and northeastern portions of the AFR. The greatest inputs for both C and N occurred in the same places regardless of the analyzed period, namely in the central, southwestern, and eastern areas (near the points 3, 4, and 8).

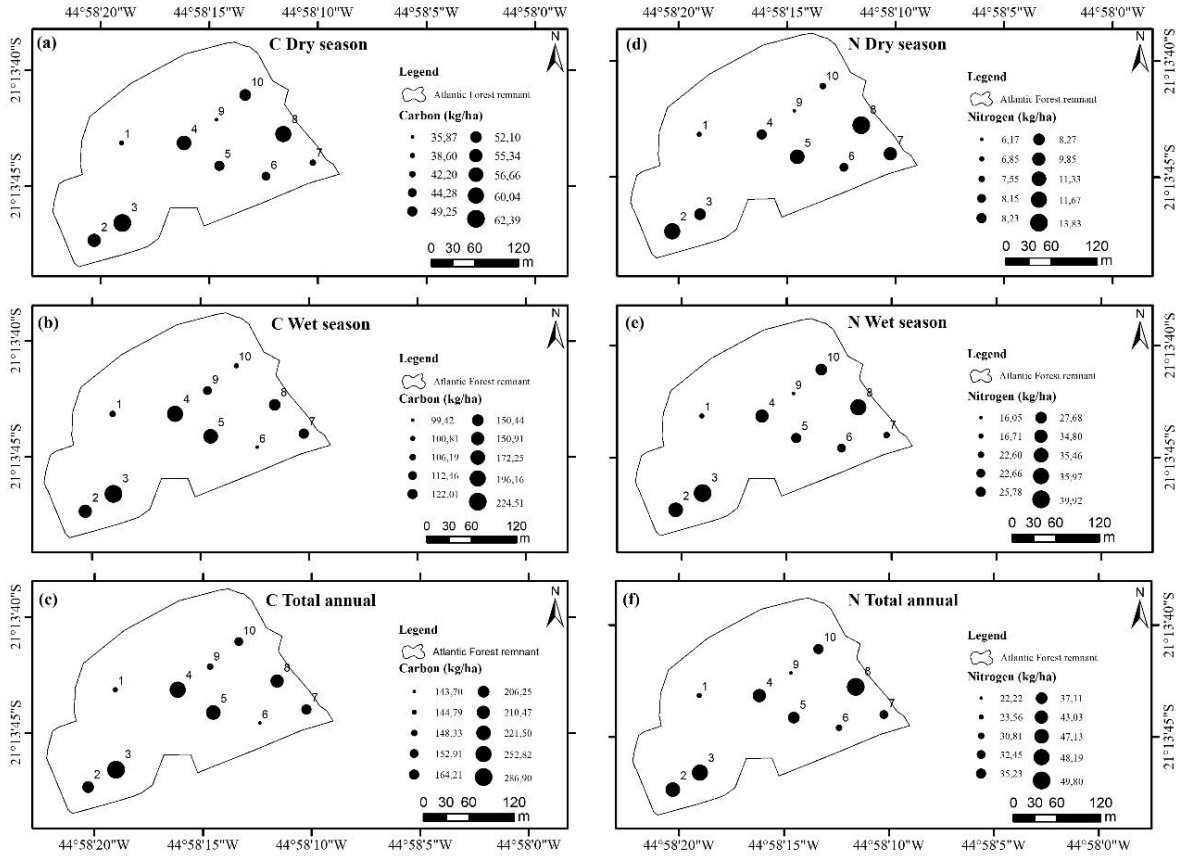

Figure 7. Carbon (C) and nitrogen (N) inputs (kg ha^{-1}) in the dry and wet seasons and the entire period (total annual).

Discussion

This study aimed to: (1) compare the changes in C and N concentration and inputs between gross precipitation and NP as rainfall is partitioned by forest canopy, (2) identify differences in C and N inputs through NP considering both seasonal (dry and wet periods) and monthly scales, and (3) identify spatial differences in C and N inputs within the AFR. Our main findings were: (1) NP inputs more C and N than GF; (2) differences were observed in the seasonal and monthly scales, with higher inputs during the wet season, accounting for almost 75% of the total contribution, although concentrations were higher in the dry season; and (3) the spatial variability was higher in the wet season, with the largest inputs for both C and N occurring in the same places within the forest.

GR x NP

The NO_3^-, NO_2^-, TKN, N, and C concentrations in GF, Tf, and Sf were similar to what have been observed in tropical and temperate forests worldwide (Hölscher et al. 2003, Lilienfein and Wilcke 2004, Markewitz et al. 2004, Oziegbe et al. 2011, Tu et al. 2013, Ukonmaanaho et al. 2014, Izquieta-Rojano et al. 2016, Neu et al. 2016, Limpert and Siegert 2019, You et al. 2020). The increase in C and N concentration results from washing the atmospheric dry deposition accumulated in forest canopy between rainfall events and leaching tree materials (Parker 1983, Schroth et al. 2001, Liu and Sheu 2003, Corti et al. 2019, You et al. 2020). The forest system is the main source of C in NP (Parker 1983, You et al. 2020), whereas N also has an influence through gaseous and aerosol depositions (Parker 1983, Schroth et al. 2001). Changes in rainfall pH and EC also highlight the nutrient enrichment in NP (Lilienfein and Wilcke 2004, Tobón et al. 2004, Corti et al. 2019). Organic acids and solid particles are leached from leaves, branches, and trunks, decreasing pH and increasing EC in both Tf and Sf (Liu and Sheu 2003, Tobón et al. 2004, Su et al. 2019).

The C input in NP (193.18 kg ha^{-1} $year^{-1}$) was 1.85 times greater than in GF (104.13 kg ha^{-1} $year^{-1}$). According to Neu et al. (2016), organic C is more representative in NP (attaining up to 90% of C) than it is in GF (68%). The presence of organic C in forests is the result of several sources, such as forest metabolism, decomposition processes, and animal excrement (Parker 1983, Neu et al. 2016). Moreover, the leaching process of the organic matter contributes to an increase in C inputs in NP (Schrumpf et al. 2006, Mellec et al. 2010). Neu et al. (2016) observed that 32% of C found in GF is from inorganic sources and that the organic fraction is influenced by agricultural activities and fires. The climate seasonality of the study region, as well as the drier vegetation of the surrounding areas, might have contributed to the incidence of natural or non-natural fires. In this regard, the carbon present in rainfall may be related to biomass burning (condensation nuclei), as we found slightly lower results than those of regions

strongly influenced by fires, such as the Cerrado and Amazonian Rainforest (Markewitz et al. 2004, Germer et al. 2007, Neu et al. 2016).

There is no consensus in the literature regarding N enrichment in Tf and Sf, which hampers finding patterns and drawing conclusions. In this study, NO_2^- concentration increased in Tf and decreased in Sf. On the other hand, considering the other N forms (NO_3^- and NTK), the concentrations increased as the rainfall passed through the forest canopy (Tf and Sf). Overall, most of the studies have observed an increase in N in the rainfall portions below the canopy (Schroth et al. 2001, Lilienfein and Wilcke 2004, Markewitz et al. 2004, Schwendenmann and Veldkamp 2005, Hofhansl et al. 2011, Souza et al. 2015). However, some studies have also shown a decrease in nitrogen concentration after rainfall crosses the forest canopy (Parron et al. 2011, Tu et al. 2013, Ukonmaanaho et al. 2014, Su et al. 2019), which is likely related to the uptake by trees. Thus, more studies related to the nitrogen and hydrological cycles in tropical forests are necessary to better frame the patterns of nitrogen redistribution. The N (36.95 kg ha^{-1} $year^{-1}$), TKN (26.46 kg ha^{-1} $year^{-1}$), NO_3^- (8.94 kg ha^{-1} $year^{-1}$), and NO_2^- (1.54 kg ha^{-1} $year^{-}1$) inputs in NP were 2.2, 2, 3.2, and 1.9 times greater than in GF, respectively. The main processes that could happen with N are tree uptake of inorganic N and leaching of organic N (provided by biological processes) after rainfall interacted with the forest canopy. These processes, combined with dry depositions and washing of reactive nitrogen forms (NO_2^-, NO_3^-, and NH_4^+) derived from anthropogenic sources (Mellec et al. 2010), provided a net increase in nitrogen inputs by NP. In this study, the anthropogenic sources are related to automobile exhaust, industries (fossil fuel combustion), fires, and agricultural activities (such as fertilizer use and cattle breeding), which are the main economic activities of southeastern Brazil (Marques et al. 2019). Considering the total area of the Atlantic Forest remnant (6.3 ha), the annual C and N inputs in GF can reach up to 656 kg $year^{-1}$ and 106 kg $year^{-1}$, respectively, whereas an amount of 1217 kg $year^{-1}$ and

233 kg year^{-1} was found for NP, respectively. The AFR is responsible for the considerable increase of local C and N, directly influencing the nutrient cycle, N availability, and C storage within the soil. Thus, Atlantic Forest environments stand out as important C and N sinks considering inputs via NP.

Temporal variations of the net precipitation in AFR

There was seasonal variability of C and N in GF, Tf, and Sf (Figure 4). The concentrations were higher in the dry (April to September) than the wet season (October to March). Such a pattern was also observed in other forest stands in seasonal climate regions, mostly because of leaf shedding during dry periods (Lilienfein and Wilcke 2004, Germer et al. 2007, Van Stan and Stubbins 2018, Neu et al. 2016).

An accumulation of particles in the atmosphere and canopy in the dry season after long dry periods ensures high C and N concentrations in the first rainfalls. These events are called "first flush events" and are responsible for "washing" the atmosphere and the forest canopy (Neu et al. 2016, You et al. 2020). Moreover, as up to 50% of the trees lose their leaves in the dry season, the amount of rainfall that passes through the canopy and the interactions between rainfall and forest are different. The accumulation of particles decreases as soon as the wet season starts because more intense and frequent rainfall events cause dilution of the compounds and further reductions in concentration (Michalzik and Matzner 1999, Zhang et al. 2016). In contrast, trees with few leaves drain more water by their trunk in dry seasons (Terra et al. 2018a), and the presence of more leaves increases interactions between rainfall and forests, affecting the nutrient inputs in wet seasons.

These conditions drive the dynamics of nutrient transport from the atmosphere to the forest floor in the dry and wet seasons, as they are strictly associated with the characteristics of both vegetation and rainfall seasonality. Conversely, evergreen forests present less variability in

both water and nutrient inputs, which are related to nonseasonal rainfall patterns and leaf shedding (Van Stan and Stubbins 2018).

The highest C inputs in the monthly-basis analyses (Figure 5) were December, October, and November, respectively, with no statistical differences. These months represent the onset of the wet season and therefore the greater inputs are because of the dry deposition accumulated throughout the dry season. On the other hand, the months with the lowest C inputs correspond to the beginning of the dry season (April, May, and June), in which canopy and atmosphere had been washed off.

November and December had the highest inputs of N (Figure 6) because they are the months with the greatest amounts of rainfall. Furthermore, October and August were also important for nitrogen inputs because both had above-average rainfall and were preceded by below-average rainfall months. This shows the influence of first rainfall events and the importance of washing off the atmospheric deposition in the crowns and branches after long dry periods. This also confirms that rainfall amount and seasonality and length of the rainless period are the main drivers of C and N inputs in the AFR.

Spatial variation of the net precipitation in AFR

There are significant differences in the spatial variability of nutrient inputs among forest types (Levia and Frost 2006). Despite some studies having tried to describe the spatial variability of solute depositions in forests by applying the CV (Raat et al. 2002, Staelens et al. 2006, Zimmermann et al. 2007, Zimmermann et al. 2008), the sampling designs, collection periods, and element analysis were very different, which impair comparisons, although our results were close to other studies carried out in temperate and tropical ecosystems. The CV throughout the study period ranged from 19% to 47% and from 17% to 60% for C and N inputs, respectively. These amounts are within the range (12% to 78%) found in other studies in which tropical forests

had the largest CV in the wet season (Raat et al. 2002, Staelens et al. 2006, Zimmermann et al. 2007, Zimmermann et al. 2008).

Overall, the wet season presented higher spatial variability than the dry season. However, N inputs presented the lowest CV at both the end of the wet season and the beginning of the dry season. The lowest CVs for C inputs were during the dry season. Except for August, the dry months with higher CV are likely associated with above average rainfall, whereas the low CV of January is related to a below average rainfall.

The potential accumulation of organic matter, the greater rainfall amounts, and the heterogeneity of the canopy are some of the factors responsible for the increased spatial variability in tropical forests (Zimmermann et al. 2008). The AFR has a heterogeneous canopy because of the high diversity of species, as well as variability in tree size, height, and age, which is expected in tropical forests. The high incidence of lianas and the canopy gaps caused by felled trees further increase the intrinsic heterogeneity of this type of forest. These conditions lead to high heterogeneity of forest canopy, which in turn acts on the high variability of NP and absence of spatial patterns (Rodrigues et al. 2020, Terra et al. 2018a). The edge effect also contributes to this variability, as it directly affects the characteristics of the vegetation, altering forest structure (tree density and size) and the abundance of species (Benítez-Malvido and Martínez- Ramos 2003).

According to Marques et al. (2019), the presence of animals in the surrounding areas may have increased the N inputs (as ammonia and ammonium) in the southwest and central portion of the AFR. The southwest area with the higher C and N inputs may also be influenced by vehicles, as this part of the forest is close to a busy road. The eastern portion, which has high N inputs throughout the year and high C inputs in the dry season, is located close to a “candeia” (*Eremanthus erythropappus*) forest stand and a *Eucalyptus* stand, which could influence the high

depositions in this location. These forest stands are a potential source of N due to past silvicultural treatments, such as nitrogen fertilizer application (Scolforo et al. 2002).

Overall, the interactions of biotic and abiotic factors (between rainfall and forests) are responsible for high spatial variability in nutrient inputs to the forest floor (Levia and Frost 2006, Zimmermann et al. 2008, Zhang et al. 2019). Despite the high amounts of rainfall being responsible for dilution, it is not possible to only select one factor that controls spatial patterns (Robson et al. 1994). Thus, there are still uncertainties regarding the factors that influence spatial variability of chemicals in tropical forests, which require more studies about canopy structure, meteorological conditions, and nutrient cycles (Levia and Frost 2006, Zhang et al. 2019).

Conclusions

Both concentration (mg L^{-1}) and N and C inputs (kg ha^{-1}) were higher in NP than in GF. The rainfall leaches the atmosphere and forest structures and can be considered an important C and N transfer pathway toward the forest floor. This forest-rainfall interaction is responsible for increasing the total amount of C and N that reaches the forest floor annually.

The seasonal variability of C and N was remarkable. The inputs were higher in the wet season and represented an average of 75% of the total annual contribution. These results confirm the hypothesis that the behavior of these nutrients is dependent on the seasonal variability of precipitation. When analyzing inputs during the year, the impact of extensive dry periods is important for increasing N rather than C. This may be a direct result of atmospheric depositions from anthropogenic sources.

The spatial variability of C and N was higher in the wet season. The spatial patterns revealed that the same locations generally had the highest inputs of both C and N throughout the year. Furthermore, the canopy heterogeneity and the proximity to potential sources seem responsible for breaking any continuity in the C and N inputs in the AFR.

The AFR increases the C and N that reaches the forest floor. The constant input of these nutrients, especially in the wet season, is extremely important in the nutrient cycle because it aids in the sustainability of ecological processes. Despite the variability of nutrient inputs, this study provides useful information on the changes of C and N input after forest-rainfall interaction. Thus, it can support estimations of atmospheric deposition and advance knowledge of the leaching and absorption processes by canopies.

Acknowledgments

The authors thank CAPES, CNPq, and FAPEMIG for funding and CAPES for the Ph.D research grant for the first author. Special thanks go to “Laboratório de Gestão de Resíduos Químicos da Universidade Federal de Lavras (LGRQ-UFLA)”,and to “Laboratório de Análise de Água da Universidade Federal de Lavras (LAADEG-UFLA)” for the facilities and equipment used in this study.

Funding

This study was funded by Coordenação de Aperfeiçoamento de Pessoal de Nível Superior—CAPES (grant number 88882.306661/2018-01); Conselho Nacional de Desenvolvimento Científico e Tecnológico—CNPq (grant number 401760/2016-2); and FAPEMIG (grant number PPMX-545/18).

References

ABNT—Associação Brasileira de Normas Técnicas. 1997. *Água. ABNT NBR 13796:1997-Determinação de nitrogênio orgânico, Kjeldahl e total—Métodos macro e semimicro Kjeldahl.* Rio de Janeiro.

Alves, L. F., S. A. Vieira, M. A. Scaranello, P. B. Camargo, F. A. M. Santos, C. A. Joly, and L.

A. Martinelli. 2010. Forest structure and live aboveground biomass variation along an elevational gradient of tropical Atlantic moist forest (Brazil). *For. Ecol. Manage.* 260(5):679–691.

Anderegg, W. R. L., A. T. Trugman, G. Badgley, C. M. Anderson, A. Bartuska, P. Ciais, D. Cullenward, *et al.* 2020. Climate-driven risks to the climate mitigation potential of forests. *Science.* 368(6497):1091–1095.

APHA—American Public Health Association. 2014. *Standard methods for examination of water and waste water.* 23th ed. Washington, DC.

Aubrey, D.P. 2020. Relevance of precipitation partitioning to the tree water and nutrient balance. I in *Precipitation partitioning by vegetation,* Van Stan, J.T. II, E. Gutmann, and J. Friesen (eds.). Springer International Publishing, Cham, Switzerland.

Benítez-Malvido, J., and M. Martínez-Ramos. 2003. Impact of forest fragmentation on understory plant species richness in Amazonia. *Conserv. Biol.* 17(2):389–400.

Ciglasch, H., J. Lilienfein, K. Kaiser, and W. Wilcke. 2004. Dissolved organic matter under native Cerrado and Pinus caribaea plantations in the Brazilian savanna. *Biogeochemistry* 67(2):157–182.

Corti, G., A. Agnelli, S. Cocco, V. Cardelli, J. Masse, and F. Courchesne. 2019. Soil affects throughfall and stemflow under Turkey oak (Quercus cerris L.). *Geoderma* 333(July 2018):43–56.

Dezzeo, N., and N. Chacón. 2006. Nutrient fluxes in incident rainfall, throughfall, and stemflow in adjacent primary and secondary forests of the Gran Sabana, southern Venezuela. *For. Ecol. Manage.* 234(1–3):218–226.

Diniz, A.R., M.G. Pereira, F.d.C. Balieiro, D.L. Machado, and C.E.G. Menezes. 2013. Precipitação e aporte de nutrientes em diferentes estádios sucessionais de floresta Atlântica,

Pinheiral—RJ. *Cienc. Florest.* 23(3):389–399.

Filoso, S., M.R. Williams, and J.M. Melack. 1999. Composition and deposition of throughfall in a flooded forest archipelago (Negro River, Brazil). *Biogeochemistry* 45(2):169–195.

Fujii, K., M. Uemura, C. Hayakawa, S. Funakawa, Sukartiningsih, T. Kosaki, and S. Ohta. 2009. Fluxes of dissolved organic carbon in two tropical forest ecosystems of East Kalimantan, Indonesia. *Geoderma* 152(1–2):127–136.

Galloway, J.N., F.J. Dentener, D.G. Capone, E.W. Boyer, R.W. Howarth, S.P. Seitzinger, G.P. Asner, *et al.* 2004. Nitrogen cycles: Past, present, and future. *Biogeochemistry* 70(2):153–226.

Germer, S., A. Zimmermann, C. Neill, A.V. Krusche, and H. Elsenbeer. 2012. Disproportionate single-species contribution to canopy-soil nutrient flux in an Amazonian rainforest. *For. Ecol. Manage.* 267:40–49.

Germer, S., C. Neill, A.V. Krusche, S.C.G. Neto, and H. Elsenbeer. 2007. Seasonal and within-event dynamics of rainfall and throughfall chemistry in an open tropical rainforest in Rondônia, Brazil. *Biogeochemistry* 86(2):155–174.

Goller, R., W. Wilcke, K. Fleischbein, C. Valarezo, and W. Zech. 2006. Dissolved nitrogen, phosphorus, and sulfur forms in the ecosystem fluxes of a montane forest in Ecuador. *Biogeochemistry* 77(1):57– 89.

Haag, H.P. 1985. *Ciclagem de nutrientes em florestas tropicais.* Fundação Cargill, Campinas, Brazil.

Hofhansl, F., W. Wanek, S. Drage, W. Huber, A. Weissenhofer, and A. Richter. 2011. Topography strongly affects atmospheric deposition and canopy exchange processes in different types of wet lowland rainforest, Southwest Costa Rica. *Biogeochemistry* 106(3):371–396.

Hofhansl, F., W. Wanek, S. Drage, W. Huber, A. Weissenhofer, and A. Richter. 2012. Controls of hydrochemical fluxes via stemflow in tropical lowland rainforests: Effects of meteorology and vegetation characteristics. *J. Hydrol.* 452–453:247–258.

Hölscher, D., L. Köhler, C. Leuschner, and M. Kappelle. 2003. Nutrient fluxes in stemflow and throughfall in three successional stages of an upper montane rain forest in Costa Rica. *J. Trop. Ecol.* 19(5):557– 565.

IBGE—Instituto Brasileiro de Geografia e Estatística. 2012. *Manual Técnico da Vegetação Brasileira.* Rio de Janeiro, RJ - Brazil.

INMET—Instituto Nacional de Meteorologia. 2018. Normais climatológicas do Brasil 1981-2010. Available at https://portal. inmet.gov.br/normais; last accessed August 8, 2018.

INMET—Instituto Nacional de Meteorologia. 2019. Banco de Dados Meteorológicos. Estação LAVRAS (83687). Available at https:// bdmep.inmet.gov.br/; last accessed December 10, 2019.

Izquieta-Rojano, S., H. García-Gomez, L. Aguillaume, J.M. Santamaría, Y.S. Tang, C. Santamaría, F. Valiño, *et al.* 2016. Throughfall and bulk deposition of dissolved organic nitrogen to holm oak forests in the Iberian Peninsula: Flux estimation and identification of potential sources. *Environ. Pollut.* 210:104–112.

Jaffe, D. A., and P. S. Weiss-Penzias. 2003. BIOGEOCHEMICAL CYCLES | Nitrogen Cycle. P. 205–213 in *Encyclopedia of Atmospheric Sciences*, Elsevier, EUA : Academic Press.

Junqueira Junior, J.A., C.R. de Mello, J.M. de Mello, H.F. Scolforo, S. Beskow, and J. McCarter. 2019. Rainfall partitioning measurement and rainfall interception modelling in a tropical semi-deciduous Atlantic forest remnant. *Agric. For. Meteorol.* 275(May):170–183.

Junqueira Junior, J.A., C.R. Mello, P.R. Owens, J.M. Mello, N. Curi, and G.J. Alves. 2017. Time-stability of soil water content (SWC) in an Atlantic Forest – Latosol site. *Geoderma*

288:64–78.

Levia, D.F., and E.E. Frost. 2006. Variability of throughfall volume and solute inputs in wooded ecosystems. *Prog. Phys. Geogr.* 30(5):605– 632.

Lilienfein, J., and W. Wilcke. 2004. Erratum: Water and element input into native, agri- and silvicultural ecosystems of the Brazilian savanna. *Biogeochemistry* 68(1):131–133.

Limpert, K., and C. Siegert. 2019. Interspecific differences in canopy-derived water, carbon, and nitrogen in upland oak-hickory forest. *Forests* 10(12):1121.

Liu, C.P., and B.H. Sheu. 2003. Dissolved organic carbon in precipitation, throughfall, stemflow, soil solution, and stream water at the Guandaushi subtropical forest in Taiwan. *For. Ecol. Manage.* 172(2–3):315–325.

Markewitz, D., E. Davidson, P. Moutinho, and D. Nepstad. 2004. Nutrient loss and redistribution after forest clearing on a highly weathered soil in Amazonia. *Ecol. Appl.* 14(4 SUPPL.):177–199.

Marques, R.F.d.P.V., M.d.C.N.S. Terra, V.A. Mantovani, A.F. Rodrigues, G.A. Pereira, R.A. da Silva, and C.R. de Mello. 2019. Rainfall water quality under different forest stands. *CERNE* 25(1):8–17.

Mellec, A., H. Meesenburg, and B. Michalzik. 2010. The importance of canopy-derived dissolved and particulate organic matter (DOM and POM)—comparing throughfall solution from broadleaved and coniferous forests. *Ann. For. Sci.* 67(4):411–411.

Mello, C.R., L.F. Ávila, H. Lin, M.C.N.S. Terra, and N.A. Chappell. 2019. Water balance in a neotropical forest catchment of southeastern Brazil. *Catena* 173(July 2018):9–21.

Michalzik, B., and E. Matzner. 1999. Dynamics of dissolved organic nitrogen and carbon in a Central European Norway spruce ecosystem. *Eur. J. Soil Sci.* 50(4):579–590.

Möller, A., K. Kaiser, and G. Guggenberger. 2005. Dissolved organic carbon and nitrogen in

precipitation, throughfall, soil solution, and stream water of the tropical highlands in northern Thailand. *J. Plant Nutr. Soil Sci.* 168(5):649–659.

Morellato, P.C., and C.F.B. Haddad. 2000. Introduction: The Brazilian Atlantic Forest. *Biotropica* 32(4b):786–792.

Myers, N., R.A. Mittermeier, C.G. Mittermeier, G.A.B. da Fonseca, and J. Kent. 2000. Biodiversity hotspots for conservation priorities. *Nature* 403(6772):853–858.

Neu, V., N.D. Ward, A.V. Krusche, and C. Neill. 2016. Dissolved organic and inorganic carbon flow paths in an Amazonian transitional forest. *Front. Mar. Sci.* 3(JUN):1–15.

Nunes, M.H., T. Jucker, T. Riutta, M. Svátek, J. Kvasnica, M. Rejžek, R. Matula, *et al.* 2021. Recovery of logged forest fragments in a human-modified tropical landscape during the 2015-16 El Niño. *Nat. Commun.* 12(1):1–11.

Oliveira-Filho, A.T., Camisao-Neto, A.A., and Volpato, M.M.L. 1996. Structure and dispersion of four tree Populations in an area of montane semideciduous forest in southeastern Brazil. *Biotropica* 28(4):762–769.

Oliveira-Filho, A.T., and M.A.L. Fontes. 2000. Patterns of floristic differentiation among Atlantic forests in southeastern Brazil and the influence of climate. *Biotropica* 32(4 B):793–810.

Oziegbe, M.B., J.I. Muoghalu, and S.O. Oke. 2011. Litterfall, precipitation and nutrient fluxes in a secondary lowland rain forest in Ile—Ife, Nigeria. *Acta Bot. Brasilica* 25(3):664–671.

Parker, G.G. 1983. Throughfall and stemflow in the forest nutrient cycle. *Adv. Ecol. Res.* 13:57–133.

Parron, L.M., M.M.C. Bustamante, and D. Markewitz. 2011. Fluxes of nitrogen and phosphorus in a gallery forest in the Cerrado of central Brazil. *Biogeochemistry* 105(1):89–104.

Phillips, O.L., G. Van Der Heijden, S.L. Lewis, G. Lo, J. Lloyd, Y. Malhi, A. Monteagudo, *et*

al. 2010. Drought–mortality relationships for tropical forests. *New Phytol.* 187:631–646.

QGIS Development Team. 2018. *QGIS Geographic Information System*. Chicago: Open Source Geospatial Foundation. https:// www.qgis.org.

R Development Core Team. 2018. *R: A language and environment for statistical computing.* R Foundation for Statistical Computing, Vienna, Austria.

Raat, K.J., G.P.J. Draaijers, M.G. Schaap, A. Tietema, and J.M. Verstraten. 2002. Spatial variability of throughfall water and chemistry and forest floor water content in a Douglas fir forest stand. *Hydrol. Earth Syst. Sci.* 6(3):363–374.

Reichstein, M., M. Bahn, P. Ciais, D. Frank, M.D. Mahecha, S.I. Seneviratne, J. Zscheischler, *et al.* 2013. Climate extremes and the carbon cycle. *Nature* 500(7462):287–295.

Ribeiro, M.C., J.P. Metzger, A.C. Martensen, F.J. Ponzoni, and M.M. Hirota. 2009. The Brazilian Atlantic Forest: How much is left, and how is the remaining forest distributed? Implications for conservation. *Biol. Conserv.* 142(6):1141–1153.

Robson, A.J., C. Neal, G.P. Ryland, and M. Harrow. 1994. Spatial variations in throughfall chemistry at the small plot scale. *J. Hydrol.* 158(1–2):107–122.

Rodrigues, A.F., C.R. de Mello, M.d.C.N.S. Terra, V.O. Silva, G.A. Pereira, and R.A. da Silva. 2020. Soil water content and net precipitation spatial variability in an Atlantic Forest remnant. *Acta Sci.—Agron.* 42:1–13.

Rodrigues, A.F., C.R. de Mello, U. Nehren, J. Pedro de Coimbra Ribeiro, V. Alves Mantovani, and J. Marcio de Mello. 2021. Modeling canopy interception under drought conditions: The relevance of evaporation and extra sources of energy. *J. Environ. Manage.* 292(January):112710.

Sadeghi S.M.M., D.A. Gordon, and J.T. Van Stan II. 2020. A global synthesis of throughfall and stemflow hydrometeorology. in *Precipitation partitioning by vegetation*, Van Stan, J.T. II,

E. Gutmann, and J. Friesen (eds.). Springer International Publishing, Cham, Switzerland.

Schroth, G., M.E.A. Elias, K. Uguen, R. Seixas, and W. Zech. 2001. Nutrient fluxes in rainfall, throughfall and stemflow in tree-based land use systems and spontaneous tree vegetation of central Amazonia. *Agric. Ecosyst. Environ.* 87(1):37–49.

Schrumpf, M., W. Zech, J. Lehmann, and H.V.C. Lyaruu. 2006. TOC, TON, TOS and TOP in rainfall, throughfall, litter percolate and soil solution of a montane rainforest succession at Mt. Kilimanjaro, Tanzania. *Biogeochemistry* 78(3):361–387.

Schwendenmann, L., and E. Veldkamp. 2005. The role of dissolved organic carbon, dissolved organic nitrogen, and dissolved inorganic nitrogen in a tropical wet forest ecosystem. *Ecosystems* 8(4):339– 351.

Scolforo, J.R., A.D. de Oliveira, A.C. Davide, J.M. de Mello, and F.W.A. Junior. 2002. *Manejo sustentado da candeia Eremanthus erythropappus (DC.) McLeisch e Eremanthus incanus (Less.) Less.). Relatório Técnico Científico.* UFLA-FAEPE- MMA, Lavras, Brazil, 214 p.

Scolforo J.R., and L.M.T. Carvalho. 2006. *Mapeamento e inventário da flora nativa e dos reflorestamentos de Minas Gerais.* Ufla, Lavras, Brazil.

Shimadzu. 2003. TOC-VCPH/CPN & TOC-control V software user manual. 384. Shimadzu Corporation. Kyoto, Japan.

Shinzato, E.T., K.C. Tonello, E.A.G. Gasparoto, and R.O.A. Valente. 2011. Escoamento pelo tronco em diferentes povoamentos florestais na Floresta Nacional de Ipanema em Iperó, Brasil. *Sci. For.* 39:395–402.

Silveira, E.M.d.O., M.d.C.N.S. Terra, H. ter Steege, E.E. Maeda, F.W. Acerbi Júnior, and J.R.S. Scolforo. 2019. Carbon-diversity hotspots and their owners in Brazilian southeastern savanna, Atlantic Forest and semi-arid woodland domains. *For. Ecol. Manage.* 452(August):117575.

Souza, C. R., V. A. Maia, N. de Aguiar-Campos, A. B. M. Santos, A. F. Rodrigues, C. L. Farrapo, F. M. Gianasi, *et al.* 2021. Long-term ecological trends of small secondary forests of the atlantic forest hotspot: A 30-year study case. *For. Ecol. Manage.* 489(February):119043.

Souza, P.A., A.G. Ponette-González, W.Z. de Mello, K.C. Weathers, and I.A. Santos. 2015. Atmospheric organic and inorganic nitrogen inputs to coastal urban and montane Atlantic Forest sites in southeastern Brazil. *Atmos. Res.* 160:126–137.

Staelens, J., A. De Schrijver, K. Verheyen, and N.E.C. Verhoest. 2006. Spatial variability and temporal stability of throughfall deposition under beech (Fagus sylvatica L.) in relationship to canopy structure. *Environ. Pollut.* 142(2):254–263.

Stubbins, A., F. Guillemette, and J.T. Van Stan. 2020. Throughfall and stemflow: The crowning headwaters of the aquatic carbon cycle. In *Precipitation partitioning by vegetation*, Van Stan, J.T. II, E. Gutmann, and J. Friesen (eds.). Springer International Publishing, Cham, Switzerland.

Su, L., C. Zhao, W. Xu, and Z. Xie. 2019. Hydrochemical fluxes in bulk precipitation, throughfall, and stemflow in a mixed evergreen and deciduous broadleaved forest. *Forests* 10(6):1–13.

Sullivan, M.J.P., S.L. Lewis, K. Affum-Baffoe, C. Castilho, F. Costa, A.C. Sanchez, C.E.N. Ewango, *et al.* 2020. Long-term thermal sensitivity of Earth's tropical forests. *Science* 368(6493):869–874.

Terra, M.d.C., C.R. de Mello, J.M. de Mello, V.A. de Oliveira, M.H. Nunes, V.O. Silva, A.F. Rodrigues, *et al.* 2018a. Stemflow in a neotropical forest remnant: Vegetative determinants, spatial distribution and correlation with soil moisture. *Trees* 32(1):323–335.

Terra, M.d.C.N.S., R.M. Dos Santos, J.A. Do Prado Júnior, J.M. de Mello, J.R.S. Scolforo, M.A.L. Fontes, I. Schiavini, *et al.* 2018b. Water availability drives gradients of tree

diversity, structure and functional traits in the Atlantic–Cerrado–Caatinga transition, Brazil. *J. Plant Ecol.* 11(6):803–814.

Tobón, C., J. Sevink, and J.M. Verstraten. 2004. Solute fluxes in throughfall and stemflow in four forest ecosystems in northwest Amazonia. *Biogeochemistry* 70(1):1–25.

Tonello, K. C., A. G. Rosa, L. C. Pereira, G. N. Matus, M. E. G. Guandique, and A. A. Navarrete. 2021. Rainfall partitioning in the Cerrado and its influence on net rainfall nutrient fluxes. *Agric. For. Meteorol.* 303(February):108372.

Trumbore, S. E., E. A. Davidson, P. Barbosa de Camargo, D. C. Nepstad, and L. A. Martinelli. 1995. Belowground cycling of carbon in forests and pastures of eastern Amazonia. *Global Biogeochem. Cycles*. 9(4):515–528.

Tu, L.H., T.X. Hu, J. Zhang, L.H. Huang, Y.L. Xiao, G. Chen, and H.L. Hu, *et al.* 2013. Nitrogen distribution and cycling through water flows in a subtropical bamboo forest under high level of atmospheric deposition. *PLoS One* 8(10):2–12.

Ukonmaanaho, L., M. Starr, A.J. Lindroos, and T.M. Nieminen. 2014. Long-term changes in acidity and DOC in throughfall and soil water in Finnish forests. *Environ. Monit. Assess.* 186(11):7733–7752.

Van Stan, J.T., and A. Stubbins. 2018. Tree-DOM: Dissolved organic matter in throughfall and stemflow. *Limnol. Oceanogr. Lett.* 3(3):199–214.

Veloso H.P., A.L.R. Rangel Filho, and J.C.A. Lima. 1991. *Classificação da Vegetação Brasileira, Adaptada a um Sistema Universal.* IBGE, Departamento de Recursos Naturais e Estudos Ambientais, Rio de Janeiro.

Vieira, S. A., L. F. Alves, P. J. Duarte-Neto, S. C. Martins, L. G. Veiga, M. A. Scaranello, M. C. Picollo, *et al.* 2011. Stocks of carbon and nitrogen and partitioning between above-and belowground pools in the Brazilian coastal Atlantic Forest elevation range. *Ecol. Evol.*

1(3):421–434.

Villela, D., E. de Mattos, A. Pinto, S. Vieira, and L. Martinelli. 2012. Carbon and nitrogen stock and fluxes in coastal Atlantic Forest of southeast Brazil: potential impacts of climate change on biogeochemical functioning. *Brazilian J. Biol.* 72(3 suppl):633–642.

Yang, J.E., J.J. Kim, E.O. Skogley, and B.E. Schaff. 1998. A simple spectrophotometric determination of nitrate in water, resin, and soil extracts. *Soil Sci. Soc. Am. J.* 62(4):1108–1115.

You, Y., W. Xiang, S. Ouyang, Z. Zhao, L. Chen, Y. Zeng, P. Lei, *et al.* 2020. Hydrological fluxes of dissolved organic carbon and total dissolved nitrogen in subtropical forests at three restoration stages in southern China. *J. Hydrol.* 583(498):124656.

Zhang, H.X., H.W. Wu, J. Li, B. He, J.F. Liu, N. Wang, W.L. Duan, *et al.* 2019. Spatial-temporal variability of throughfall in a subtropical deciduous forest from the hilly regions of eastern China. *J. Mt. Sci.* 16(8):1788–1801.

Zhang, Y., X. Wang, Y. Pan, and R. Hu. 2016. Variations of Nutrients in Gross Rainfall, Stemflow, and Throughfall Within Revegetated Desert Ecosystems. *Water, Air, Soil Pollut.* 227(6):183.

Zheng, C., and L. Jia. 2020. Global canopy rainfall interception loss derived from satellite earth observations. *Ecohydrology*. 13(2):1– 13.

Zhu, X., Z. He, J. Du, L. Chen, P. Lin, E. Q. Tian. 2021. Spatial heterogeneity of throughfall and its contributions to the variability in near-surface soil water-content in semiarid mountains of China. *For. Ecol. Manage.* 488(December 2020):119008.

Zimmermann, A., S. Germer, C. Neill, A.V. Krusche, and H. Elsenbeer. 2008. Spatio-temporal patterns of throughfall and solute deposition in an open tropical rain forest. *J. Hydrol.* 360(1–4):87–102.

Zimmermann, A., W. Wilcke, and H. Elsenbeer. 2007. Spatial and temporal patterns of throughfall quantity and quality in a tropical montane forest in Ecuador. *J. Hydrol.* 343(1–2):80–96.

Supplementary Material

Table S1. Physical and chemical water variables evaluated, preservation procedures, the lab method used, and respective reference.

Variable	Preservation procedures	Lab Method	References
pH	Refrigerated at 4 ºC	Eletrometric method (Method 4500 $H^{+)}$	APHA (2014)
EC	Refrigerated at 4 ºC	Conductimetric method (Method 2510 B)	APHA (2014)
C	Filtered and refrigerated at 4 ºC	Shimadzu total carbon analyzer (TOC-V CPH) (Method TC-IC)	Shimadzu (2003)
NO_3^-	Filtered and frozen	Yang et al. (1998) Method	Yang et al. (1998)
NO_2^-	Filtered and frozen	Colorimetric Method (Method 4500- NO_2^-B)	APHA (2014)
TKN	Acidification and refrigerated at 4 ºC	NBR 13.796:1997 Method	ABNT (1997)

Table S2. Comparison of the rainfall in the dry and wet seasons (INMET and AFR) against the long-term average (1981-2010).

	INMET meteorological station (mm)	Atlantic Forest remnant (AFR) (mm)	Long-term average rainfall (1981-2010) - (mm)
Dry season	226.4	241.0	218.0
Wet season	1308.9	1360.5	1243.8
Entire period	1535.3	1601.6	1461.8

Table S3. Gross rainfall (GR), average throughfall (Tf) and average stemflow (Sf) with their respective standard deviations and coefficients of variation (CV).

Months	GR (mm)	Tf (mm)	Sf (mm)
May 2018	10.61	8.32 ± 1.84 (22%)	0.005 ± 0.006 (120%)
Jun 2018	14.08	11.13 ± 2.62 (24%)	0.007 ± 0.007 (100%)
Jul 2018	0.00	0.00 ± 0.00 (0%)	0.000 ± 0.000 (0%)
Aug 2018	60.20	46.39 ± 9.34 (20%)	0.287 ± 0.209 (73%)
Sep 2018	46.37	38.25 ± 5.18 (14%)	0.079 ± 0.060 (76%)
Oct 2018	205.95	164.11 ± 21.26 (13%)	0.364 ± 0.188 (52%)
Nov 2018	240.64	182.03 ± 32.19 (18%)	0.638 ± 0.576 (90%)
Dec 2018	319.86	276.54 ± 35.08 (13%)	0.699 ± 0.389 (56%)
Jan 2019	147.76	117.89 ± 22.64 (19%)	0.342 ± 0.215 (63%)
Feb 2019	201.50	159.57 ± 32.35 (20%)	0.277 ± 0.173 (62%)
Mar 2019	199.21	160.88 ± 23.49 (15%)	0.292 ± 0.246 (84%)
Apr 2019	90.30	71.60 ± 11.07 (15%)	0.121 ± 0.102 (84%)
Entire period (mm)	1536.48 (82%)	1236.71 (84%)	3.111 (90%)

Table S4. Carbon and nitrogen concentration from gross rainfall (GR), average throughfall (Tf), and average stemflow (Sf) with their respective standard deviations and coefficients of variation (CV).

	GR (mg L^{-1})		Tf (mg L^{-1})		Sf (mg L^{-1})	
	C	N	C	N	C	N
May 2018	18.0	9.2	111.6±3.02 (29%)	13.8±6.9 (50%)	126.8±76.5 (60%)	11.5±16.6 (144%)
Jun 2018	22.9	2.3	50.6±13.2 (26%)	5.4±3.9 (72%)	70.0±28.4 (41%)	12.1±14.2 (118%)
Jul 2018	0.0	0.0	0±0 (0%)	0±0 (0%)	0±0 (0%)	0± 0 (0%)
Aug 2018	14.0	1.7	32.7±17.1 (52%)	8.9±4.4 (49%)	83.4±35.9 (43%)	14.0±6.5 (47%)
Sep 2018	12.8	1.9	30.5±9.8 (32%)	3.8±1.7 (46%)	96.7±52.0 (54%)	11.8±7.7 (66%)
Oct 2018	6.0	0.8	18.4±6.4 (35%)	2.9±1.5 (52%)	45.9±22.2 (48%)	8.9±5.9 (67%)
Nov 2018	7.8	0.8	14.2±4.8 (34%)	4.0±2.2 (54%)	27.3±13.4 (49%)	10.9±5.8 (53%)
Dec 2018	6.5	0.9	12.2±3.5 (29%)	2.5±1.5 (59%)	24.9±13.9 (56%)	6.8±5.9 (87%)
Jan 2019	6.2	1.1	12.4±3.7 (29%)	3.0±1.3 (42%)	22.7±11.3 (50%)	4.9±2.8 (56%)
Feb 2019	5.4	1.1	12.7±3.3 (26%)	1.5±0.3 (19%)	33.0±18.5 (56%)	4.1±3.2 (77%)
Mar 2019	4.3	1.2	10.8±3.6 (34%)	1.7±0.6 (33%)	27.7±17.1 (62%)	3.4±1.9 (55%)
Apr 2019	4.3	1.1	11.1±2.5 (22%)	2.4±1.1 (48%)	23.0±11.4 (49%)	3.2±2.2 (70%)
Mean annual	9.8 (73%)	2.0 (130%)	28.8 (113%)	4.5 (91%)	52.9 (77%)	8.3 (59%)

Table S5. Carbon and nitrogen monthly inputs (kg ha^{-1}) from gross rainfall (GR), throughfall (Tf), and stemflow (Sf) in the AFR.

	GR (kg ha^{-1})		Tf (kg ha^{-1})		Sf (kg ha^{-1})	
Months	C	N	C	N	C	N
May 2018	1.91	0.97	8.94	1.10	0.00	0.00
Jun 2018	3.23	0.32	5.47	0.55	0.00	0.00
Jul 2018*	0.00	0.00	0.00	0.00	0.00	0.00
Aug 2018	8.43	1.01	15.53	4.46	0.25	0.04
Sep 2018	5.95	0.87	11.48	1.42	0.09	0.01
Oct 2018	12.43	1.74	29.65	4.63	0.19	0.04
Nov 2018	18.84	1.96	26.04	7.18	0.20	0.08
Dec 2018	20.89	2.88	34.56	7.18	0.19	0.05
Jan 2019	9.21	1.59	14.09	3.40	0.07	0.02
Feb 2019	10.80	2.11	20.84	2.49	0.11	0.01
Mar 2019	8.55	2.41	17.50	2.68	0.09	0.01
Apr 2019	3.89	0.94	7.88	1.60	0.02	0.00
Annual total	104.13	16.81	191.97	36.69	1.21	0.27

*Means no observed rain in the month.

Table S6. Coefficient of variation (CV) of the carbon and nitrogen inputs (kg ha^{-1}) in the AFR.

	Coefficient of variation (%) in C and N inputs from net precipitation	
Months	Carbon	Nitrogen
May 2018	22	43
Jun 2018	22	52
Jul 2018*	0	0
Aug 2018	47	44
Sep 2018	29	60
Oct 2018	29	44
Nov 2018	38	50
Dec 2018	39	58
Jan 2019	19	31
Feb 2019	29	17
Mar 2019	41	20
Apr 2019	24	27
Dry season	18	26
Wet season	30	30
Annual total	26	27

*July 2018 there was no rainfall events

Table S7 Summary of the key carbon and nitrogen inputs (kg ha^{-1} $year^{-1}$) in rainfall portions (gross rainfall, throughfall and, stemflow) in forests around the world.

		Rainfall		**Gross rainfall (kg ha^{-1} $year^{-1}$)**							
Reference	**Forest type**	**Long-term (mm)**	**Mean annual (mm)**	**NH_4+**	**NO_3^-**	**NO_2^-**	**DON**	**TKN**	**N**	**DOC**	**C**
This study	Atlantic Forest	1461.8	1601.6	-	2.82	0.81	-	13.08	16.81	-	104.13
Schroth et al. (2001)	Amazonia Rainforest	2622	2672	1.8	1.4	-	2.3	4.1*	5.5	-	-
Hölscher et al. (2003)	Rainforest	2812	2900	1.4-2.2	1.7-2.0	-	-	-	-	-	-
Markewitz et al. (2004)	Tropical Moist Forest	1803	-	1.5	0.2	-	-	-	4	123.4	-
Lilienfein and Wilcke (2004)	Cerrado	1550	1815	2.7-3.1	2.1-2.4	-	-	-	5.7-6.4	47-55	-
Schwendenmann and Veldkamp (2005)	Tropical Wet Forest	4200	4073	-	-	-	1-6	-	5-14	22- 36	-
Schrumpf et al. (2006)	Rainforest	1840	1960 to 2600	-	-	-	3.36-5.97	-	-	59.4-143.9	-

Germer et al. (2007)	Tropical Rainforest	2300	2286	4.46	0.8	-	-	-	-	106.45	-
Souza and Marques (2010)	Atlantic Rainforest	2240.1	2406.96	-	2.3	-	-	-	-	-	-
Hofhansl et al. (2011)	Wet Tropical Rainforest	5810	5720	-	-	-	-	-	7.7	30.9	
Oziegbe et al. (2011)	Rainforest	1413	1079	-	10.43	-	-	-	-	-	-
Parron et al. (2011)	Cerrado	-	1400	-	-	-	-	-	12.6	-	-
Souza et al. (2015)	Atlantic Forest	2800	2649	6	5	-	4.1	10.1 *	15.1	-	-
Zhou et al. (2016)	Tropical Forest	1557	-	-	-	-	-	-	-	41.9	-
Neu et al. (2016)	Evergreen Tropical Forest	1905	1829	-	-	-	-	-	-	82.3	121.2
Tonello et al. (2021)	Cerrado	-	1337	-	0.33	-	-	-	-	-	-
Liu and Sheu (2003)	Subtropical Forest	2300 to 2700	-	-	-	-	-	-	-	142.8	-
Tu et al. (2013)	Subtropical Forest	1490	1984.2	61.9	24.9	-	26.9	88.8 *	113.8	-	-
Izquieta-Rojano et al. (2016)	Evergreen Holm Oak Forests	364-840	-	0.68-6.55	1.08-3.54	-	1.08-12.27	1.76 - 18.82*	-	-	-
You et al. (2020)	Coniferous, Deciduous and Evergreen forest	1416.4	-	-	-	-	-	-	30.4	22.6	-

		Rainfall		**Throughfall (kg ha^{-1} year^{-1})**							
Reference	**Forest type**	**Long-term (mm)**	**Mean annual (mm)**	**NH_4+**	**NO_3^-**	**NO_2^-**	**DON**	**TKN**	**N**	**DOC**	**C**
This study	Atlantic Forest	1461.8	1601.6		8.89	1.54	-	26.25	36.68	-	191.97
Schroth et al. (2001)	Amazonia Rainforest	2622	2672	2.2	1.9	-	7.2	9.4*	11.3	-	-
Hölscher et al. (2003)	Rainforest	2812	2900	2.4 - 5.7	0.6-1	-	-	-	-	-	-
Markewitz et al. (2004)	Tropical Moist Forest	1803	-	2.9	1.7	-	-	-	9.5	83.1	-
Tobón et al. (2004)	Tropical Rainforest	3100	3400	9.72 - 12.98	17.07-31.98	-	-	-	-	148.43 - 190.42	-
Lilienfein and Wilcke (2004)	Cerrado	1550	1815	2.3-3.4	3-3.9	-	-	-	9.9-11	66-70	-

Schwendenmann and Veldkamp (2005)	Tropical Wet Forest	4200	4073	-	-	-	9	-	17	232	-
Schrumpf et al (2006)	Montane Rainforest	1840	1960 to 2600	-	-	-	6.24-10.31	-	-	102.8-218.5	-
Germer et al. (2007)	Tropical Rainforest	2300	2286	5.71	2.11	-	-	-	-	301.59	-
Fujii et al. (2009)	Tropical Forest	-	2187 - 2427	-	-	-	-	-	-	97-182	-
Souza and Marques (2010)	Atlantic Rainforest	2240.1	2406.96	-	2.51-5.93	-	-	-	-	-	-
Schmidt et al. (2010)	Subtropical Montane Forest	2000 to 5000	4169	1.9	2.8	-	3.4	5.3*	-	106	-
Hofhansl et al. (2011)	Wet Tropical Rainforest	5810	5720	-	-		-	-	10.5-13.8	74.7-94.9	-
Oziegbe et al. (2011)	Rainforest	1413	1079	-	39.27	-	-	-	-	-	-
Parron et al. (2011)	Cerrado	-	1400	-	-	-	-	-	5.9 - 8.3	-	-
Diniz et al. (2013)	Atlantic Forest	1300	1533.3	-	-	-	-	-	-	-	23.1-30.5
Souza et al. (2015)	Atlantic Forest	2800	2649	9.1	5.3	0.2	19.7	28.8*	34.3	-	-
Tonello et al. (2021)	Cerrado	-	1337	-	27.49	-	-	-	-	-	-
Zhou et al. (2016)	Tropical Forest	1557	-	-	-		-	-	-	113.5	-
Neu et al. (2016)	Evergreen Tropical Forest	1905	1829	-	-	-	-	-	-	150.8	167.4
Liu and Sheu (2003)	Subtropical Forest	2300 to 2700	-	-	-	-	-	-	-	188.8-231.3	-
Tu et al. (2013)	Subtropical Forest	1490	1984.2	80.1	13.7	-	20.1	-	113.8	-	-
Izquieta-Rojano et al. (2016)	Evergreen Holm Oak Forests	364-840	-	0.44-3.7	1.66-8.81	-	5.3-11.91	-	-	-	-
Van Stan et al. (2017)	Oak - Cedar Forest	750 to 1200	-	-	-	-	-	-	9-29	230-480	-
You et al. (2020)	Coniferous, Deciduous and Evergreen Forest	1416.4	-	-	-		-	-	22.92-27.38	52-75.94	-

		Rainfall		**Stemflow (kg ha^{-1} year^{-1})**							
Reference	**Forest type**	**Long-term (mm)**	**Mean annual (mm)**	**NH_4+**	**NO_3^-**	**NO_2^-**	**DON**	**TKN**	**N**	**DOC**	**C**

This study	Atlantic Forest	1461.8	1601.6	-	0.05	0.001	-	0.21	0.261	-	1.21
Hölscher et al. (2003)	Rainforest	2812	2900	0.1 - 0.4	0.1		-		-	-	-
Tobón et al. (2004)	Tropical Rainforest	3100	3400	0.18 - 0.26	0.32-0.62		-		-	2.82-6.14	-
Hofhansl et al. (2012)	Tropical Rainforest	5810	-	-	-		-		0.16	2.75	-
Diniz et al. (2013)	Atlantic Forest	1300	1533.3	-	-		-		-	-	0.93-1.55
Neu et al. (2016)	Evergreen Tropical Forest	1905	1829	-	-		-		-	1.5	2.1
Tonello et al. (2021)	Cerrado	-	1337	-	1.45	-	-	-	-	-	-
Liu and Sheu (2003)	Subtropical Forest	2300 to 2700	-	-	-		-		-	6.7-15.3	-
Van Stan et al. (2017)	Oak - Cedar Forest	750 to 1200	-	-	-		-		0.15-2.4	7-75	-
You et al. (2020)	Coniferous, Deciduous and Evergreen forest	1416.4	-	-	-		-		0.14-0.91	0.43-4.43	-

Legend: C: carbon; N: nitrogen; TKN: total kjeldahl nitrogen; DON: dissolved organic nitrogen; DOC: dissolved organic carbon; NH_4^+: ammonia; NO_3^-: nitrate; NO_2^-: nitrite. *TKN = DON + NH_4^+

ARTIGO 2 - BIOTIC AND ABIOTIC DRIVERS OF STEMFLOW CARBON ENRICHMENT RATIO IN TROPICAL TREES

Vanessa Alves Mantovani[1*], Marcela de Castro Nunes Santos Terra[2], André Ferreira Rodrigues[1], Natielle Gomes Cordeiro[2], José Marcio de Mello[2], Carlos Rogério de Mello[1]

[1]Water Resources Department, Federal University of Lavras, C.P. 3037, 37200-900, Lavras MG, Brazil

[2]Forest Science Department, Federal University of Lavras, C.P. 3037, 37200-000, Lavras MG, Brazil

vanismantovani@hotmail.com*

* corresponding author

Artigo submetido no periódico -*Trees Structure and Function* - **Electronic ISSN** 1432-2285, e apresentado segundo as normas de publicação do periódico.

Abstract: Stemflow is an often-neglected concentrated water path in the forest, carrying nutrients along the tree trunks, affecting the biogeochemistry processes, and accelerating the nutrients redistribution in forest ecosystems. Here we assessed what are the effects of tree structural features (height, bark roughness, projected crown area), seasonality (wet and dry season, and previous dry period - PDP), and maximum rainfall intensity on stemflow total carbon enrichment ratios in a semideciduous tropical forest. The enrichment ratio allows quantifying the contribution of stemflow to delivery carbon to the forest soil. To evaluate the increase in total carbon concentration (TC) in the stemflow, we sampled and analyzed sixty-one rainfall events (gross rainfall, throughfall, and stemflow) and modeling the enrichment ratios using potential biotic and abiotic drivers through generalized linear models. The stemflow carbon enrichment ratios ranged from 1 to 30 relative to gross rainfall and from 0.8 to 11 relative to throughfall. The carbon concentration in stemflow was higher in the dry season, however, the greater rainfall amount in the wet season provided higher carbon inputs. Moreover, the carbon enrichment ratios were sensitive to variation on tree structural features and meteorological conditions, highlighting bark structure, crown area, maximum rainfall intensity and season. Our findings demonstrate the role of the stemflow as a relevant source of total carbon input into tropical forests soils.

Keywords: Tropical Critical Zones; Carbon cycle in Tropical Forest; Trees structural features; Carbon-water relationship in tropical forests.

Key message: Tree bark structure, crown area, maximum rainfall intensity and season are the main biotic drivers of carbon input via stemflow in a neotropical forest.

Author contributions: Conceived and designed the study: VAM, MdCNST and CRdM. Led the research project: CRdM. Performed the experiments, collected data and samples in the field: VAM and AFR. Processed samples in the lab: VAM. Wrote the paper: VAM, MdCNST and NGC. Critical Revision: CRdM, AFR, and JMdM. Statistical Support: MdCNST. All authors read and approved the final manuscript.

Acknowledgements: We acknowledge the Coordenação de Aperfeiçoamento de Pessoal de Nível Superior - CAPES (for the Ph.D research grant for the first author, and grant number 88882.306661/2018-01); the Conselho Nacional de Desenvolvimento Científico e Tecnológico - CNPq (grant number 401760/2016-2); and FAPEMIG (grant number PPMX-545/18) for supporting and funding this work. Special thanks go to "Laboratório de Gestão de Resíduos Químicos da Universidade Federal de Lavras (LGRQ-UFLA)" for the facilities and equipment used in this study.

Funding: This work was financially by Coordenação de Aperfeiçoamento de Pessoal de Nível Superior - CAPES (grant number 88882.306661/2018-01); the Conselho Nacional de Desenvolvimento Científico e Tecnológico – CNPq (grant number 401760/2016-2); and FAPEMIG (grant number PPMX-545/18).

Introduction

Forest ecological processes are essential to provide several ecosystem services, such as water quality and quantity, carbon uptake and storage, and nutrient cycling (Carmo et al. 2012; Alves et al. 2010, Harris et al. 2021). Tropical forests play an essential role in the global carbon cycle and are ultimately crucial to mitigate the ongoing climate change (Ribeiro et al. 2009; Joly et al. 2014; Townsend et al. 2011). The relevance of tropical forests should be highlighted as they have been severely threatened by several anthropogenic factors, mainly fragmentation and habitat loss, pollution, rising temperatures, and changes in rainfall patterns which compromises the forest provision and mitigation capacity (Anderegg et al. 2020; Brando et al. 2019).

Interactions between rainfall and vegetation coverage are the beginning of the terrestrial hydrological cycle and affect the rainfall partitioning and solute concentrations in forest stands (Van Stan and Friesen, 2020). Rainfall partitioning in forests is conditioned by the forest canopy and structure, along with the meteorological conditions (Klamerus-Iwan et al. 2020). Throughfall is the rainfall portion that crosses the forest canopy and reaches the forest floor (Su et al. 2019). Stemflow is the rainfall fraction that drains through tree branches and trunks, reaching the forest floor nearby the tree. Stemflow has been neglected in forest hydrology assessments because, in most cases, it represents a small percentage of gross precipitation (Levia and Germer 2015). Nevertheless, stemflow is a local water path in the forest, carrying and redistributing water and nutrients to the forest floor, and has a relevant role on the biogeochemistry processes, such as water infiltration, and nutrient redistribution in forest ecosystems (Germer et al. 2012; Su et al. 2019; Johnson and Lehmann 2006). In this sense, the soil next to the trees can receive a significant amount of carbon, being up to 70x more than an area without vegetation (Duval et al. 2019; Van Stan and Stubbins 2018). Therefore, it is important to address the increase in carbon to forest soil via stemflow, because this process is able to generate a substantial load of carbon to soil near to the tree (Johnson and Lehmann 2006).

The entire process that conditioned the stemflow is still unknown as well as its real contribution to the geochemical cycle, thus, in further analysis of the nutrient inputs, Levia and Germer (2015) suggested that the inclusion of stemflow enrichment ratios in relation to gross precipitation and throughfall is relevant for understanding the forests as one of the main ecosystem services providers. The funneling ratio is the relation between rainfall amount that reaches the forest ground via stemflow and the amount that would reach in the absence of the tree (Herwitz 1986). It allows quantifying the water input at the stem basal area. Similarly, the enrichment ratio allows quantifying the nutrient input in the stem basal area and represents the relationship between the amount of nutrient that reaches the forest floor via stemflow and the amount that would reach in the absence of the tree (Levia and Herwitz 2000). These ratios are enabling the stemflow assessment as a hotspot channeling water and nutrients to the forest ground (Levia and Germer 2015; Levia et al. 2011a). Enrichment ratios can be used to analyze the real changes in the rainfall solute concentration after the rainfall drain by the tree trunks, the spatiotemporal variability of solute inputs, and to compare the nutrient inputs among different forests and tree species (Levia and Herwitz 2000). Also, enrichment ratios make it possible to compare nutrient inputs during different phenological phases of the forest (Levia et al. 2011b, Andre et al. 2008). For instance, Zhang et al. (2013) used the funneling and enrichment ratios to analyze the importance of stemflow in soil water and nutrients inputs and Andre et al. (2008) used the enrichment ratios to analyze the effects of seasons and species in stemflow chemistry.

Stemflow carbon concentration has been reported to be higher than carbon concentration in throughfall and rainfall in tropical and temperate forests (Tobón et al. 2004; Neu et al. 2016; Liu and Sheu 2003; Van Stan et al. 2017; You et al. 2020). The carbon carried by throughfall and stemflow derives from biotic factors, such as forest metabolism, organic matter decomposition as well as abiotic factors, mainly atmospheric deposition (Parker 1983; Neu et al.

2016; Schrumpf et al. 2006; Mellec et al. 2010; Liu and Sheu 2003). The stemflow solute enrichment ratio has high variability, and is related to several abiotic and biotic factors, and could be useful to evaluate spatiotemporal patterns of biogeochemical cycles (Levia and Germer 2015; Levia et al. 2011b). The main abiotic factors are related to atmosphere conditions and pollution, such as distance of pollution sources, air mass provenance, rainfall pattern, rainfall intensity and amount, and wind velocity and direction (André et al. 2008; Levia et al. 2011a). The biotic factors are related to characteristics of the tree species, such as diameter at breast height (DBH), tree height, crown area and architecture, and tree bark roughness, which are determinant in the residence time of intercepted rainfall, impacting the volume and chemistry of stemflow (Levia et al. 2011a; Chen et al. 2019). Furthermore, the stemflow retention time also influences carbon concentration (Michalzik et al. 2001). Both abiotic and biotic factors are determinants of stemflow chemistry, which result in high variability of the enrichment ratios (Chen et al. 2019; Dowtin et al. 2020; Schooling et al. 2017; Levia et al. 2011b).

Biological carbon production by the forest itself and carbon atmospheric deposition are driven to forest soil as significant inputs via stemflow. Studying the carbon enrichment ratios and identifying the main biotic and abiotic drivers can improve our understanding regarding sustainability and the ecological functioning of the forest fragments. Tobon et al. (2004) found the previous dry period as a factor can explain the dissolved organic carbon concentration in stemflow. The development of models that make possible to assess nutrient inputs via stemflow as a function of the vegetation traits, tree species, seasonality, and meteorological variables, may potentially leap our understanding of how each driver could influence water and carbon flow in the stemflow, and improve yields in forests and agricultural land (Levia and Frost 2003). Thus, it is imperative to continue investigating the variability of nutrients and pollutants inputs in the

forest ecosystem, and how this can affect the biogeochemical cycles (Dowtin et al. 2020; Limpert and Siegert 2019).

In this regard, we sought to quantify and describe the stemflow carbon concentration and stemflow carbon enrichment ratio in relation to both gross rainfall and throughfall in a seasonally dry tropical forest to provide a better understanding of the importance of trees on water and carbon cycles. The main question here is: what are the effects of tree structural features (height, bark roughness, projected crown area), seasonality (wet and dry season, and previous dry period - PDP) and maximum rainfall intensity on stemflow carbon enrichment ratios in a seasonally dry tropical forest? To address this question, we will rely on an experimental dataset (encompassing sixty-one rainfall events) and on modeling the enrichment ratios using potential biotic and abiotic drivers through generalized linear regression models. We expect the stemflow enrichment ratios to show seasonal behavior and to be sensitive to a variation on tree structural features.

Material and methods

Site description

Our study covered a 6.30 ha seasonally dry tropical forest fragment (semideciduous forest *sensu* Oliveira-Filho and Fontes, 2000) in late successional stage, located in an urban and agricultural area in Southeastern Brazil (21º13’40’’S and 44º57’50’’W, 925 m a.s.l) (Souza et al. 2021) (Fig 1). The long-term (1981-2010) average annual precipitation is 1461.8 mm, in which 85% falls during the wet period between October and March (INMET 2018). The annual mean air temperature is 20.3 ºC, ranging from 16.9 ºC (June and July) to 22.5 ºC in February (INMET 2018). The Köppen-type climate of the studied region is Cwa, characterized by rainfall concentration in the summer (December to March) and well-defined seasons (Silva and Mello 2021; Junqueira Junior et al. 2019). The soil is a Dystrophic Red Latosol (Rhodic Hapludox) and the relief is slightly undulated (Junqueira Junior et al. 2017). Semideciduous forests are

widespread across the inland portion of the Atlantic Forest biome in Southeastern Brazil (Oliveira-Filho and Fontes 2000). This forest type is characterized by up to 50% of deciduous trees, which lose their leaves to cope with the up-to-six-months dry season (IBGE 2012; Morellato and Haddad 2000; Vitória et al. 2019).

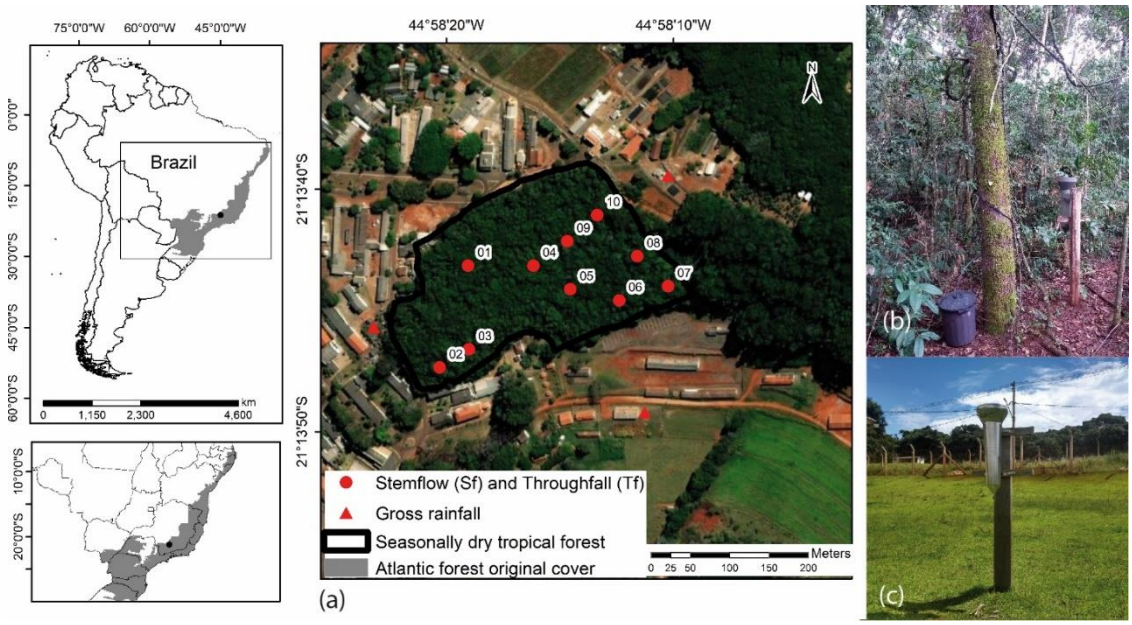

Fig. 1. Semideciduous seasonally dry tropical forest geographic location in South America and Brazil and the positions of the sampling points (GR, Tf and Sf) (a), Rain-gauge to Tf sampling and Sf collection system (b) Rain-gauge to GR sampling (c)

Forest attributes

In 2017, a forest census was carried out in the study area providing species identification and tree traits information for all trees with diameter at breast height (DBH) ≥ 5 cm. We found a forest tree density of 1021 trees.ha^{-1}, and basal area equal to 120.85 m².ha^{-1}. Among the most abundant tree species found in the area were *Xylopia brasiliensis* Spreng. (Annonaceae) (the most abundant), *Copaifera langsdorffii* Desf. (Fabaceae) (second most abundant), and *Miconia willdenowii* Klotzsch ex Naudin (Melastomataceae) (5th most abundant) (Fig 2). These species together account for more than 30% of the forest cover value index (Souza et al. 2021). In addition to the greatest abundance to our study area, *Xylopia brasiliensis*, *Copaifera langsdorffii*

and *Miconia willdenowii* are species with great population size in Southeastern region of Brazil, thus showing notable importance in local and regional scales (Goldenberg and Caddah 2015; Pontes Pires and Johnson 2020; Terra et al. 2017).

Fig. 2 Details of the crown architecture of the tree species *X. brasiliensis* (a), *C. langsdorffii* (b) and *M. willdenowii* (c). Bark roughness of trees species *X. brasiliensis* (d), *C. langsdorffii* (e) and *M. willdenowii* (f)

X. brasiliensis is an evergreen and heliophyte species of fast-growing, which diameter of 30-60 cm and height of 10-30 m in mature trees. Its wood density is about 0.70 g.cm^{-3} (Lorenzi 2016; Scolforo et al. 2017). The species shows alternated simple leaves, straight trunk, and a conical crown. *C. langsdorffii*, a deciduous and heliophyte species, is characterized by its capacity of adaptation in different vegetation type, as well as being a late secondary or light demanding climax species. The species presents a wood density of 0.70 g cm^{-3}, which classifies

the wood as moderately heavy. Usually, this species shows a dense crown, diameter ranging from 50 to 80 cm, height between 10 and 15 m, compound leaves and a furrowed-bark (Lorenzi 2016).

For the stemflow assessment, we selected 10 spatially well-distributed trees of the above-mentioned species (four *X. brasiliensis*, three *C. langsdorffii* and three *M. willdenowii*), to represent the forest characteristics (Table 1). Diameter at breast height (DBH; measured at 1.3 m aboveground), sectional area (BA), and projected crown area (CA) were obtained using metric tape (Table 1). CA was measured according to Shinzato et al. (2011) in the wet (March 2019) and dry (July 2018) periods, through eight vertical projections over the ground from the trunk to the end of the crown at 45°. After that, the eight triangles' areas obtained from the projection were calculated and summed. Tree height (H) along with bark structure (tree bark) – classified as rough (R), very-rough (VR), and smooth (S) – were determined by visual estimation (always made by the same person to prevent increasing bias).

The selected trees, which species cover approximately 30% of the forest fragment (Souza et al. 2021), have DBH ranging from 9 to 50 cm, basal area ranging from 0.01 to 0.20 m², projected crown area ranging from 4.41 to 112.74 m², height ranging from 13 to 26 m, and tree barks were classified by smooth, rough and very-rough (Table 1).

Table 1. Trees identification (ID), species classification and attributes (DBH, BA, CA, H, tree bark)

ID	Scientific name (Family)	DBH[a] (m)	BA[b] (m²)	CA[c] (m²)	H[d] (m)	Tree bark
1	*Xylopia brasiliensis* Spreng. *(Annonaceae)*	0.27	0.06	42.64	18.00	R[e]
2	*Copaifera langsdorffii* Desf.. *(Fabaceae)*	0.32	0.08	65.27	16.00	R[e]
3	*Copaifera langsdorffii* Desf. *(Fabaceae)*	0.15	0.02	16.04	15.00	VR[f]
4	*Copaifera langsdorffii* Desf. *(Fabaceae)*	0.32	0.08	95.97	21.00	VR[f]
5	*Miconia willdenowii* Klotzsch ex Naudin *(Melastomataceae)*	0.22	0.04	18.65	13.50	R[e]
6	*Miconia willdenowii* Klotzsch ex Naudin *(Melastomataceae)*	0.16	0.02	14.02	15.00	S[g]
7	*Xylopia brasiliensis* Spreng. *(Annonaceae)*	0.50	0.20	112.74	26.00	VR[f]
8	*Xylopia brasiliensis* Spreng. *(Annonaceae)*	0.11	0.01	14.33	14.00	R[e]
9	*Miconia willdenowii* Klotzsch ex Naudin *(Melastomataceae)*	0.24	0.05	20.47	14.00	S[g]
10	*Xylopia brasiliensis* Spreng. *(Annonaceae)*	0.09	0.01	4.41	13.00	S[g]

[a] diameter at 1.3 m above ground; [b] basal area; [c] average crown area considering the two measurements; [d] height; [e] roughness; [f] very roughness; [g] smooth.

Stemflow, throughfall, and gross rainfall measurements, and carbon laboratory analysis

Gross rainfall (GR), throughfall (Tf), and stemflow (Sf) were monitored and sampled from May 2018 to April 2019, totalizing sixty-one rainfall events. Due to the minimum volume necessary for lab analysis, only events greater than 4.7 mm were considered. GR was measured and sampled through three fixed Ville de Paris-type rain gauges placed outside the forest fragment (Fig. 1a and Fig. 1c). To assess the GR contribution over the forest, the Thiessen Polygon approach was considered as there are three external rain gauges (Fig. 1a). Tf was measured and sampled through ten fixed Ville de Paris-type rain gauges installed inside the forest fragment, near to the selected trees, considering 1.5 m above the forest floor in order to avoid splash-in (Fig. 1b). GR and Tf were converted to depth by dividing the collected volume (L) by the rain-gauge catchment area (m²). In a broad study of throughfall monitoring, Zimmermann and Zimmerman (2014) recommended that small collectors should be used (instead of troughs) in heterogeneous forests (such as the Atlantic Forest fragment) to better frame the spatial structure of throughfall. However, aiming to reduce costs involved with laboratory analyzes and

field measurement, we choose to install one rain gauge beside each representative tree, thus making it possible to calculate the enrichment ratios. As the enrichment ratio study is conducted by individual trees, we believe the spatial variability is not the main concern here, but the choice of trees following the dominance criteria. To monitor and sample Sf, collectors were built with a hose slit open toward the length that has been nailed in a spiral around the tree trunk and connected to a collection bin (Fig.1b). The measurements of the GR, Tf and Sf volumes were carried out with a graduated cylinder, with a precision of 10 ml.

The water samples were collected and analyzed after each rainfall event. For preservation purposes, samples were filtered with a qualitative filter paper (80g) and refrigerated at 4 ºC until lab analysis. Total dissolved carbon analyses were performed with a total carbon analyzer (TOC-VCPH) Shimadzu. This procedure consisted of inserting the samples in a combustion tube, which was filled with an oxidation catalyst and subsequently burned at a temperature of 680ºC. The total carbon was converted to carbon dioxide and quantified in a non-dispersive infrared sensor (NDIR) (Shimadzu 2003).

The maximum rainfall intensity (mm. h^{-1}) of each rainfall event was calculated using the rainfall amount and duration of each rainfall event, in the hourly steps. These data were obtained through an automatic monitoring tipping bucket rain gauge with a covered area of 324.3 cm^2 (Campbell Scientific CR10X) installed at the top of a meteorological tower (22 m) inside of the forest fragment.

Stemflow carbon enrichment ratio

We calculated the enrichment ratio to quantify the stemflow carbon funneling in relation to gross rainfall (E_{GR}) and throughfall (E_{Tf}). The enrichment ratio makes it possible to quantify the carbon funneling in trees (Levia and Germer 2015); improve the understanding of the factors that may influence carbon transport; and highlight the stemflow role in the carbon cycle. E_{GR}

and E_{Tf} were calculated for the ten selected trees (Table 1) in the sixty-one rainfall events (May 2018 to April 2019) (Levia and Herwitz 2000):

$$E_{GR} = \frac{C_{Sf} . V_{Sf}}{C_{GR} . GR. BA.}$$

$$E_{Tf} = \frac{C_{Sf} . V_{Sf}}{C_{Tf} . Tf. BA.}$$

where E_{GR} is the stemflow enrichment ratio in relation to gross rainfall (dimensionless); C_{Sf} is the stemflow carbon concentration (mg L^{-1}); V_{Sf} is the stemflow volume (L); C_{GR} is the gross rainfall carbon concentration (mg L^{-1}); GR is gross rainfall (mm); BA is tree basal area (m^2); E_{Tf} is the stemflow enrichment ratio in relation to throughfall (dimensionless); C_{Tf} is the throughfall carbon concentration (mg L^{-1}), Tf is the throughfall (mm).

Statistical analysis

We calculated descriptive statistics – mean, median, standard deviation and coefficient of variation – to total dissolved carbon concentration in GR, Tf, and Sf, and to the enrichment ratios (E_{GR} and E_{Tf}), considering rainfall events separated in dry and wet season. Differences between total dissolved carbon concentration of the dry and wet season was assessed by means paired *t*-tests. Also, we generated violin plots using the "ggplot" package in the statistical software R (version 3.6.2) (R Core Team 2018) to present the frequency distribution of carbon concentrations in Sf, Tf and the enrichment ratios (E_{GR} and E_{Tf}) of the trees. The relationships between E_{GR} and E_{Tf} for the ten trees in the sixty-one rainfall events were assessed by linear regression.

To identify the effects of tree structural features (crown area, height, tree bark), seasonality (wet and dry season, and previous dry period), and maximum rainfall intensity on the stemflow carbon enrichment ratios (E_{GR} and E_{Tf}), we made use of generalized linear models (GLMs) with multi-model inference. Generalized linear models (GLMs) allow the modeling of

response variables belonging to different probability distribution functions (e.g., Binomial, Poisson, and Gaussian) and to accommodate categorical and continuous variables as predictors (Guisan et al. 2002).

Frequency distribution of E_{GR} and E_{Tf} were checked and as long as normality was detected for both of them (Fig. A1. Histogram - Supplementary Material), our GLMs were fitted using Gaussian family and identity link-function. Log-transformation was used to standardize the independent variables. Following the multi-model inference approach, models of E_{GR} and E_{Tf} against the explanatory variables were fitted by means of the "glm" (Dobson et al. 2001) and "dredge" functions (MuMIn package; Burnham and Anderson 2002). The initial structure of the models was as it follows

Log (EGR) ~ Bark + log(I) + Season + log(PDP) + log(Height) + log(CA)

Log (ETf) ~ Bark + log(I) + Season + log(PDP) + log(Height) + log(CA)

All possible models were ranked based on the Akaike Information Criterion of the Second Order (AICc), value. Models with $\Delta AICc < 2$ were considered equally suitable (Burnham and Anderson 2002). The final model coefficients were the average of the best models, considering only the predictors that appeared in the suitable models. The final model and the significance (p-values < 0.05 were considered significant) of the selected variables were obtained using the "model.avg" function of MuMin package. All the analyses were performed in the software R (version 3.6.2) (R Core Team 2018). The models selected by $\Delta AICc < 2$ criterium and the average coefficients are presented in Supplementary Materials (Tables A5) and in Tables 2 and 3.

Results

Carbon concentration and stemflow enrichment ratio

During the study period Sf, Tf, and, GR were measured, sampled, and analyzed after sixty-one rainfall events, totaling 1536.5 mm (ranging from 4.7 to 152.8 mm) of gross rainfall, being 14 rainfall events in the dry season (221.6 mm), and 47 in the wet season (1314.9 mm) (Supplementary Material Table A1). Considering the average of ten rain-gauges, Tf summed 1246.8 mm, being 1067.6 mm in the wet season and 179.3 mm in the dry season. Average Sf summed 3.2 mm, being 2.7 mm in the wet season and 0.5 mm in the dry season. The total carbon input via gross rainfall was 104.13 $kg.ha^{-1}$;191.97 $kg.ha^{-1}$ in throughfall; and 1.21 $kg.ha^{-1}$ in stemflow, which approximately 75% was observed in the wet season (Mantovani et al., 2021).

The total dissolved carbon concentrations were higher in the dry season than in the wet season, considering Tf (p-value < 0.05) and Sf (p-value < 0.05). Besides, they were higher in Sf than in Tf (p-value < 0.05) (Supplementary Material Table A1 and Table A2). GR, Tf, and Sf carbon concentration, considering all samples, ranged from 2.50 to 22.94 mg L^{-1}, from 4.83 to 150.40 mg L^{-1}, and from 6.77 to 276.60 mg L^{-1}, respectively. The average GR carbon concentration was 7.65 $\pm$ 4.38 mg L^{-1}, over the entire period. It was 9.99 $\pm$ 6.59 mg L^{-1} in the dry season, and 6.95 $\pm$ 3.25 mg L^{-1} in the wet season. The coefficient of variation was higher in the dry season (Supplementary Material Table A1). The Tf and Sf carbon concentration statistics were calculated considering all the rainfall events for each Tf/Sf location (Fig. 1). Tf carbon concentration average value considering all Tf location in the entire period ranged from 14.67 $\pm$ 11.22 to 29.42 $\pm$ 24.04 mg L^{-1}; in the dry season, the average ranged from 24.41 $\pm$ 19.99 to 45.23 $\pm$ 42.19 mg L^{-1}; and in wet season, from 11.97 $\pm$ 4.78 to 24.72 $\pm$ 12.34 mg L^{-1}. Sf carbon concentration average value, considering all tree location, ranged from 24.28 $\pm$ 21.72 to 65.05 $\pm$ 33.21 mg L^{-1} in the entire period, whereas in the dry season, varied from 43.33 $\pm$ 38.71 to 84.00 $\pm$ 80.35 mg L^{-1}; and in wet season, ranged from 19.31 $\pm$ 10.46 to 62.26 $\pm$ 28.14 mg L^{-1}. The coefficient of variation was higher in the dry season than in the wet season considering all Tf

and Sf location. The general data distribution of GR, Tf and Sf total dissolved carbon concentration showed high variability between the dry (14 rainfall events) and wet (47 rainfall events) seasons (Fig. 3 and Fig. 4) and was observed that the carbon concentration for both Tf and Sf showed higher values in the dry season.

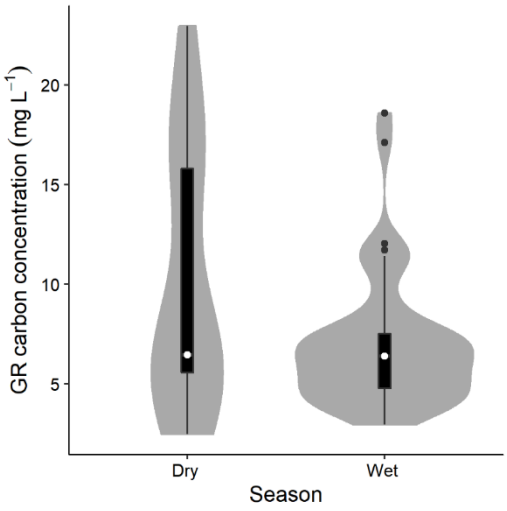

Fig. 3 Violin plots showing data distribution of GR total dissolved carbon concentration (mg L^{-1}) in the dry (a and b) and wet (c and d) seasons. The dry and wet seasons encompass 14 and 47 rainfall events, respectively. The gray shade represents the full carbon concentration data distribution (kernel density plot), the white dots represent the median, the black-boxes are box-plots with the 25, 50 and 75 quartiles, and the black dots represents the outlier data.

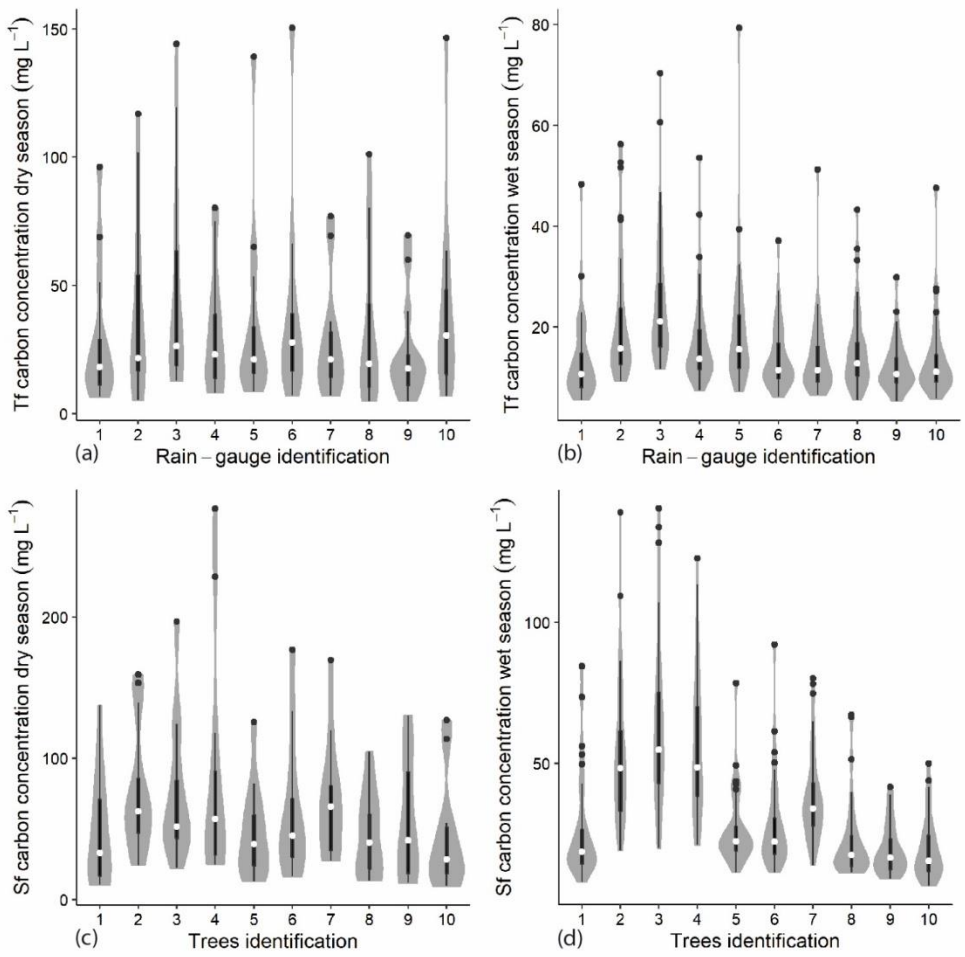

Fig. 4 Violin plots showing data distribution of Tf and Sf total dissolved carbon concentration (mg L^{-1}) in the dry (a and b) and wet (c and d) seasons. The dry and wet seasons encompass 14 and 47 rainfall events, respectively. The gray shade represents the full carbon concentration data distribution (kernel density plot), the white dots represent the median, the black-boxes are box-plots with the 25, 50 and 75 quartiles, and the black dots represents the outlier data.

Violins more stretched show a greater distribution of data over the entire concentration range, especially for Tf (ID 2, 3 and 10) in the dry season, and Sf (ID 2, 3 and 4: *C. langsdorffii*. trees) in the wet season. More flattened violins represent a higher concentration of data around the median. We observed that the carbon concentrations in Tf and Sf showed great variability in relation to the Tf location (especially in the dry season), and trees (especially in the wet season).

The variability of Sf enrichment ratio in relation to gross rainfall (E_{GR}) and to throughfall (E_{TF}) was substantial for any given tree across both seasons, dry (14 rainfall events) and wet (47

rainfall events), and the entire period (sixty-one rainfall events) (Supplementary Material: Table A3 and A4). As to the E_{GR} and E_{TF}, among all tree species, the *C. langsdorffii* (ID:3) showed the highest values of mean (wet season), and the *M. willdenowii* (ID:9) presented the smallest value of mean (wet season) (Table A3 – Supplementary Material). The enrichment ratios (E_{GR} and E_{Tf}) were highly variable within and among tree species and seasons (Fig. 5 and Fig. 6).

As concern to the stemflow enrichment ratio relative to Tf (E_{Tf}) and to GR (E_{GR}), we found a correlation as E_{Tf} linearly increased with increasing E_{GR} (Fig. A2 – Supplementary Material). These relationships were observed by analyzing the E_{Tf} and E_{GR} for each individual tree, with R^2 ranged from 0.688 to 0.933 (Supplementary Material: Fig. A3 a to A3j).

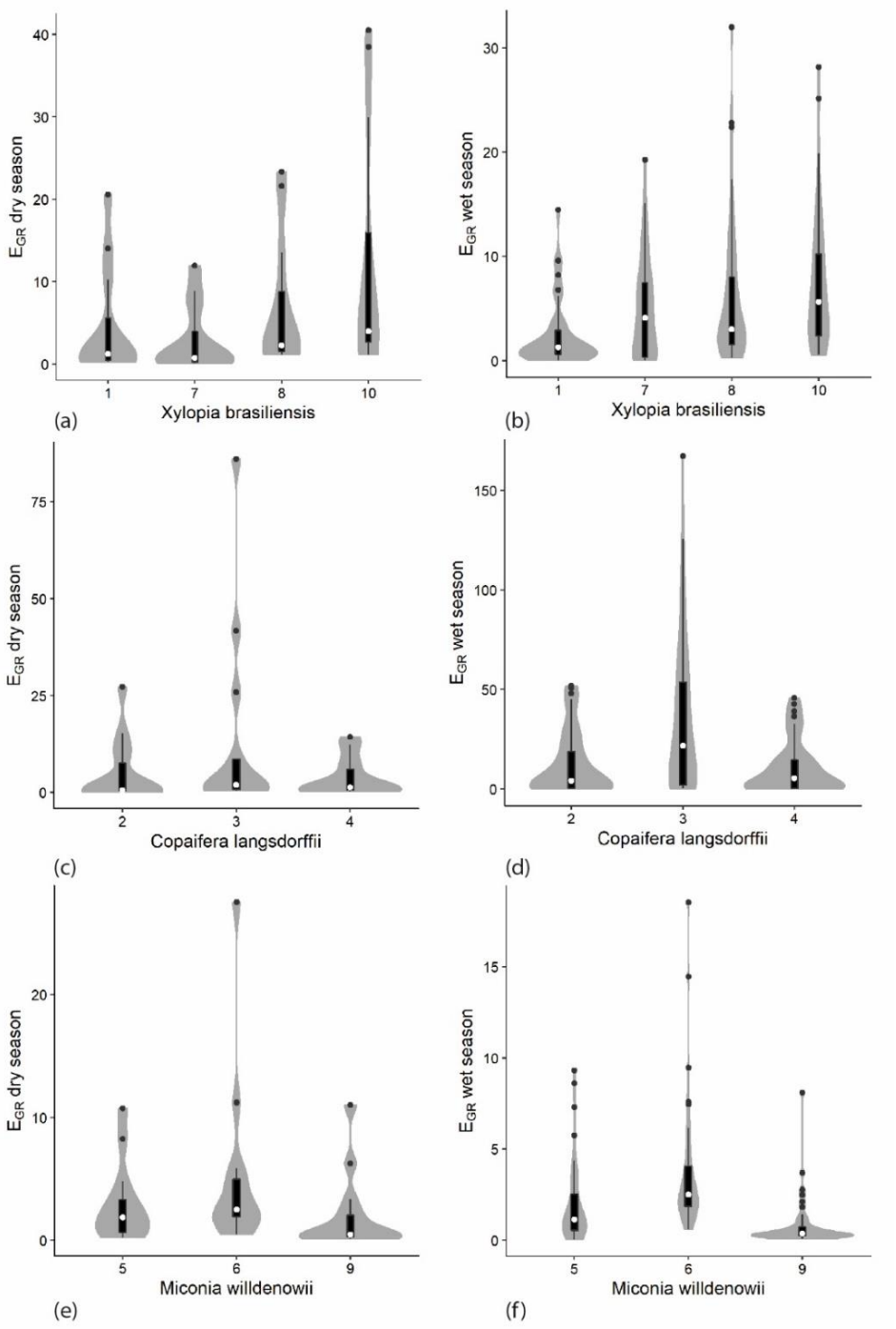

Fig. 5. Violin plots showing E_{GR} data distribution of three studied species, considering the dry (14 rainfall events) and wet (47 rainfall events) seasons: *Xylopia brasiliensis* (a and b), *Copaifera langsdorffii* (c and d), *Miconia willdenowii* (e and f). The gray shade represents the full carbon concentration data distribution (kernel density plot), the white dots represent the median, the black-boxes is are box-plots with the 25, 50 and 75 quartiles, and the black dots represents the outlier data

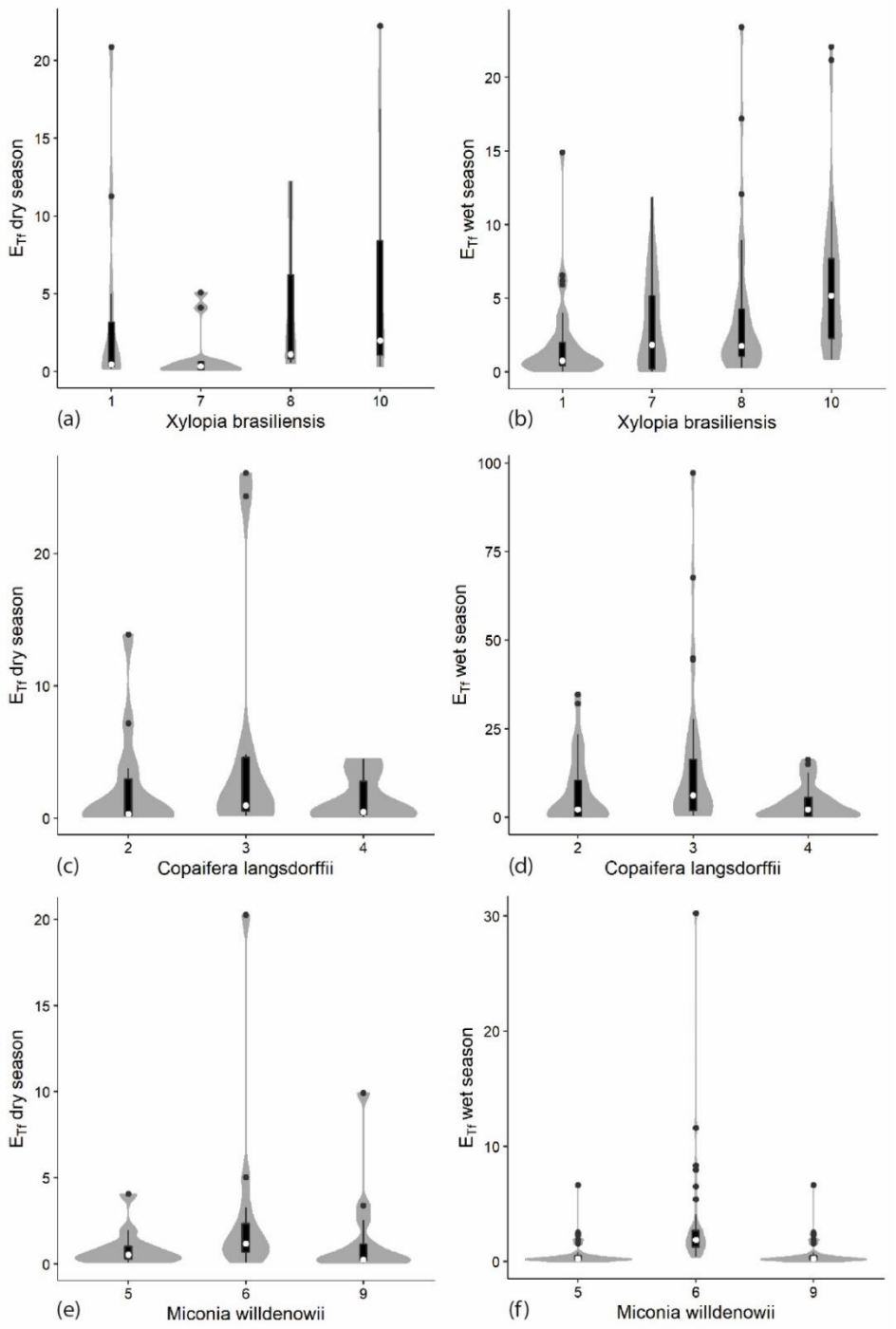

Fig. 6. Violin plots showing E_{Tf} data distribution of three studied species, considering the dry (14 rainfall events) and wet (47 rainfall events) seasons: *Xylopia brasiliensis* (a and b), *Copaifera langsdorffii* (c and d), *Miconia willdenowii* (e and f). The gray shade represents the full carbon concentration data distribution (kernel density plot), the white dots represent the median, the black-boxes is are box-plots with the 25, 50 and 75 quartiles, and the black dots represents the outlier data

Effects of biotic and abiotic drivers on stemflow enrichment ratio

Generalized linear models indicated roughly the same predictors as significants for E_{GR} and E_{Tf} (Fig. 7; Table A5 – Supplementary material). Season, maximum rainfall intensity, projected crown area, and tree bark were significant drivers for both enrichment ratios (E_{GR} and E_{Tf}), and tree height was significant for E_{Tf} (see Fig A4 - Supplementary material with the graphic relation between enrichment ratios (E_{GR} and E_{Tf}) and each non-categorical variable - I, CA, height and PDP).

The very-rough bark, maximum rainfall intensity, projected crown area, and smooth-bark showed higher magnitude effects on E_{GR} with average coefficients > 0.75, followed by wet season (> 0.5). The very-rough bark and maximum rainfall intensity showed a positive correlation with E_{GR}, and projected canopy area, smooth-bark and wet season had a negative correlation (Table 2).

Tree height, projected crown area, and maximum rainfall intensity showed higher magnitude effects on E_{Tf}, with average coefficients > 0.75, followed by very-rough bark, smooth-bark, and wet season (> 0.45). The tree height, maximum rainfall intensity, and very-rough bark had a positive correlation with $E_{Tf,}$ and projected canopy area, smooth bark, and wet season had a negative correlation (Table 3).

Table 2. Model-average coefficients for the relation between stemflow enrichment rate (E_{GR}) and the biotic and abiotic drivers

	Estimate	Std. Error	Adjusted SE	z value	Pr(>|z|)	Signif. Codes
(Intercept)	1.87174	0.95256	0.95521	1.96	5.01E-02	.
BarkS	-0.78086	0.19932	0.19992	3.906	9.39E-05	***
BarkVR	1.1713	0.19286	0.19344	6.055	< 2e-16	***
log(I)	0.93206	0.08499	0.08525	10.933	< 2e-16	***
log(CA)	-0.80322	0.11924	0.11958	6.717	< 2e-16	***
SeasonW	-0.66313	0.20665	0.20727	3.199	1.38E-03	**
log(PDP)	0.08878	0.08288	0.08313	1.068	2.86E-01	
log(Height)	0.35037	0.85254	0.85514	0.41	6.82E-01	

BarkS = smooth bark, BarkVR = very rough bark, I = maximum rainfall intensity, CA = projected canopy area, SeasonW = Wet season, PDP = previous dry period, Height)

Table 3 Model-average coefficients for the relation between stemflow enrichment rate (E_{Tf}) and the biotic and abiotic drivers

	Estimate	Std. Error	Adjusted SE	z value	Pr(>|z|)	Signif. Codes
(Intercept)	-2.99964	1.80955	1.81513	1.653	9.84E-02	.
BarkS	-0.60475	0.20064	0.20125	3.005	2.66E-03	**
BarkVR	0.70196	0.22043	0.22111	3.175	1.50E-03	**
log(Height)	1.91365	0.81873	0.82125	2.33	0.0198	*
log(I)	0.91021	0.08099	0.08124	11.204	< 2e-16	***
log(CA)	-1.05131	0.1683	0.16882	6.227	< 2e-16	***
SeasonW	-0.46829	0.20141	0.20203	2.318	2.05E-02	*
log(PDP)	0.03651	0.07993	0.08018	0.455	6.49E-01	

BarkS = smooth bark, BarkVR = very rough bark, Height, I = maximum rainfall intensity, CA = projected canopy area, SeasonW = Wet season, PDP = previous dry period)

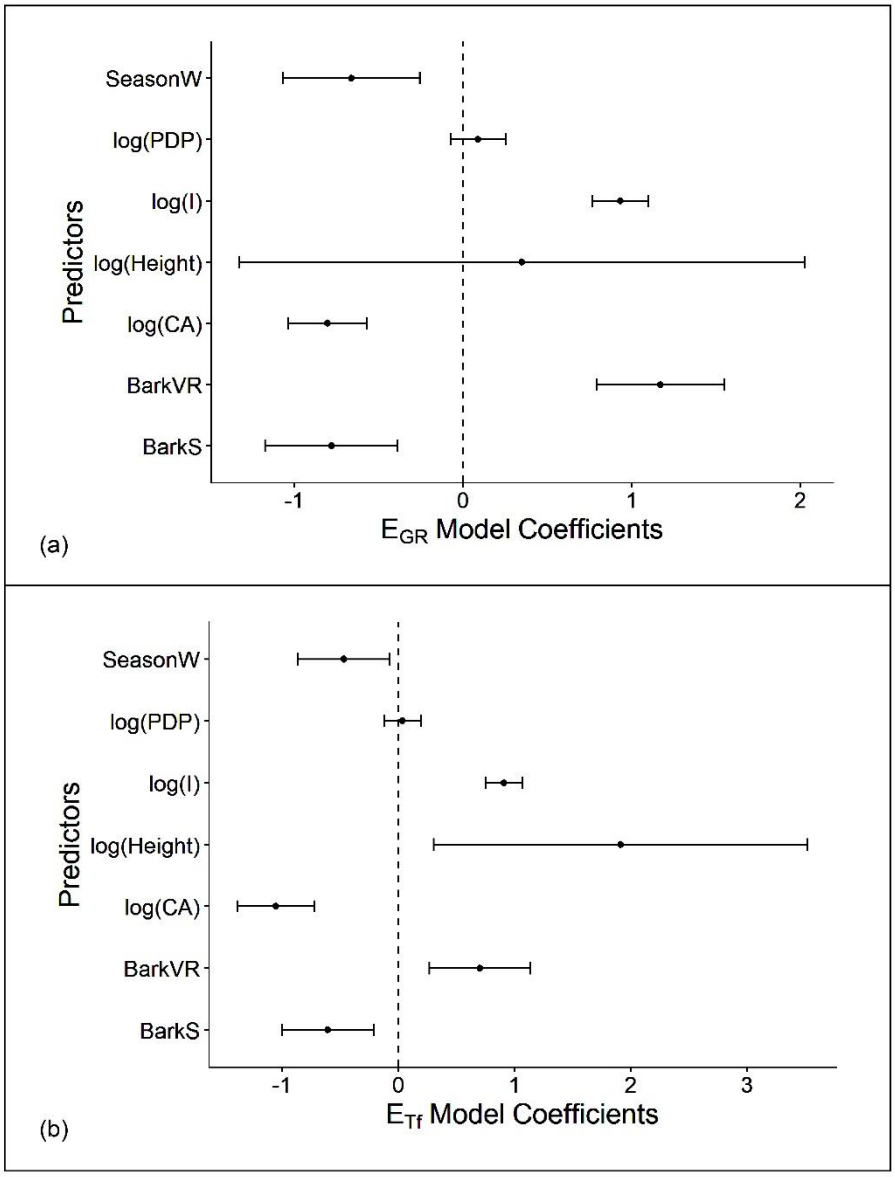

Fig. 7. Relationship between the enrichment ratios (a) E_{GR} and (b) E_{Tf} and predictors (SeasonW = Wet season, PDP = previous dry period, I = maximum rainfall intensity, CA = projected canopy area, Height, BarkVR = very rough bark, BarkS = smooth bark). The black dots represent the estimated model coefficients and the horizontal bars the confidence interval. The significant variables do not touch the dotted vertical line.

Discussion

Overall, the total dissolved carbon concentrations were higher in the dry season than in the wet season, and higher in Sf than in Tf and GR (Fig. 8). There was a linear correlation between the stemflow enrichment ratio relative to Tf (E_{Tf}) and the stemflow enrichment ratio relative to GR (E_{GR}). The biotic and abiotic drivers were significant to the total carbon stemflow enrichment ratios. Our findings demonstrate the role of the stemflow as a relevant source of carbon input in a tropical forest fragment, highlighting that this process is mainly affected by season, maximum rainfall intensity, projected crown area (CA), and tree bark (Fig. 8).

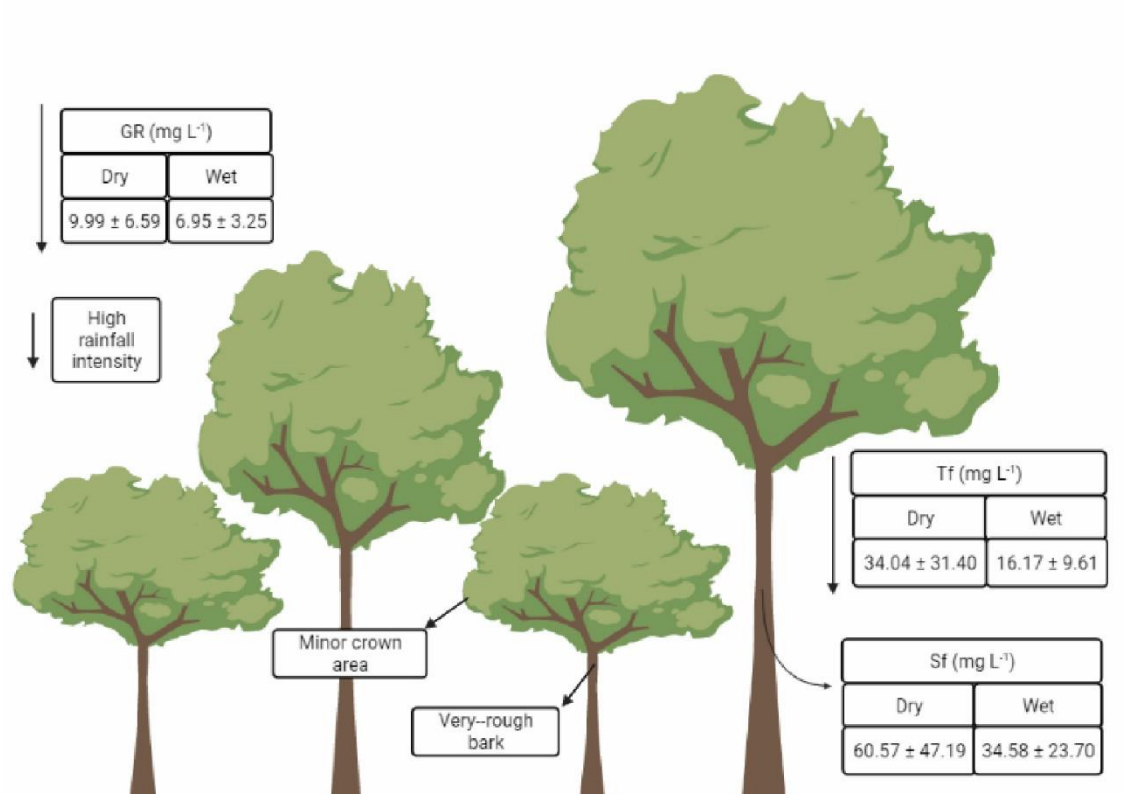

Fig. 8. Summary of the main results: total carbon concentration on the gross rainfall (GR), throughfall (Tf), and stemflow (Sf), considering the average values in the dry and wet season, and the biotic and abiotic drivers responsible to increase the stemflow carbon enrichment ratio.

Carbon concentration in stemflow was higher than in throughfall and gross rainfall, and higher in the dry season than in the wet season, which corroborates with previous studies carried

out in tropical (Ciglasch et al. 2004; Lilienfein and Wilcke 2004; Goller et al. 2006) and temperate forests (Limpert and Siegert 2019; You et al. 2020). The average duration of the previous dry period was four days in the wet season and fifteen days in the dry season, thus, the absence of continuous rainfall events in the dry season provided accumulation of carbon atmospheric deposition in the crowns, trunks, and leaves, and consequently increased the total carbon concentrations (Neu et al. 2016; You et al. 2020). However, the rainfall amount was responsible for the highest inputs, being the wet season responsible for almost 75% of the total carbon input via throughfall and stemflow to the forest floor in the studied period (Mantovani et al., 2021).

The mean stemflow carbon enrichment ratios observed in this study for *X. brasiliensis*, *C. langsdorffii*, and *M. willdenowii* relative to GR (ratios ranging from 1 to 30) in a seasonally dry tropical forest were lower than those observed in a mixed cedar swamp in Ontario, Canada (16 to 68) (Duval et al. 2019), in an Oak-Hickory Forest in Mississippi, EUA (6 to 122) (Limpert and Siegert 2019), in an evergreen broad-leafed in Mt. Kinka, Japan (53 to 87) (Chen et al. 2019), and in a temperate forest (sugar maple and yellow birch trees) in New England region of the USA (110 and 122) (Ryan et al. 2021). Considering the mean stemflow carbon enrichment ratios relative to throughfall, the mean values of this study (0.8 to 11) were similar to those observed for Duval et al. (2019) (2 to 9), but lower than observed for Ryan t al. (2021) (17 to 20). The lower values of enrichment rates found in our study may be associated with the higher carbon concentration in gross rainfall than other studies, such as Duval et al. (2019) and Ryan et al. (2021). The higher carbon concentration is probably due to the presence of important sources of carbon like agricultural activities and fires in the surroundings (Neu et al., 2016; Mantovani et al., 2021). Additionally, we considered the inorganic portion of the carbon in the analysis, which wasn't considered in other studies. The frequent rainfall and the occurrence of large rainfall

amounts, typically for tropical regions, could influence the lower stemflow carbon concentration values when compared to temperate regions due to the stay time of the carbon deposited in these forests (Duval et al., 2019; Ryan et al., 2021). The enrichment rates allow identifying that the forest soil near the base of the trees receives more carbon than inputs via gross rainfall and throughfall. Throughfall and stemflow are important carbon inputs into forest soil due to the frequency and high rate of deposition, especially in the wet season. They influence litter decomposition, carbon availability, and reincorporation into the system (Qualls, 2020; Aubrey, 2020).

Previous studies have examined the stemflow solute enrichment rates, and some studies have associated the solutes enrichments with driving factors including trees species, trees traits, meteorological conditions, and rainfall characteristics (Andre et al. 2008; Levia et al. 2011b; Schooling et al. 2017; Siegert et al. 2017; Liu et al. 2019; Dowtin et al. 2020; Tonello et al. 2021a). Considering the stemflow carbon enrichment ratios, the studies that connecting them with specific tree traits are even more scarce (Limpert and Siegert 2019; Chen et al. 2019; Ryan et al. 2021), especially in tropical forests. In this study, the stemflow carbon enrichment ratios (E_{GR} and E_{Tf}) were driven by biotic and abiotic characteristics. Biotic drivers associated with stemflow carbon enrichment rates in our study were tree bark structure and crown area, and abiotic drivers were season and maximum rainfall intensity. Tree height was significant only for stemflow carbon enrichment ratios in relation to throughfall. The longest water pathway on tree stems provides more carbon leaching. This tree trait is known as one of the main boosters of stemflow in tropical forests (Terra et al. 2018).

Previous studies have shown that smaller trees are more effective in the process of rainfall funneling (Siegert and Levia 2014; Su et al. 2016), and the same occurs with the solute enrichment ratio, smaller trees were able to supply more solutes per unit of trunk basal area

(Chen et al. 2019; Schooling et al. 2017, Liu et al. 2019; Su et al. 2016). In our study area, smaller crowns trees were more effective in stemflow carbon enrichment (projected crown area had a negative correlation), leading to a greater carbon input into the soil. This is probably associated with a greater ability of smaller trees to funnel rainwater, being more efficient to leach dry deposition and the organic matter present in trees, increasing the carbon that reaches the forest floor (Terra et al. 2018; Chen et al. 2019). Additionally, the stratified canopy can affect, as smaller trees eventually receive rainwater that drips from taller ones, located in an emergent layer, which brings a greater amount of carbon, and when reach the smaller crowns can further increase the concentration.

Very-rough bark and smooth-bark showed, respectively, positive and negative correlation with the enrichment ratios. In our study, trees with smooth-bark generated smaller stemflow volumes per event than very-rough bark trees. This is contrary to what has been observed by other authors. For instance, a previous study in the Brazilian Cerrado found that trees with smooth bark drain more rainwater when compared with rough bark trees (Tonello et al., 2021b). On the other hand, trees with a rougher bark retained more water during stemflow, increasing the leaching of compounds and generating a more concentrated flow of nutrients (Parker 1983; Levia et al. 2012; Limpert and Siegert 2019). These aspects explain the higher enrichment ratio in trees with very-rough bark.

Considering the abiotic drivers, maximum rainfall intensity was positively correlated and more significant for the dynamics of carbon inputs into the forest floor than the wet season variable (Table 2 and Table 3). The negative influence of the wet season in both enrichment ratios can be linked to a lower carbon accumulation from dry deposition. The average interval between rainfall events in the wet season is four days, with more frequent and large rainfall events, the carbon concentration tends to be diluted. Maximum rainfall intensity ranged from

0.76 mm h^{-1} (dry season) to 29.21 mm h^{-1} (wet season), and previous studies evidenced that there is no consensus, i.e., stemflow can be positively and negatively influenced by rainfall intensity (Chen et al., 2019; Van Stan et al., 2014; Staelens et al., 2008; Levia et al., 2010). The positive correlation between stemflow carbon enrichment ratio and maximum rainfall intensity was likely due to an increase in the carbon leaching present in leaves, branches and stems of the trees.

Therefore, the synergistic action of both abiotic and biotic factors drives the carbon enrichment ratio in our studied forest stand. Our findings represent an advance in the understanding of the stemflow role in forest carbon cycle and were useful to indicate that tree's structural features and meteorological conditions have an important role to deliver carbon from the atmosphere and canopy to the forest floor. For instance, tree structural features, like very-rough bark and smaller crown area, provide higher carbon enrichment rates, and consequently, more carbon reaches the forest floor. Moreover, it is important to investigate the carbon dynamic in the stemflow, to better understand the contribution from rainfall on the carbon inputs into forest soil.

From our findings, a holistic understanding about the biotic and abiotic factors that influence the stemflow carbon enrichment is provided. Also, our study reinforces the importance of the tropical forest and rainfall interactions to the ecohydrological processes in a climate-changing world. A comprehensive understanding of each influencing variable in stemflow carbon enrichment ratio may aid in the modeling of carbon and water fluxes by stemflow and in selecting trees based on structural features for increasing soil carbon inputs.

Conclusion

We investigated carbon enrichment in stemflow in sixty-one individual rainfall events for ten trees of the three most abundant species, with different DBH. The stemflow carbon concentration was higher in the dry season, however, the highest rainfall amount in the wet season provided higher carbon inputs. The stemflow carbon enrichment was influenced by trees

structural features and meteorological condition. Also, we concluded that trees with very-rough bark and smaller crown area during events with higher rainfall intensity can provide more carbon input via stemflow to the forest floor. Studies that aim to identify tree species with structural features that boost carbon enrichment rates are scarce, especially in tropical forests.

Our findings expand our perception of the role played by trees in carbon cycling. Trees not only contribute to carbon storage and uptake and return the carbon to the soil and to the atmosphere via decomposition and eventual burning. They are frequently washed by the rainwater and this process contributes to carbon inputs in the forest soil. This information might be useful to decision making in forest conservation, restoration, and management, highlighting the role of small tropical forest fragments in climate change, and making it possible to select tree species (or traits) more capable of delivering carbon to the forest floor.

References

Alves LF, Vieira SA, Scaranello MA, et al (2010) Forest structure and live aboveground biomass variation along an elevational gradient of tropical Atlantic moist forest (Brazil). For Ecol Manage 260:679–691. https://doi.org/10.1016/j.foreco.2010.05.023

Anderegg WRL, Trugman AT, Badgley G, et al (2020) Divergent forest sensitivity to repeated extreme droughts. Nat Clim Chang 10:1091–1095. https://doi.org/10.1038/s41558-020-00919-1

André F, Jonard M, Ponette Q (2008) Effects of biological and meteorological factors on stemflow chemistry within a temperate mixed oak-beech stand. Sci Total Environ 393:72–83. https://doi.org/10.1016/j.scitotenv.2007.12.002

Brando PM, Paolucci L, Ummenhofer CC, et al (2019) Droughts, Wildfires, and Forest Carbon Cycling: A Pantropical Synthesis. Annu Rev Earth Planet Sci 47:555–581. https://doi.org/10.1146/annurev-earth-082517-010235

Burnham KP, Anderson DR (2002) Model Selection and Multimodel Inference: A Practical Information-Theoretic Approach

Carmo JB do, de Sousa Neto ER, Duarte-Neto PJ, et al (2012) Conversion of the coastal Atlantic forest to pasture: Consequences for the nitrogen cycle and soil greenhouse gas emissions. Agric Ecosyst Environ 148:37–43. https://doi.org/10.1016/j.agee.2011.11.010

Chen S, Cao R, Yoshitake S, Ohtsuka T (2019) Stemflow hydrology and DOM flux in relation to tree size and rainfall event characteristics. Agric For Meteorol 279:. https://doi.org/10.1016/j.agrformet.2019.107753

Ciglasch H, Lilienfein J, Kaiser K, Wilcke W (2004) Dissolved organic matter under native Cerrado and Pinus caribaea plantations in the Brazilian savanna. Biogeochemistry 67:157–182. https://doi.org/10.1023/B:BIOG.0000015281.74705.f8

Dobson AJ (2001) An introduction to Generalized Linear Models, 2nd edn. Chapman & Hall/CRC, USA

Dowtin AL, Siegert CM, Levia DF (2020) Comparisons of flux-based stemflow enrichment ratios for two Quercus spp. within the megalopolis of the eastern USA. Urban Ecosyst. https://doi.org/10.1007/s11252-020-01064-5

Duval TP (2019) Rainfall partitioning through a mixed cedar swamp and associated C and N fluxes in Southern Ontario, Canada. Hydrol Process 33:1510–1524. https://doi.org/10.1002/hyp.13414

Germer S, Werther L, Elsenbeer H (2010) Have we underestimated stemflow? Lessons from an open tropical rainforest. J Hydrol 395:169–179. https://doi.org/10.1016/j.jhydrol.2010.10.022

Germer S, Zimmermann A, Neill C, et al (2012) Disproportionate single-species contribution to canopy-soil nutrient flux in an Amazonian rainforest. For Ecol Manage 267:40–49.

https://doi.org/10.1016/j.foreco.2011.11.041

Goldenberg R, Caddah MK (2015) Miconia in Lista de Espécies da Flora do Brasil. Jardim Botânico do Rio de Janeiro. Available at: <http://floradobrasil.jbrj.gov.br/jabot/floradobrasil/FB9779>. Accessed in: July 20, 2021.

Goller R, Wilcke W, Fleischbein K, et al (2006) Dissolved nitrogen, phosphorus, and sulfur forms in the ecosystem fluxes of a montane forest in Ecuador. Biogeochemistry 77:57–89. https://doi.org/10.1007/s10533-005-1061-1

Guisan A, Edwards TC, Hastie T (2002) Generalized linear and generalized additive models in studies of species distributions: setting the scene. Ecol Modell 157:89–100. https://doi.org/10.1016/S0304-3800(02)00204-1

Harris NL, Gibbs DA, Baccini A, et al (2021) Global maps of twenty-first century forest carbon fluxes. Nat Clim Chang 11:234–240. https://doi.org/10.1038/s41558-020-00976-6

Herwitz SR (1986) Infiltration-excess caused by Stemflow in a cyclone-prone tropical rainforest. Earth Surf Process Landforms 11:401–412. https://doi.org/10.1002/esp.3290110406

IBGE (2012) Manual Técnico da Vegetação Brasileira, 2nd edn. Rio de Janeiro

INMET - Instituto Nacional de Meteorologia, 2018. Normais climatológicas do Brasil 1981-2010. Available at: https://portal.inmet.gov.br/normais Accessed 8 August 2018

Johnson MS, Lehmann J (2006) Double-funneling of trees: Stemflow and root-induced preferential flow. Ecoscience 13:324–333. https://doi.org/10.2980/i1195-6860-13-3-324.1

Joly CA, Metzger JP, Tabarelli M (2014) Experiences from the Brazilian Atlantic Forest: Ecological findings and conservation initiatives. New Phytol 204:459–473. https://doi.org/10.1111/nph.12989

Junqueira Junior JA, de Mello CR, de Mello JM, et al (2019) Rainfall partitioning

measurement and rainfall interception modelling in a tropical semi-deciduous Atlantic forest remnant. Agric For Meteorol 275:170–183. https://doi.org/10.1016/j.agrformet.2019.05.016

Junqueira Junior JA, Mello CR, Owens PR, et al (2017) Time-stability of soil water content (SWC) in an Atlantic Forest - Latosol site. Geoderma 288:64–78. https://doi.org/10.1016/j.geoderma.2016.10.034

Klamerus-Iwan A, Link TE, Keim RF, Van Stan II JT (2020) Storage and Routing of Precipitation Through Canopies. In: Van Stan, II JT, Gutmann E, Friesen J (eds) Precipitation Partitioning by Vegetation. Springer International Publishing, Switzerland.

Levia DF, Frost EE (2003) A review and evaluation of stemflow literature in the hydrologic and biogeochemical cycles of forested and agricultural ecosystems. J Hydrol 274:1–29. https://doi.org/10.1016/S0022-1694(02)00399-2

Levia DF, Germer S (2015) A review of stemflow generation dynamics and stemflow-environment interactions in forests and shrublands. Rev Geophys 53:673–714. https://doi.org/10.1002/2015RG000479

Levia DF, Herwitz SR (2000) Physical properties of water in relation to stemflow leachate dynamics: Implications for nutrient cycling. Can J For Res 30:662–666. https://doi.org/10.1139/cjfr-30-4-662

Levia DF, Keim RF, Darryl E. Carlyle-Moses A, Frost EE (2011a) Throughfall and Stemflow in Wooded Ecosystems. In: Forest hydrology and biogeochemistry, Synthesis of past research and future directions

Levia DF, Van Stan JT, Siegert CM, et al (2011b) Atmospheric deposition and corresponding variability of stemflow chemistry across temporal scales in a mid-Atlantic broadleaved deciduous forest. Atmos Environ 45:3046–3054.

https://doi.org/10.1016/j.atmosenv.2011.03.022

Levia DF, Van Stan JT, Inamdar SP, et al (2012) Stemflow and dissolved organic carbon cycling : temporal variability in concentration , flux , and UV- Vis spectral metrics in a temperate broadleaved deciduous forest in the eastern United States. 216:207–216. https://doi.org/10.1139/X11-173

Lilienfein J, Wilcke W (2004) Erratum: Water and element input into native, agri- And silvicultural ecosystems of the Brazilian savanna (Biogeochemistry 67 (183-212)). Biogeochemistry 68:131–133. https://doi.org/10.1023/B:BIOG.0000025925.56087.8e

Limpert K, Siegert C (2019) Interspecific Differences in Canopy-Derived Water, Carbon, and Nitrogen in Upland Oak-Hickory Forest. Forests 10:1121. https://doi.org/10.3390/f10121121

Liu CP, Sheu BH (2003) Dissolved organic carbon in precipitation, throughfall, stemflow, soil solution, and stream water at the Guandaushi subtropical forest in Taiwan. For Ecol Manage 172:315–325. https://doi.org/10.1016/S0378-1127(01)00793-9

Liu Y, Jiang L, You C, et al (2019) Base cation fluxes from the stemflow in three mixed plantations in the rainy zone of Western China. Forests 10:1–13. https://doi.org/10.3390/F10121101

Lorenzi H (2016) Árvores Brasileiras. Manual de Identificação e Cultivo de Plantas Arbóreas Nativas do Brasil - Volume 2. Instituto Plantarum, São Paulo

Mellec A, Meesenburg H, Michalzik B (2010) The importance of canopy-derived dissolved and particulate organic matter (DOM and POM) — comparing throughfall solution from broadleaved and coniferous forests. Ann For Sci 67:411–411. https://doi.org/10.1051/forest/2009130

Michalzik B, Kalbitz K, Park JH, et al (2001) Fluxes and concentrations of dissolved organic

carbon and nitrogen - A synthesis for temperate forests. Biogeochemistry 52:173–205. https://doi.org/10.1023/A:1006441620810

Morellato PC, Haddad CFB (2000) Introduction: the Brazilian Atlantic Forest. Biotropica 32:786–792. https://doi.org/10.1111/j.1744-7429.2000.tb00618.x

Neu V, Ward ND, Krusche A V, Neill C (2016) Dissolved organic and inorganic carbon flow paths in an amazonian transitional forest. Front Mar Sci 3:1–15. https://doi.org/10.3389/fmars.2016.00114

Oliveira-Filho AT, Fontes MAL (2000) Patterns of floristic differentiation among atlantic forests in southeastern Brazil and the influence of climate. Biotropica 32:793–810. https://doi.org/10.1111/j.1744-7429.2000.tb00619.x

Parker GG (1983) Throughfall and Stemflow in the Forest Nutrient Cycle

Pontes Pires AF, Johnson D (2020) Xylopia in Flora do Brasil 2020. Jardim Botânico do Rio de Janeiro. Available at: <http://reflora.jbrj.gov.br/reflora/floradobrasil/FB110560>. Accessed in: July 20, 2021

R Development Core Team. (2018) R: a language and environment for statistical computing. R Foundation for Statistical Computing, Vienna. http://www.R-project.org/.

Ribeiro MC, Metzger JP, Martensen AC, et al (2009) The Brazilian Atlantic Forest: How much is left, and how is the remaining forest distributed? Implications for conservation. Biol Conserv 142:1141–1153. https://doi.org/10.1016/j.biocon.2009.02.021

Rodrigues AF, Mello CR de, Nehren U, et al (2021) Modeling canopy interception under drought conditions: The relevance of evaporation and extra sources of energy. J Environ Manage 292:112710. https://doi.org/10.1016/j.jenvman.2021.112710

Ryan KA, Adler T, Chalmers A, et al (2021) Event Scale Relationships of DOC and TDN Fluxes in Throughfall and Stemflow Diverge From Stream Exports in a Forested

Catchment. J Geophys Res Biogeosciences 126:1–23. https://doi.org/10.1029/2021jg006281

Sadeghi SMM, Gordon DA, Van Stan II JT (2020) A Global Synthesis of Throughfall and Stemflow Hydrometeorology. In: Van Stan, II JT, Gutmann E, Friesen J (eds) Precipitation Partitioning by Vegetation. Springer International Publishing, Switzerland.

Schooling JT, Levia DF, Carlyle-Moses DE, et al (2017) Stemflow chemistry in relation to tree size: A preliminary investigation of eleven urban park trees in British Columbia, Canada. Urban For Urban Green 21:129–133. https://doi.org/10.1016/j.ufug.2016.11.013

Schrumpf M, Zech W, Lehmann J, Lyaruu HVC (2006) TOC, TON, TOS and TOP in rainfall, throughfall, litter percolate and soil solution of a montane rainforest succession at Mt. Kilimanjaro, Tanzania. Biogeochemistry 78:361–387. https://doi.org/10.1007/s10533-005-4428-4

Scolforo HF, Scolforo JRS, Thiersch CR, et al (2017) A new model of tropical tree diameter growth rate and its application to identify fast-growing native tree species. For Ecol Manage 400:578–586. https://doi.org/10.1016/j.foreco.2017.06.048

Shimadzu, 2003. TOC-VCPH/CPN & TOC-Control V Software User Manual. 384.

Shinzato ET, Tonello KC, Gasparoto EAG, Valente ROA (2011) Escoamento pelo tronco em diferentes povoamentos florestais na Floresta Nacional de Ipanema em Iperó , Brasil. Sci For 39:395–402

Siegert CM, Levia DF (2014) Seasonal and meteorological effects on differential stemflow funneling ratios for two deciduous tree species. J Hydrol 519:446–454. https://doi.org/10.1016/j.jhydrol.2014.07.038

Siegert CM, Levia DF, Leathers DJ, et al (2017) Do storm synoptic patterns affect biogeochemical fluxes from temperate deciduous forest canopies? Biogeochemistry

132:273–292. https://doi.org/10.1007/s10533-017-0300-6

Silva VO, Mello CR (2021) Meteorological droughts in part of southeastern Brazil: Understanding the last 100 years. An Acad Bras Cienc 93:1–17. https://doi.org/10.1590/0001-3765202120201130

Souza CR, Maia VA, Aguiar-Campos N de, et al (2021) Long-term ecological trends of small secondary forests of the atlantic forest hotspot: A 30-year study case. For Ecol Manage 489:https://doi.org/10.1016/j.foreco.2021.119043

Staelens J, De Schrijver A, Verheyen K, Verhoest NEC (2008) Rainfall partitioning into throughfall, stemflow, and interception within a single beech (Fagus sylvatica L.) canopy: influence of foliation, rain event characteristics, and meteorology. Hydrol Process 22:33–45. https://doi.org/10.1002/hyp.6610

Su L, Xu W, Zhao C, et al (2016) Inter- and intra-specific variation in stemflow for evergreen species and deciduous tree species in a subtropical forest. J Hydrol 537:1–9. https://doi.org/10.1016/j.jhydrol.2016.03.028

Su L, Zhao C, Xu W, Xie Z (2019) Hydrochemical fluxes in bulk precipitation, throughfall, and stemflow in a mixed evergreen and deciduous broadleaved forest. Forests 10:1–13. https://doi.org/10.3390/f10060507

Terra M de CNS, de Mello CR, de Mello JM, et al (2018) Stemflow in a neotropical forest remnant: vegetative determinants, spatial distribution and correlation with soil moisture. Trees 32:323–335. https://doi.org/10.1007/s00468-017-1634-3

Terra M de CNS, dos Santos RM, Fontes MAL, et al (2017) Tree dominance and diversity in Minas Gerais, Brazil. Biodivers Conserv 26:2133–2153. https://doi.org/10.1007/s10531-017-1349-1

Tobón C, Sevink J, Verstraten JM (2004) Solute fluxes in throughfall and stemflow in four

forest ecosystems in northwest Amazonia. Biogeochemistry 70:1–25. https://doi.org/10.1023/B:BIOG.0000049334.10381.f8

Tonello KC, Rosa AG, Pereira LC, et al (2021a) Rainfall partitioning in the Cerrado and its influence on net rainfall nutrient fluxes. Agric For Meteorol 303:. https://doi.org/10.1016/j.agrformet.2021.108372

Tonello KC, Van Stan JT, Rosa AG, et al (2021) Stemflow variability across tree stem and canopy traits in the Brazilian Cerrado. Agric For Meteorol 308–309:108551. https://doi.org/10.1016/j.agrformet.2021.108551

Townsend AR, Cleveland CC, Houlton BZ, et al (2011) Multi-element regulation of the tropical forest carbon cycle. Front Ecol Environ 9:9–17. https://doi.org/10.1890/100047

Van Stan II JT, Friesen J (2020) Precipitation Partitioning, or to the Surface and Back Again: Historical Overview

of the First Process in the Terrestrial Hydrologic Pathway. In: Van Stan, II JT, Gutmann E, Friesen J (eds) Precipitation Partitioning by Vegetation. Springer International Publishing, Switzerland.

Van Stan JT, Stubbins A (2018) Tree-DOM: Dissolved organic matter in throughfall and stemflow. Limnol Oceanogr Lett 3:199–214. https://doi.org/10.1002/lol2.10059

Van Stan JT, Van Stan JH, Levia DF (2014) Meteorological influences on stemflow generation across diameter size classes of two morphologically distinct deciduous species. Int J Biometeorol 58:2059–2069. https://doi.org/10.1007/s00484-014-0807-7

Van Stan JT, Wagner S, Guillemette F, et al (2017) Temporal Dynamics in the Concentration, Flux, and Optical Properties of Tree-Derived Dissolved Organic Matter in an Epiphyte-Laden Oak-Cedar Forest. J Geophys Res Biogeosciences 122:2982–2997. https://doi.org/10.1002/2017JG004111

Vitória AP, Alves LF, Santiago LS (2019) Atlantic forest and leaf traits: an overview. Trees - Struct Funct 33:1535–1547. https://doi.org/10.1007/s00468-019-01864-z

You Y, Xiang W, Ouyang S, et al (2020) Hydrological fluxes of dissolved organic carbon and total dissolved nitrogen in subtropical forests at three restoration stages in southern China. J Hydrol 583: https://doi.org/10.1016/j.jhydrol.2020.124656

Zhang Y feng, Wang X ping, Hu R, et al (2013) Stemflow in two xerophytic shrubs and its significance to soil water and nutrient enrichment. Ecol Res 28:567–579. https://doi.org/10.1007/s11284-013-1046-9

Zimmermann A, Germer S, Neill C, et al (2008) Spatio-temporal patterns of throughfall and solute deposition in an open tropical rain forest. J Hydrol 360:87–102. https://doi.org/10.1016/j.jhydrol.2008.07.028

Zimmermann A, Zimmermann B (2014) Requirements for throughfall monitoring: The roles of temporal scale and canopy complexity. Agric For Meteorol 189–190:125–139. https://doi.org/10.1016/j.agrformet.2014.01.014

Supplementary Material

Table A1. Gross rainfall (GR) and throughfall carbon concentration in dry and wet seasons, and in the entire period with respective maximum, minimum, median, mean, standard deviation (SD), coefficient of variation (CV), and the rainfall in the period.

Gross rainfall carbon concentration (mg L^{-1})									
ID	Season	n	Maximum	Minimum	Median	Mean	SD[a]	CV[b]	Gross Rainfall (mm)
GR	Dry	14	22.94	2.50	6.45	9.99	6.59	66%	221.6
	Wet	47	18.59	2.97	6.39	6.95	3.25	47%	1314.9
	Entire period	61	22.94	2.50	6.39	7.65	4.38	57%	1536.5
Throughfall carbon concentration (mg L^{-1})									
ID	Season	n	Maximum	Minimum	Median	Mean	SD[a]	CV[b]	Throughfall (mm)
1	Dry	14	96.19	6.60	18.22	28.51	26.11	92%	159.0
	Wet	47	48.35	5.54	10.63	13.01	7.58	58%	1031.0
	Entire period	61	96.19	5.54	11.62	16.57	15.33	93%	1189.9
2	Dry	14	116.90	5.24	21.67	39.97	34.98	88%	161.8
	Wet	47	56.27	9.22	15.71	20.66	11.75	57%	918.1
	Entire period	61	116.90	5.24	16.67	25.09	20.93	83%	1079.8
3	Dry	14	144.10	12.82	26.37	45.23	42.19	93%	152.3
	Wet	47	70.39	11.65	21.09	24.72	12.34	50%	1017.3
	Entire period	61	144.10	11.65	21.81	29.42	24.04	82%	1169.6
4	Dry	14	80.24	8.09	23.02	31.40	23.32	74%	193.6
	Wet	46	53.54	7.42	13.67	16.87	8.92	53%	1259.7
	Entire period	60	80.24	7.42	14.71	20.26	14.79	73%	1453.2
5	Dry	13	139.20	8.49	21.26	34.56	35.58	103%	213.8
	Wet	47	79.31	7.22	15.56	18.66	11.44	61%	1182.9
	Entire period	60	139.20	7.22	16.19	22.10	20.25	92%	1396.6
6	Dry	13	150.40	7.01	27.77	36.45	37.79	104%	161.9
	Wet	47	37.11	6.11	11.47	13.71	6.09	44%	872.5
	Entire period	60	150.40	6.11	12.35	18.64	20.21	108%	1034.4
7	Dry	12	77.07	6.94	21.15	28.40	22.65	80%	215.8
	Wet	47	51.24	6.49	11.42	13.59	7.36	54%	1130.7
	Entire period	59	77.07	6.49	12.95	16.66	13.35	80%	1346.5
8	Dry	14	101.10	4.87	19.48	31.92	30.92	97%	187.5
	Wet	47	43.21	5.60	12.79	15.18	7.82	51%	1216.4
	Entire period	61	101.10	4.87	13.19	19.03	17.45	92%	1403.8

9	Dry	13	69.52	4.83	17.61	24.41	19.99	82%	186.6
	Wet	47	29.80	5.26	10.63	11.97	4.78	40%	1114.9
	Entire period	60	69.52	4.83	11.08	14.67	11.22	76%	1301.4
10	Dry	13	146.50	6.92	30.60	38.59	36.70	95%	160.3
	Wet	46	47.62	5.75	11.14	13.24	7.30	55%	932.9
	Entire period	59	146.50	5.75	12.12	18.82	20.79	110%	1093.2

[a] standard deviation, [b] coefficient of variation

Table A2. Stemflow carbon concentration in dry and wet seasons, and in the entire period with respective maximum, minimum, median, mean, standard deviation (SD), coefficient of variation (CV), and the rainfall in the period.

Stemflow carbon concentration (mg L^{-1})									
ID	Season	n	Maximum	Minimum	Median	Mean	SD[a]	CV[b]	Stemflow (mm)
1	Dry	12	137.40	10.52	33.15	46.85	39.44	84%	0.4
	Wet	45	84.38	8.09	18.81	24.78	16.51	67%	2.6
	Entire period	57	137.40	8.09	19.89	29.43	24.54	83%	3.1
2	Dry	14	159.20	24.21	62.56	75.71	44.25	58%	0.4
	Wet	44	138.90	19.17	48.36	52.84	25.40	48%	2.2
	Entire period	58	159.20	19.17	50.07	58.36	32.11	55%	2.6
3	Dry	13	196.90	22.39	51.64	74.70	48.31	65%	1.1
	Wet	45	140.30	20.03	54.86	62.26	28.14	45%	5.6
	Entire period	58	196.90	20.03	54.84	65.05	33.61	52%	6.6
4	Dry	13	276.60	24.90	56.99	84.00	80.35	96%	0.1
	Wet	43	122.70	21.19	48.68	55.30	25.00	45%	1.8
	Entire period	56	276.60	21.19	49.61	61.97	45.11	73%	1.9
5	Dry	13	125.50	12.95	39.12	46.35	31.85	69%	0.3
	Wet	43	78.56	11.54	22.45	26.13	12.28	47%	2.2
	Entire period	56	125.50	11.54	23.41	30.83	20.27	66%	2.6
6	Dry	13	176.80	16.47	45.20	61.33	47.86	78%	0.6
	Wet	44	92.10	11.46	22.31	27.59	15.30	55%	2.2
	Entire period	57	176.80	11.46	25.34	35.28	29.57	84%	2.8
7	Dry	12	169.60	27.50	65.75	69.40	41.92	60%	0.3
	Wet	45	80.18	13.88	34.09	37.66	15.42	41%	2.5
	Entire period	57	169.60	13.88	35.97	44.34	26.50	60%	2.8
8	Dry	12	104.60	13.39	40.25	45.52	29.82	66%	0.5
	Wet	46	67.33	11.37	17.58	21.78	12.72	58%	1.8
	Entire period	58	104.60	11.37	19.45	26.69	19.84	74%	2.3
9	Dry	14	130.50	11.72	41.74	54.89	43.01	78%	0.3
	Wet	44	41.70	9.21	16.68	19.19	8.61	45%	0.8
	Entire period	58	130.50	9.21	17.92	27.80	26.75	96%	1.1
10	Dry	12	127.00	9.67	28.52	43.33	38.71	89%	1.0

Wet	46	50.00	6.77	15.53	19.31	10.46	54%	5.1
Entire period	58	127.00	6.77	17.78	24.28	21.72	89%	6.1

[a] standard deviation, [b] coefficient of variation

Table A3: The stemflow carbon enrichment rate in relation to gross rainfall (E_{GR}) in the dry and wet seasons, and in the entire period, with their respective maximum, minimum, median, mean, standard deviation (SD), and coefficient of variation (CV).

Stemflow carbon enrichment rate (E_{GR})								
ID	Season	n	Maximum	Minimum	Median	Mean	SD[a]	CV[b]
1	Dry	12	20.57	0.25	1.20	4.57	6.72	147%
	Wet	45	14.44	0.03	1.28	2.40	3.12	130%
	Entire period	57	20.6	0.03	1.3	2.9	4.2	146%
2	Dry	14	27.28	0.22	0.61	4.94	8.12	164%
	Wet	44	51.92	0.07	4.17	12.45	15.95	128%
	Entire period	58	51.9	0.07	2.5	10.6	14.7	139%
3	Dry	13	86.05	0.47	1.98	13.61	25.04	184%
	Wet	45	167.27	0.22	21.72	34.57	39.60	115%
	Entire period	58	167.3	0.22	9.9	29.9	37.7	126%
4	Dry	13	14.31	0.28	1.35	3.75	4.89	130%
	Wet	43	45.79	0.13	5.51	10.53	13.21	125%
	Entire period	56	45.8	0.13	2.5	9	12.1	135%
5	Dry	13	10.76	0.23	1.87	2.99	3.22	108%
	Wet	43	9.31	0.06	1.13	2.01	2.23	111%
	Entire period	56	10.8	0.06	1.3	2.2	2.5	112%
6	Dry	13	27.51	0.48	2.51	5.22	7.28	139%
	Wet	44	18.52	0.57	2.50	3.65	3.47	95%
	Entire period	57	27.5	0.48	2.5	4	4.6	114%
7	Dry	12	11.94	0.09	0.75	2.92	4.03	138%
	Wet	45	19.26	0.02	4.09	4.71	4.78	101%
	Entire period	57	19.3	0.02	3	4.3	4.7	107%
8	Dry	12	23.31	1.19	2.28	6.96	8.09	116%
	Wet	46	31.97	0.26	2.99	6.23	6.79	109%
	Entire period	58	32	0.26	2.8	6.4	7	110%
9	Dry	14	11.00	0.14	0.47	1.98	3.11	157%
	Wet	44	8.09	0.08	0.37	0.84	1.36	162%
	Entire period	58	11	0.08	0.4	1.1	2	176%
10	Dry	12	40.50	1.18	3.98	12.51	14.91	119%
	Wet	46	28.15	0.55	5.64	7.40	6.32	85%
	Entire period	58	40.5	0.55	5.5	8.5	8.9	105%

[a] standard deviation, [b] coefficient of variation

Table A4: The stemflow carbon enrichment rate in relation to throughfall (E_{TF}) in the dry and wet seasons, and in the entire period, with their respective maximum, minimum, median, mean, standard deviation (SD), and coefficient of variation (CV).

Stemflow carbon enrichment rate (E_{TF})								
ID	Season	n	Maximum	Minimum	Median	Mean	SD[a]	CV[b]
1	Dry	12	20.84	0.16	0.44	3.54	6.35	180%
	Wet	45	14.90	0.02	0.75	1.77	2.59	146%
	Entire period	57	20.8	0.02	0.7	2.1	3.7	173%
2	Dry	14	13.85	0.08	0.31	2.25	3.93	175%
	Wet	44	34.61	0.09	2.12	6.78	9.08	134%
	Entire period	58	34.6	0.08	1.5	5.7	8.3	147%
3	Dry	13	26.06	0.20	0.93	5.17	9.02	174%
	Wet	45	97.16	0.36	6.12	13.06	18.80	144%
	Entire period	58	97.2	0.2	4.1	11.3	17.3	154%
4	Dry	13	4.48	0.11	0.46	1.43	1.70	119%
	Wet	42	16.26	0.08	2.72	4.12	4.98	121%
	Entire period	55	16.3	0.08	1.1	3.3	4.3	131%
5	Dry	12	4.05	0.07	0.52	0.91	1.12	122%
	Wet	42	4.81	0.03	0.44	0.98	1.13	116%
	Entire period	54	4.8	0.03	0.4	0.9	1	112%
6	Dry	12	20.25	0.09	1.17	3.14	5.56	177%
	Wet	44	30.20	0.40	1.87	3.13	4.74	151%
	Entire period	56	30.2	0.09	1.9	3.1	4.9	156%
7	Dry	12	5.07	0.06	0.33	1.01	1.69	168%
	Wet	45	11.83	0.02	1.83	3.06	3.11	102%
	Entire period	57	11.8	0.02	1.3	2.7	3	112%
8	Dry	12	12.22	0.53	1.08	3.80	4.60	121%
	Wet	46	23.42	0.28	1.79	3.96	5.34	135%
	Entire period	58	23.4	0.28	1.6	3.6	4.5	126%
9	Dry	13	9.93	0.07	0.24	1.51	2.73	181%
	Wet	44	6.63	0.03	0.24	0.77	1.42	183%
	Entire period	57	9.9	0.03	0.2	0.8	1.6	196%
10	Dry	12	22.20	0.32	1.99	6.23	7.69	123%
	Wet	46	22.06	0.85	5.30	6.07	5.10	84%
	Entire period	58	22.2	0.32	4.6	5.8	5.3	91%

[a] standard deviation, [b] coefficient of variation

Figure A1. Histogram

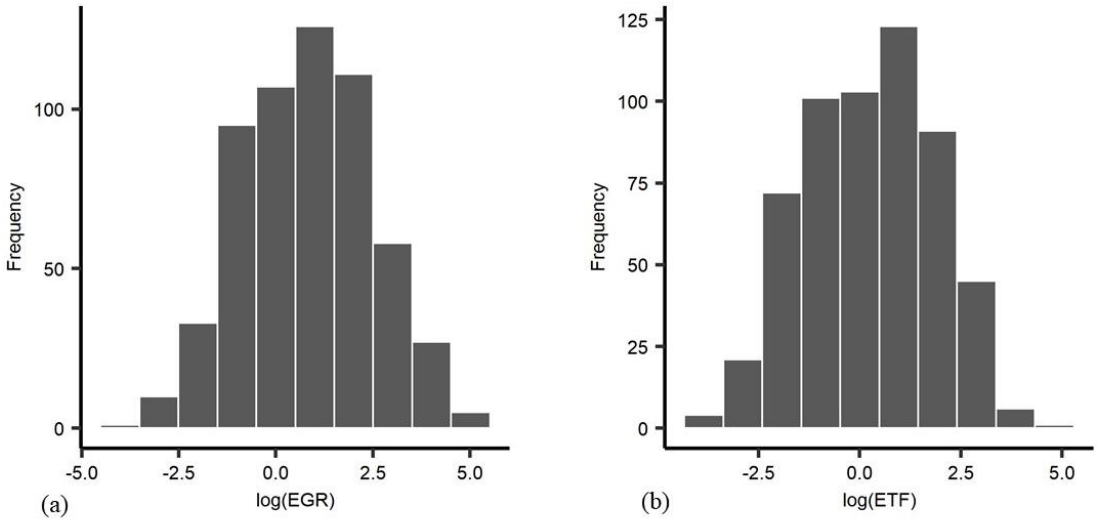

Figure A2. The regression relationship between EGR and ETf which was based on ratios from 10 trees in all 61 rainfall events.

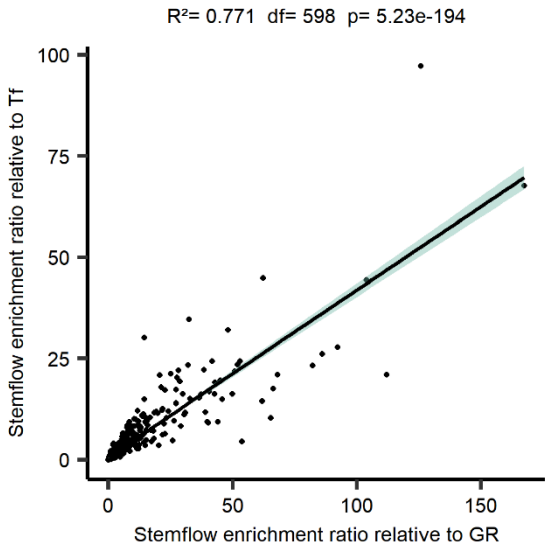

Figure A3. The regression relationship between E_{GR} and E_{Tf} which was based on the individual rates from 10 trees (a to j) in all 61 rainfall events.

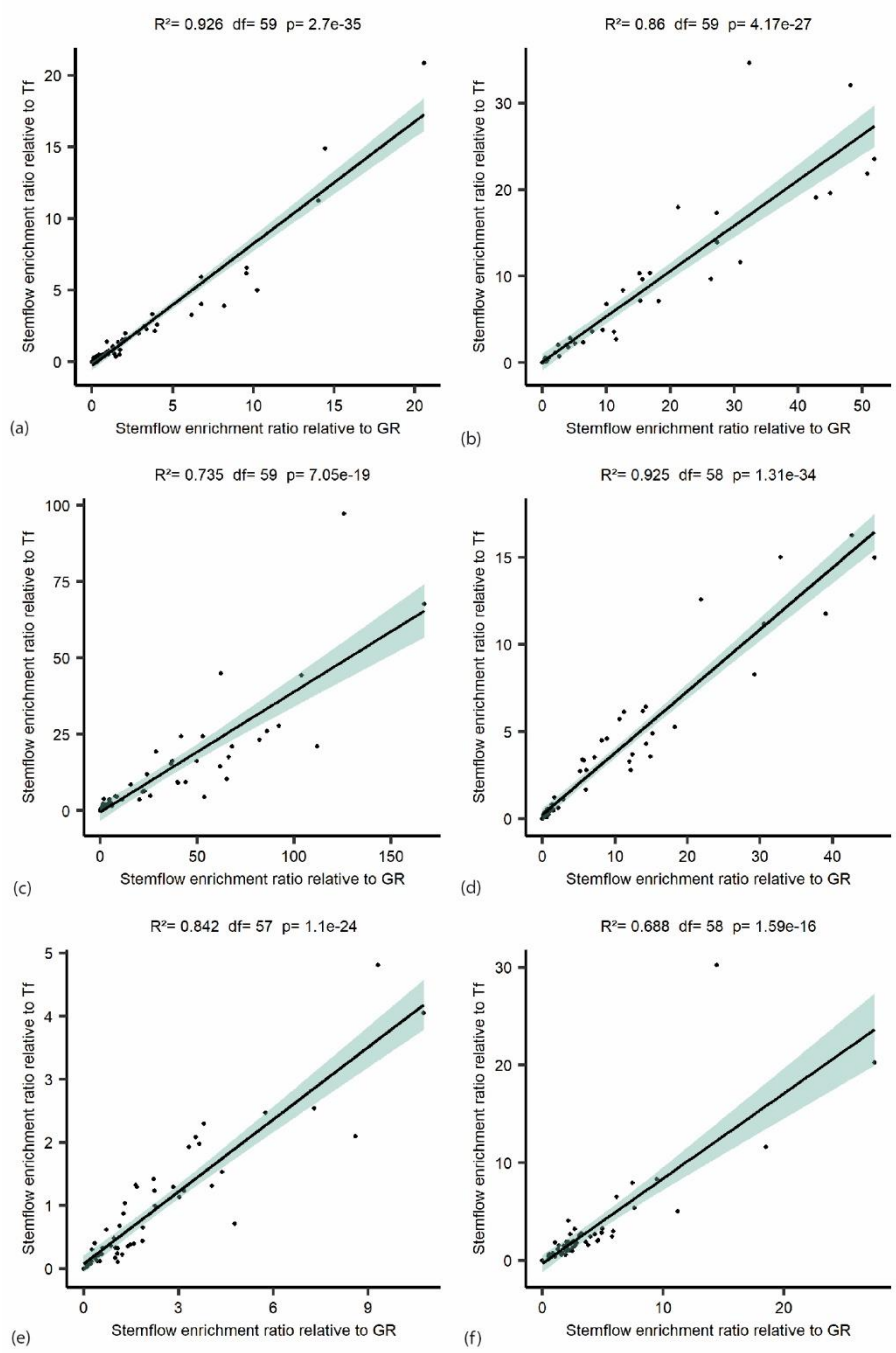

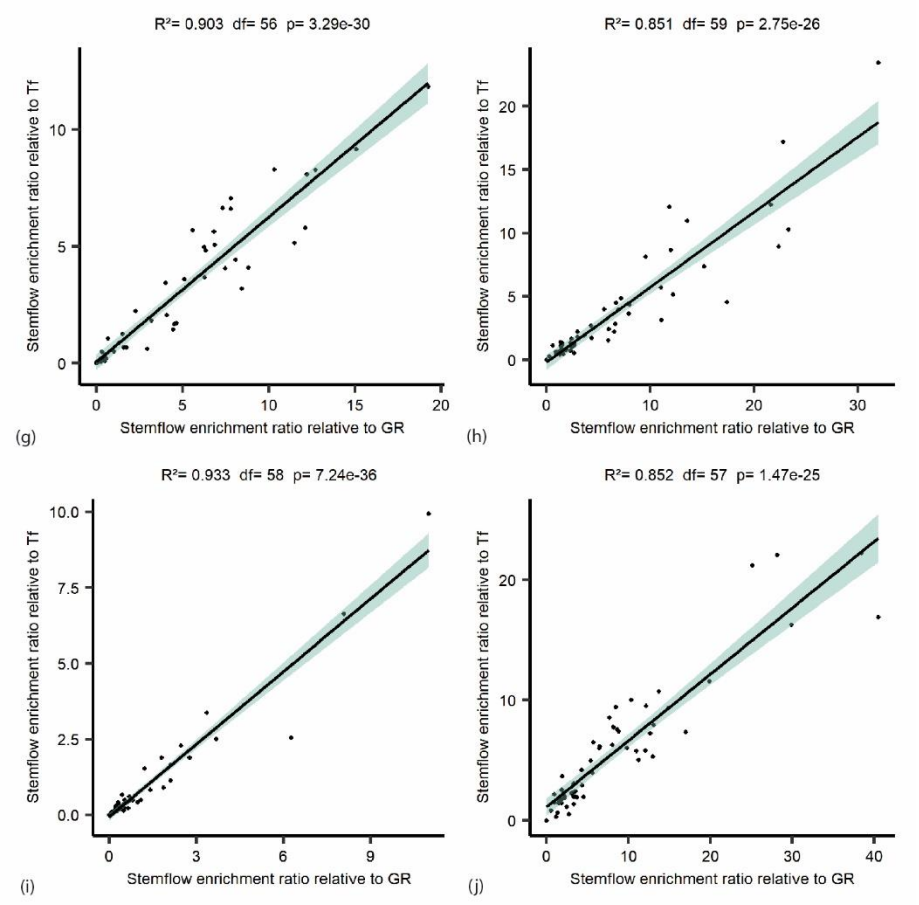

Table A5. Global models selected by ΔAICc < 2 for estimating stemflow enrichment rate (E_{GR} and E_{Tf}).

log (E_{GR}) ~ Bark + log(PDP) + log(Height) + log(I) + log(CA) + Season									
Int[a]	Brk[b]	log(PDP[c])	log(Hgh[d])	log(I[e])	log(CA[f])	Ssn[g]	Df[h]	logLik[i]	AICc[j]
2.079	+			0.9256	-0.7922	+	7	-714.538	1443.4
1.876	+	0.08878		0.9458	-0.7908	+	8	-713.955	1444.3
1.326	+		0.3504	0.9264	-0.8521	+	8	-714.452	1445.3
log (E_{Tf}) ~ Bark + log(PDP) + log(Height) + log(I) + log(CA) + Season									
Int[a]	Brk[b]	log(PDP[c])	log(Hgh[d])	log(I[e])	log(CA[f])	Ssn[g]	Df[h]	logLik[i]	AICc[j]
-2.978	+		1.915	0.9081	-1.052	+	8	-686.603	1389.6
-3.054	+	0.03651	1.911	0.9157	-1.051	+	9	-686.496	1391.5

[a] Intercept value estimated for each model, [b] tree bark, [c] previous dry period, [d] height, [e] maximum rainfall intensity, [f] projected canopy area, [g] season, [h] degrees of freedom, [i] Likelihood ratio of each model; [j] Akaike Information Criteria.

Figure A4. Relation between predictor variable and stemflow carbon enrichment rate (E_{GR} and E_{Tf}) and I (a,b), CA (c,d), height (e,f) and PDP (g,h).

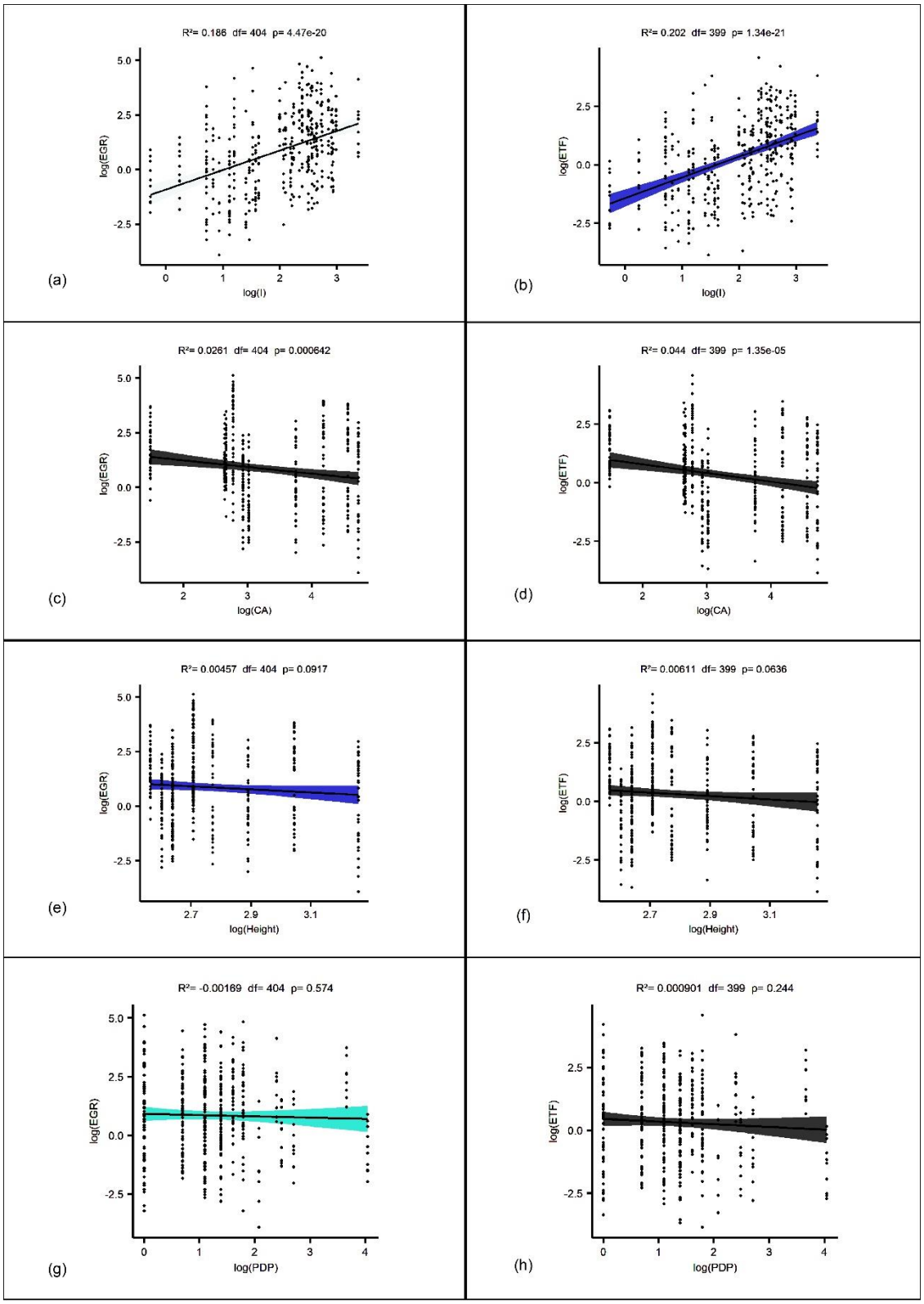

ARTIGO 3 – SOIL CARBON STOCKS AND THEIR MICROSCALE DRIVERS IN DRY AND WET SEASONS OF A DRY TROPICAL FOREST FRAGMENT IN BRAZIL*

Vanessa Alves Mantovani, Marcela de Castro Nunes Santos Terra, André Ferreira Rodrigues, Carlos Alberto Silva, Carlos Rogério de Mello

*Preliminary version. To be submitted to the journal *Forests* (ISSN: 1999-4907) – **Special Issue "Carbon and Nutrient Transfer via Above and Belowground Litter in Forests"**

Abstract

There is currently a gap in the literature regarding forest soil carbon stock evaluation and their potential drivers controlling factors. As soils are the main carbon reservoir on Earth, this information is critical in the face of climate change. We aimed to (i) determine the soil carbon stocks up to 1 meter depth in a forest fragment in hotspot Atlantic Forest; (ii) describe the soil carbon stock variability among the dry season and the wet season, (ii) identify the main biotic and abiotic drivers that affect the soil carbon stock. Soil carbon stocks up to 1 meter ranged from 201.0 Mg ha^{-1} C to 396 Mg ha^{-1} C (with a mean value for soil carbon stock up to 1 m depth of 268.5 Mg ha^{-1} C). We reinforced the vertical pattern of carbon distribution in the soil profile and the key differences in soil carbon stock variation between dry and wet seasons. Finally, our results pointed out that carbon concentration in dry biomass and hydraulic conductivity are positively related to soil carbon in shallower layers. Soil temperature and the coefficient of variation of the diameter at breast height in forest plots are positively related to soil carbon in deeper soil layers.

Key words: Biogeochemical cycles; Forest soil; Carbon stock; Carbon distribution in soil profile.

Acknowledgements: We acknowledge the Coordenação de Aperfeiçoamento de Pessoal de Nível Superior - CAPES (for the Ph.D research grant for the first author, and grant number 88882.306661/2018-01); the Conselho Nacional de Desenvolvimento Científico e Tecnológico - CNPq (grant number 401760/2016-2); and FAPEMIG (grant number PPMX-545/18) for supporting and funding this work. Special thanks go to "Laboratório de Gestão de Resíduos Químicos da Universidade Federal de Lavras (LGRQ-UFLA)" and "Laboratório de Estudo da Matéria Orgânica do Solo (LEMOS-UFLA)" for the facilities and equipment used in this study.

Funding: This work was financially by Coordenação de Aperfeiçoamento de Pessoal de Nível Superior - CAPES (grant number 88882.306661/2018-01); the Conselho Nacional de Desenvolvimento Científico e Tecnológico – CNPq (grant number 401760/2016-2); and FAPEMIG (grant number PPMX-545/18).

Introduction

The carbon cycle has drawn the attention of scientists and non-scientists around the world because of the increasing concern about the ongoing climate change (Anderegg et al., 2020; Brando et al., 2019). Forests have an ambiguous role on climate change as both a drain and a source of greenhouse gas emissions. In this context, tropical forests play a key role a strong carbon sinking, a matrix to sequester carbon anthropogenic sources, and regulating climate change (Hubau et al., 2020; Tian et al., 2015). However, deforestation of tropical forests has increased CO_2 emissions, decreased the soil carbon stocks, and instead of behaving like a true C sink faces the risk to become a strong carbon source (Anderegg et al., 2020; Brando et al., 2019; Moomaw et al., 2020). For instance, in Brazil, land use change, especially the conversion of forest into pasture area, figure as one of the main activities contributing to CO_2 emission (MCTI, 2020). The carbon stored in forest soils represents an important compartment of the overall carbon stored in the forest ecosystem (De Vos et al., 2015) and therefore plays a crucial role in mitigating the negative effects of climate change (Walker et al., 2019). Moreover, soil carbon (organic matter) has a crucial biological function in regulating nutrients dynamics, forms, flow and cycling (Haghverdi and Kooch, 2019), and key hole in improving soil aggregation and structure, preventing erosion and soil loss (Pimentel et al., 2005; Guillaume et al., 2015).

Rainfall is an important pathway for input solutes into forest soil due to the constancy and speed at which the dissolved elements reach the soil ground. Thus, the heterogeneity of water and nutrient inputs influences the litter decomposition processes, nutrient availability and cycling, including carbon organic compounds and carbon stored in soils (Qualls, 2020; Aubrey, 2020). Nevertheless, litterfall mass and carbon contained on it are considered the main sources of carbon input and flow to the forest soil due to deposition (Tobón et al., 2004; Aubrey, 2020; Macinnis-Ng and Schwendenmann, 2014). The high rate of organic matter deposition leads the forest in upper soil layers to present higher carbon stock than deeper layers (Morais et al., 2013).

Additionally, the low solubility of organic compounds associated with litter and reduced leaching of carbon in the soil profile are the main drive factors ruling the vertical distribution of organic matter and carbon stocks in tropical forest soils (Calazans et al., 2017).

The soil carbon stock under natural vegetation has been often underestimated. For instance, the soil carbon stocks quantified in the Minas Gerais Cerrado (Brazil) were approximately 53% higher than previously reported averages for the biome (Morais et al., 2020). This probably happened as a result of using more accurate full carbon contents recuperation with automatic dry combustion analyzers, and stratification for the correct determination of density in each soil layer, allowing to improve the assessment of full stocks of carbon in forest soils (Fernandes et al., 2015; Gomes et al., 2019; Morais et al., 2020). More than properly quantifying the soil carbon stocks, it is crucial to identify the potential drivers of carbon stock in forests types, and, within the same and small forest fragment, the variation of carbon both horizontal and throughout the soil profile. Knowing the variables that directly or indirectly affect carbon soil stock is a suitable and feasible strategy to model and ultimately to build scenarios of the forest soil carbon gain and loss under variations of its conditioning factors. Successfully attempts have been made in this direction. Large-scale soil carbon stock mapping carried out in the Cerrado has revealed that temperature, rainfall, altitude, silt and clay content are key factors ruling carbon stocks in forest soils (Morais et al., 2020). Doetterl et al. (2015) identified that soil geochemical variables have more significance to predict soil carbon stock than meteorological ones. The predictors with significant influence in soil carbon stock variation in tropical secondary forests were soil type, soil pH, and woody plant diversity (Paz et al., 2016). In small and apparently homogeneous forest fragments, soil type, tree height, canopy, litter input, amount of water leached through the soil profile, biota diversity and activity across the forest fragment

are eligible factors controlling carbon stocks in soils and their spatial variations across the forest ecosystem.

The Atlantic Forest is considered a global hotspot (Myers et al., 2000) because it is threatened by deforestation, fragmentation, anthropic pressures, replacement of native forest by not environmental-friendly land use and soil management practices, and shelters plenty of endemic species, which requires constant efforts for the preservation of vegetation and maintenance of its environmental services (Ribeiro et al., 2009). Despite being highly threatened, this biome contributes to a significant amount of total carbon stores in soil in Brazilian territory (Gomes et al. 2019). Studies performed with the aim to correct quantify soil carbon stocks in tropical forests, and specifically in the Atlantic Forest are scarce and lacking in small scale range of the forest fragments (e.g. Sayer et al., 2019). Therefore, it is necessary to carry out studies of soil carbon quantification on regional, small and local scales to improve the estimates and the understanding of forest role in climate change mitigation. Thus, raising awareness on the importance of forest conservation to boost fixation of carbon highly emitted from soil to atmosphere (Moomaw et al., 2020; Anderson-Teixeira and Belair, 2022).

Here, we aimed to (i) determine the carbon stocks in seven different layers up to 1 meter soil depth (0-5, 5-10, 10-20, 20-30, 30-40, 40-60, 60-100) in a semideciduous seasonally dry tropical forest fragment in the southeast region of Brazil; (ii) describe the soil carbon stock variability across the forest fragment in 4 months soil sampling scheme, 2 months in the dry season, and 2 months in the wet season, (ii) identify the main biotic and abiotic local drivers ruling the soil carbon stock in soil layers up to 1 meter depth.

Material and methods

Site description

The study area, located in the southeastern Brazil, is a 6.30 ha seasonally dry tropical forest fragment in the late-successional stage (21º13'40''S and 44º57'50''W, 925 m a.s.l) (Souza et al. 2021) (Fig 1). The seasonally dry tropical forest comprises up to 50% of deciduous trees, which lose their leaves to support long dry periods (IBGE 2012; Morellato and Haddad 2000; Vitória et al. 2019). The relief is slightly undulated with slopes ranging from 5 to 15% (Junqueira Junior et al. 2017). The forest fragment characterizes as a typical landscape of the Atlantic Forest biome because it is over a homogeneous area of Oxisols, which forms the Atlantic Forest-Oxisols site (Junqueira Junior. 2017). The Köppen climate classification is Cwa, characterized by rainfall seasonality with two well-defined seasons: wet (October to March) and dry (April to September) (Junqueira Junior et al. 2019). The long-term (1981-2010) average annual rainfall is 1462 mm, in which 85% of rain falls during the wet period (INMET 2020).

The seasonally dry tropical forest inventory

A forest survey was carried out in the study area in 2017, providing species identification and tree traits information for all arboreal individuals with a diameter at breast height (DBH) ≥ 5 cm in 126 plots. The mean of diameter at breast height (DBH) in the plots ranged from 11.2 to 20.1 m, the number of individuals (n) ranged from 18 to 62, and the basal area ranged from 0.46 to 1.81 m. The seasonally dry tropical forest fragment has a heterogeneous and stratified canopy (Terra et al., 2018), and is reaching a late-successional stage after entire protection establishment in 1986 (Souza et al., 2021). Fragments with complete protection contribute to preventing losses in both biodiversity and carbon stock (de Lima et al., 2020).

Soil sampling and carbon content

Ten locations were selected in the seasonally dry tropical forest fragment for soil sampling to carbon quantification and bulk density determination (Fig. 01). Before soil sampling, we removed the superficial litterfall to guarantee no interference of litter on carbon stored in Oxisol. Undisturbed soil samples were collected from six layers: 0-10, 10-20, 20-30, 30-40, 40-

60, and 60-100 cm with a volumetric ring, totalizing sixty samples (six in each location). Samples were dried at 105°C for 48 hours in an oven and weighed to obtain the dried mass (Embrapa 1997). Soil bulk density (ρ) was calculated as the dry weight of soil divided by its volume.

Soil samples were collected to determine total carbon concentration from seven layers: 0-5, 5-10, 10-20, 20-30, 30-40, 40-60, and 60-100 cm, in the first week of the four months (May and August 2018 representing the beginning and the middle of the dry season, respectively, and December 2018 and April 2019 representing the middle and the end of the wet season, respectively) totalizing 280 samples. The samples were air-dried, crushed with a porcelain pestle, sieved through a mesh of 0.25 mm, and dried in a forced-draft oven at 50 °C until constant weight (~48 hours). For the carbon content determination, samples were submitted to dry combustion in a TOC analyzer (Elementar Vario TOC Cube model, Hanau, Germany). The carbon determination followed standard methods and quality control were monitored using certified standards to guarantee the suitability of the results. The carbon stocks were calculated for each soil layer as follows:

$$C_{stock} = \rho \,.\, c \,.\, L.\, 100$$

Where C_{stock} is expressed in Mg ha^{-1}, ρ is the soil bulk density in Mg m^{-3}, c is the carbon content in %, L is the layer soil thickness (m), 100 is the unit's conversion factor.

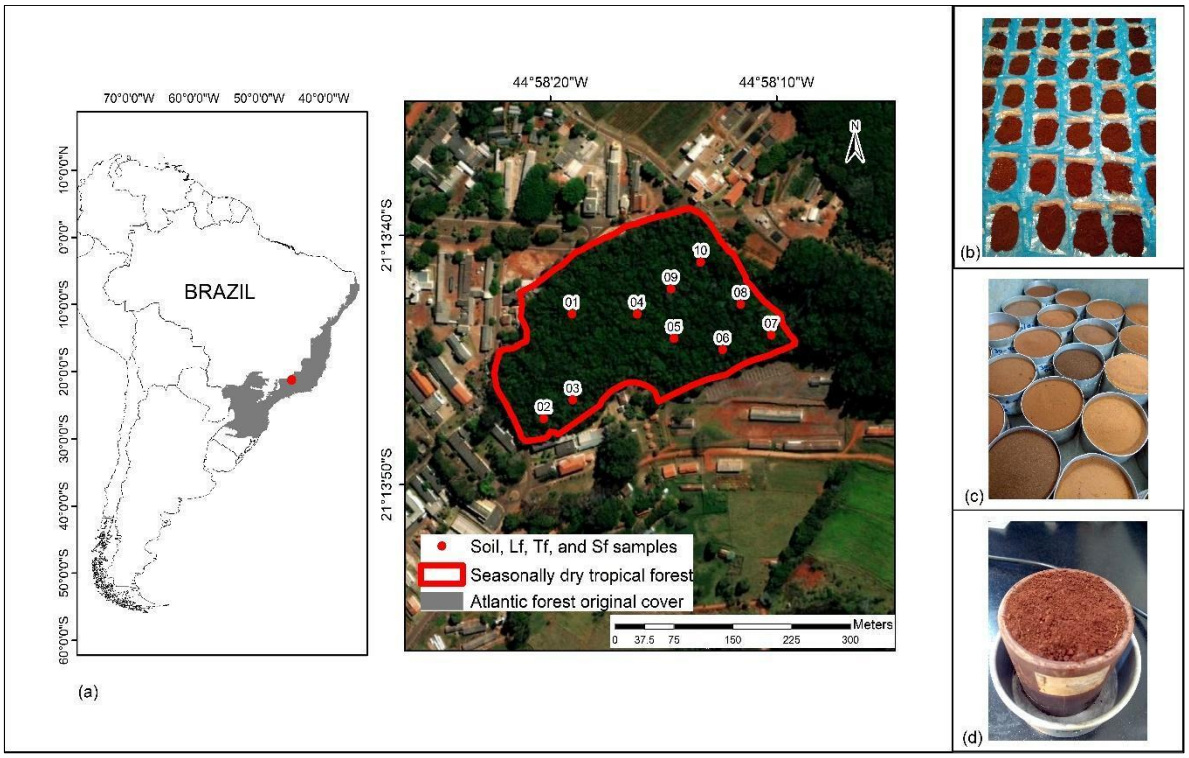

Figure 01. Seasonally dry tropical forest fragment location, and soil, litterfall (Lt) throughfall (Tf), and stemflow (Sf) sample's location (a), air-dried soil samples (b), soil samples prepared for carbon determination (c), undisturbed soil sample (d)

Biotic and abiotic variables

In the location of soil samples (Fig 01), throughfall (Tf), stemflow (Sf), and litterfall (Lt) were measured and sampled from May 2018 to April 2019. Tf and Sf were collected at least for hours after each rainfall event, totaling sixty-one events, whereas Lt was collected monthly. Tf was collected through ten fixed Ville de Paris-type rain gauges installed inside the forest fragment (Fig. 2a). Sf was collected by a hose nailed spiral around the tree trunk and connected to a collection bin (Fig. 2a). Both (Tf and Sf) were located near the soil sample collecting places. Tf and Sf were sampled for carbon analyses after each rainfall event more significant than 4.7 mm, due to the necessary volume to perform the lab analyses. For preservation purposes, samples were filtered and refrigerated at 4 ºC until lab analyses. Total dissolved carbon analyses were performed with a total carbon analyzer (TOC-VCPH) Shimadzu by quantification in a non-

dispersive infrared sensor (NDIR) (Shimadzu 2003). The mean monthly carbon concentrations in Tf and Sf were estimated by the volume-weighted mean (VWM) as follows:

$$VWM = \frac{\sum_{n=1}^{i} C_{i,e} \ . V_{i,e}}{\sum_{n=1}^{i} V_{i,e}} \quad (2)$$

In which C represents the total dissolved carbon concentration and V represents the total volume at collector *i* for event *e*. With the mean concentration and the monthly Tf, and Sf depth (mm) was possible to quantify net precipitation inputs (Tf+Sf) in each month, and the entire period.

Litterfall was monthly collected using fixed litter traps installed in each of the ten selected points, totaling 40 collectors in the study area (Fig. 2b). The litter traps were seated close to the ground, each measuring 0.25 m², constructed with PVC pipes, and attached the shading material with cable ties (Fig 2c). The deposited material in the litter traps was collected in the first week of each month from May 2018 to April 2019 (Fig. 3a). The samples were weighed with an accuracy of 0.01 g and dried in a forced-draft oven in paper bags at 50°C (Fig. 3b) until they reached a constant weight (~ 48 hours). After that, the material was weighed again on a 0.01g precision scale for dry biomass determination. The samples were then crushed in a knife mill, and sieved (60 mesh) (Fig. 3c), dried in a forced-draft oven at 50 °C until constant weight (~48 hours). We selected the samples of the same months in which soil carbon was quantified (May, August, December 2018, and April 2019). The samples were submitted to dry combustion in a TOC analyzer (Elementar Vario TOC Cube model, Hanau, Germany). Dry biomass was calculated for each month (May 2018 to April 2019), while the carbon stored in dry biomass (Mg C. ha^{-1}) was calculated for four months (May and August 2018 representing the dry season, and December 2018, and April 2019 the wet season).

Figure 02. Throughfall (Tf), stemflow (Sf), and litterfall (Lt) collection plots (a), litter traps installed 30 days before the first collection (b), the clean area before the installation.

Figure 03. Litterfall deposited during the period between the collections (c), forced-draft oven (d), samples after crushed and sieved (e)

We obtained a suite of variables potentially related to soil carbon stock (see Table1). Most of these variables were obtained from forest inventory (2017) and describe the forest structure: diameter at breast height (DBH), number of individuals (n), basal area (BA), coefficient of variation of the diameter at breast height (CV DBH), carbon stock in aboveground biomass (C), species richness (S), Shannon diversity index (H'), Pielou equability index (J). Moreover, we obtained some soil-related variables: soil temperature (measured in the field), clay content (measured in the laboratory), and hydraulic conductivity (from Junqueira Junior et al., 2017); litterfall-related variables: dry biomass (DB) and carbon concentration in dry biomass

(CDB), and rainfall-related variables: net precipitation (NP), and carbon input via net precipitation (CNP).

Table 01. Set of environmental variables potentially related to forest soil carbon, gathered for the present study.

Forest inventory	**Description and Determination**
DBH (cm): Diameter at breast height	Represents the measurement of the tree's diameter at 1.30 meters high in relation to the ground level.
n	Number of individuals of each species sampled in a plot.
BA (m^2/ha): Basal area	Represents the plant community density, that is, provides the occupation level of a soil specific area.
CV DBH (%): Coefficient of variation of the diameter at breast height	Express the variability of a characteristic of interest, that is, allows to analyze the variable dispersion in relation to its mean value.
C (Ton/ha): carbon stock in aboveground biomass	Defined as carbon presents in all living biomass above the soil, expressed as a mass per unit area. May includes stem, stump, branches, bark, seeds and foliage.
S: Species richness	Express the number of species sampled in a specific area.
H' (nats.ind^{-1}): Shannon diversity index	Diversity index based on the proportional abundance of the community species. In other words, it represents the measurement of the number of different species in a specific area.
J (nats.ind^{-1}): Pielou equability index	Express the number of individuals in relation to the species.
Other variables	**Description and Determination**

Clay (soil particle size) (%)	Clay content determined by soil fractions separation was performed by sieving followed by sedimentation (ABNT, 2018)
Hydraulic conductivity (Ko) (cm h^{-1})	Guelph permeameter method at 40 cm depth (Junqueira Junior et al., 2017)
Soil temperature (T) (°C)	Measured in the field in each soil sample (considering the average of each soil layer).
Dry biomass (DB) (Mg ha^{-1})	Litterfall after drier processes, considering the total litterfall in period (May 2018 to April 2019)
Carbon concentration in dry biomass (CDB) (%)	Total carbon analysis (TOC analyzer – Elementar Vario TOC Cube model, Hanau, Germany). Considering the average of 4 months of analysis.
Net precipitation (NP) (mm)	Rainfall that reaches soil (Tf+Sf), considering the period (May 2018 to April 2019)
Carbon in NP (CNP) (Mg ha^{-1})	Carbon inputs via net precipitation (throughfall + stemflow), considering the period (May 2018 to April 2019)

Data analyses

We have performed descriptive statistical analyses (mean, median, minimum, maximum, standard deviation coefficient of variation) of soil bulk density (ρ, Mg m^{-3}), and soil carbon concentration (C, %), up to 1,0 m depth across de ten soil samples located in the seasonally dry tropical forest fragment. The statistical analyses were performed for each soil depth (n=10). The descriptive analyses were performed for soil carbon concentration considering the four months of analyses (May, August, and December 2018, and April 2019 – temporally) and the soil depth (n=10). The carbon concentration for each layer was tested for normality (Shapiro–Wilk test).

In the cases of non-normal distribution, the carbon concentration was compared by the Wilcoxon test at the 0.05 significance level to determine statistical differences between the four months (May and August 2018 representing the dry season, December 2018, and April 2019 the wet season).

To evaluate the biotic and abiotic drivers (Table 01) of soil carbon stock, we used a multivariate modeling approach. Therefore, we built a "response matrix" with the carbon stock in each soil layer as columns and the samples as rows; and an "explanatory matrix" containing all the variables presented in Table 1 as columns and again the sample points as rows. We used Redundancy Analysis (RDA) to fit the response matrix against the explanatory matrix. RDA is a constrained ordination technique (ordination with covariates or predictors) used to explain a dataset "Y" using a dataset "X" (Ter Braak and Looman, 1994; Legendre et al., 2011). Subsequently, for the selection of explanatory variables, we made use of the *envfit* function ("vegan" package for R; Oksanen et al., 2020; Powell et al., 2019), which tests the significance of the explanatory variables by permutation test (number of permutations used = 999). The significant variables ($p>0.1$) pointed by the *envfit* function were then used to build a final RDA diagram.

Results

Soil carbon concentration and bulk density

The soil bulk density (Table 2) and carbon concentration (Supplementary Material - Table 1 e 2) were used to calculate each layer's soil carbon storage. The average soil bulk density increased with soil depth (n=10), ranging from 0.85 to 0.95 Mg m^{-3} in the 0-10 and 60-100 cm soil layer, respectively. The lowest soil bulk density value was observed in the 0-10 cm soil layer (0.78 Mg m^{-3}), and the greatest was determined for the 20-30 cm soil layer (1.09 Mg m^{-3}).

Table 2. Descriptive statistics of soil bulk density (ρ, Mg m^{-3})

Depth (cm)	Mean	Min	Max	SD	CV (%)
0-10	0.85	0.78	0.92	0.05	6%
10-20	0.93	0.81	0.97	0.05	5%
20-30	0.94	0.81	1.09	0.08	8%
30-40	0.98	0.92	1.08	0.05	5%
40-60	0.97	0.87	1.04	0.05	5%
60-100	0.95	0.84	1.02	0.05	6%

Min: minimum; Max: maximum, SD: standard deviation; CV: coefficient of variation

The average carbon concentration (%) of the ten locations decreased with soil depth, in the four months of analysis (Supplementary Material – Table 1). The average carbon concentration in the superficial layer (0-5 cm) ranging from 9.8 ± 5.8 in August, to 14.8 ± 6.1 % in December, and the deeper layer ranged from 1.6 ± 0.3 in April to 2.0 ± 0.2 % in May. Considering the spatial distribution of soil carbon concentration, the coefficient of variation decreased with soil depth (CV>40% in 0-10 cm depth, and CV<40% in 10-100 cm depth), indicating a decrease in the spatial variability of carbon concentration in the deeper layers (Supplementary Material – Table 1). Considering the temporal distribution, the coefficient of variation was lower, being less than 35% in all locations and all depths (Supplementary Material – Table 2). The vertical distribution of the average carbon concentration in each location shows that the superficial layers (0-5 and 5-10 cm) present the highest values in all locations, and from 10-20 cm layer, carbon concentrations showed similar values and a less accentuated reduction with depth (Supplementary Material - Fig 01).

The carbon concentration in the first superficial layer (0-5 cm) was higher in December. However, there were no significant differences in the other months (May, August, and April). The concentration in December was higher than in May and August. However, there were no

significant differences from April considering the 5-10 cm layer. We could notice changes in the carbon concentration dynamics with depth. For example, the concentration was higher at the beginning of the dry season (May) in the 30-40 cm and 40-60 cm layers (Table 3).

Table 3: Average soil carbon concentration to 1-m depth across the locations (n=10 for each soil depth). Carbon concentration followed by the same letter in the line is not significantly different by Wilcoxon test (p-value < 0.05).

	Carbon concentration (%)			
Soil layer (cm)	May-18	Aug-18	Dec-18	Apr-19
0-5	10.0[a]	9.8a	14.8[b]	10.7[a]
05-10	6.2[ab]	5.6a	7.9[c]	7.2[bc]
10-20	3.2[a]	3.3[a]	3.2[a]	3.2[a]
20-30	3.3[a]	2.9[ab]	3.0[ab]	2.9[b]
30-40	3.0[a]	2.2[b]	2.4[b]	2.4[b]
40-60	2.4[a]	1.9[b]	2.1[c]	2.1[bc]
60-100	2.0[a]	1.7[ab]	1.8[a]	1.6[b]

Overall, the soil carbon stocks up to 1 meter ranged from 201.0 Mg C ha^{-1} to 396 Mg C ha^{-1}, averaging 268.5 Mg C ha^{-1} (Table 4). With the greatest carbon storages (396 .0 Mg C ha^{-1} and 335.3 Mg C ha^{-1}) located on opposite sides (northwest and southeast) of the forest fragment (locations 01 and 07, see Fig. 01). And the lower carbon storages (201.0 Mg C ha^{-1} and 210.3 Mg C ha^{-1}) are located next to and in the southwest of the forest fragment (location 02 and 03, see Fig. 01).

Table 4: Carbon stock (Mg C ha^{-1}) in ten locations in the Atlantic Forest fragment, considering the average of 4 months of analysis, in each soil depth, and the total up to 1-m. [a]Average of carbon stock, considering the 10 locations, [b] proportion (%) of the carbon stored at 0–100 cm, considering the average of 10 locations.

ID	0-5 cm	05-10 cm	10-20 cm	20-30 cm	30-40 cm	40-60 cm	60-100 cm	0-100 cm
1	125.1	74.4	32.4	28.7	22.5	45.7	67.3	396.0
2	30.0	16.9	20.9	20.1	19.0	37.8	65.6	210.3
3	30.2	20.0	28.8	27.0	20.4	29.9	44.6	201.0
4	28.9	20.0	29.0	30.1	26.0	42.8	74.3	251.0
5	38.2	19.2	27.0	24.2	26.4	49.4	84.2	268.6
6	39.4	24.3	35.4	29.4	26.6	39.1	70.5	264.7
7	71.2	36.7	30.6	38.9	30.6	45.7	81.5	335.3
8	50.5	32.2	34.6	33.2	27.7	45.4	67.9	291.5
9	37.9	21.9	34.2	29.1	22.1	37.2	60.0	242.5
10	35.0	22.8	25.2	21.9	21.2	36.9	61.1	224.2
Mean[a]	48.6	28.8	29.8	28.3	24.3	41.0	67.7	268.5
C (%)[b]	18.1	10.7	11.1	10.5	9.0	15.3	25.2	100.0

The analysis of carbon stock per layer identified that the first soil layer (0-10 cm) is responsible for almost 30% of total carbon stock in the soil profile up to 1 m, and on average, represents 77.5 Mg C ha^{-1}. When we consider the 30 cm depth, 50% of total soil carbon stock up to 1 m is stored in this layer (Table 4).

The dry biomass of litterfall sampled from May 2018 to April 2019 (12 months) was on average 13.02 ± 3.77 Mg ha^{-1} (Table 3 – Supplementary Material). Almost 60% of the total litter sampled in the study period fell between August and January from the middle of the dry season to the middle to the wet season. The average carbon concentration of the litterfall showed low variability, ranging from 46.3 $\pm$ 2.0 in samples from April 2019 to 48.8 $\pm$ 2.0 in May 2018 (Table 4 – Supplementary Material). The litterfall carbon stock was higher in the wet months and ranged

from 0.24 Mg ha^{-1} month^{-1}, and the accumulated over 12 months was 6.23 Mg C ha^{-1} (Table 4 – Supplementary Material).

According to the RDA, the explanatory matrix explained 80.36% of the forest soil carbon matrix variation. The *envfit* function pointed hydraulic conductivity (K0), soil temperature in 40-60 cm layer (T60), carbon concentration in dry biomass (CDB), and coefficient of variation of the diameter at breast height (CV_DBH) as significant ($p < 0.1$) explanatory variables (p-values: 0.03, 0.087, 0.004, and 0.031, respectively). The final RDA diagram shows two main trends: (i) CDB and K0 positively related to forest soil carbon stock in soil shallower layers, and (ii) CV_DBH and T60 positively correlated to soil carbon stock in deeper layers.

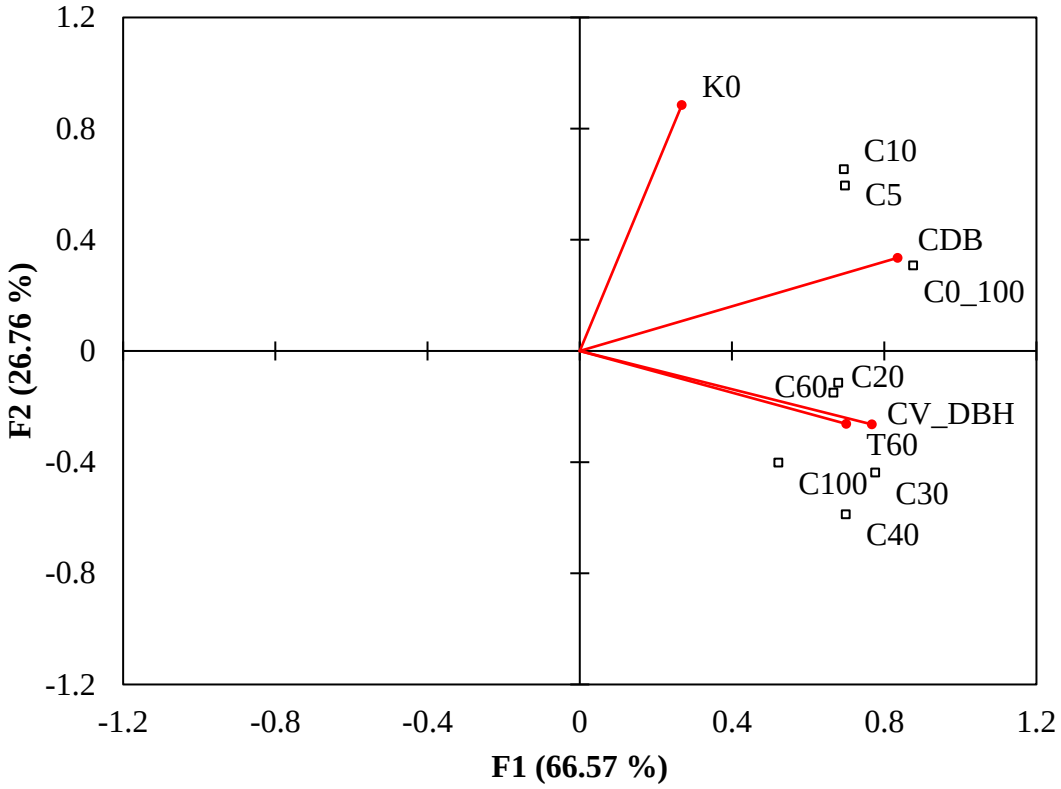

Figure 04. Redundancy analysis (RDA) diagram of forest soil carbon stock in different soil layers: 0-5 cm (C5), 5-10 cm (C10), 10-20 cm (C20), 20-30 cm (C30), 30-40 cm (C40), 40-60 cm (C60), 60-100 cm (C100), and 0-100 cm (C0_100). Red vectors represent the significant environmental variables: hydraulic conductivity (K0), soil temperature in 40-60 cm layer (T60), carbon concentration in dry biomass (CDB), and coefficient of variation of the diameter at breast height (CV_DBH).

Discussion

Overall, our study fills a gap in the literature by presenting determined forest soil carbon stock for Atlantic Forest. Moreover, we reinforced the vertical pattern of carbon distribution in the soil profile and showed differences in soil carbon with higher concentrations in upper layers in the wet season and lower concentrations in deeper layers in the dry seasons. Finally, our results pointed to carbon concentration in dry biomass (CDB) and hydraulic conductivity (K0) as positively related to soil carbon in shallower layers, and soil temperature (T60) and coefficient of variation of the diameter at breast height in forest plots (CV DBH) positively related to soil carbon in deeper layers.

Forest soil carbon stock

The soil carbon stocks up to 1 meter ranged from 201.0 Mg C ha^{-1} to 396 Mg C ha^{-1}. Our mean value for soil carbon stock up to 1 m depth (268.5 Mg C ha^{-1}) is comparable to the values found in Amazon ombrophilous forests by Marques et al. (2016), who found values of soil carbon of 136 to 240 Mg C ha^{-1}. Such a high value found for our forest is probably due to its long-term protection and advanced succession stage (Souza et al., 2021).

Our results reinforce the widespread pattern of decreasing carbon stocks with depth, the "vertical pattern." Soil carbon storage depends primarily on balance between inputs mainly from the vegetation (Jobbágy and Jackson, 2000) and eventually from rainfall (Mantovani et al., 2022) and losses through decomposition. As these inputs are essentially vertical, the decrease in carbon stock in deeper layers is expected (D'Amore and Kane, 2016; Marques et al., 2016). We found in the Atlantic Forest that 50% of total soil carbon stock up to 1 m is stored in the 0-30 cm layer. The disparity in the distribution of carbon stocks through the soil profile is expected for forests, where up to 50% of all carbon in the top 1 m is contained in the uppermost 20 cm (Jobbágy and Jackson, 2000).

We observed some differences between wet and dry seasons, especially for upper layers. Overall, deeper layers seem to be more time stable, by other studies (e.g. Fontaine et al., 2007). However, upper layers showing variations between seasons, with the wet season presenting higher carbon stocks than the dry one. Although, there is a greater deposition of litterfall in the dry season more significant as a consequence of tree deciduousness (Costa et al., 2019), the lower temperature and moisture of this period contribute to slowing the incorporation of this matter into the soil (de Queiroz et al., 2019). In the wet season, the higher mean temperature and moisture certainly contribute to incorporating of the organic matter into the soil, leading to higher values in shallower layers during this season.

Forest soil carbon stock drivers

We found only hydraulic conductivity, carbon concentration in dry biomass, coefficient of variation of the DBH in forest plots, and soil temperature to be significantly correlated to forest soil carbon stock in our study area. We found different variables associated with upper and deeper soil layers more interestingly.

Carbon concentration in the dry biomass and hydraulic conductivity were positively related to soil carbon in shallower layers. Carbon concentration in the dry biomass represents the direct input of carbon into the soil (Jobbágy and Jackson, 2000). Also, studies have pointed out that tree species regulate soil carbon via the different composition of their tissues (Angst et al., 2018) thus the different species in our sample points may have caused variation in soil carbon stocks in our study area. The hydraulic conductivity, pointed to as one of the main drivers of soil water content in our study area (Junqueira-Junior et al., 2017), is probably related to higher carbon stocks in upper layers because carbon plays an important role in soil aggregation (Pimentel et al., 2005), ultimately increasing hydraulic conductivity in forest soils.

Soil temperature and coefficient of variation of the tree diameter at breast height in forest plots were positively related to soil carbon in deeper layers. Soil temperature and moisture,

together with net primary productivity have been considered the main drivers of soil carbon storage (Todd-Brown et al., 2013). Temperature is related to several processes in the soil, including microbial activity (Cotrufo et al., 2015). In deeper layers where there are relatively lower carbon stocks, this variable can decisively affect decomposition rates. Surprisingly, variation in the size of trees was positively correlated to carbon stocks in deeper layers. Variation in the size of trees may indicate stability in forests. Late-successional forests present a stratified canopy and trees belonging to different sizes and ages, as opposed to disturbing early-stage succession forests that usually are dominated by fast-growing pioneer species (Tabarelli et al., 2012). As disturbance usually reduces carbon stocks (Johnson, 1992; Jandi et al., 2007), it is expected that stable/conserved forests have greater soil carbon stocks.

It is important to mention that our environmental data have limitations that could be affecting the results. For instance, mismatches between forest data (2017) and soil data (2018/2019) could mask the effect of some variables. There is little information about an ideal time match for these variables to be paired. Nevertheless, given the scarcity of studies on soil carbon drivers in the Atlantic Forest, our study remains important although somehow exploratory. Finally, we provide a more holistic view of the forest ecosystem, correlating vegetation, climate, and soil variables. Moreover, we reinforce the soil's potential to store carbon and, therefore, its crucial role in climate change mitigation.

Conclusion

The soil carbon stocks up to 1 meter ranged from 201.0 Mg C ha^{-1} to 396 Mg C ha^{-1} (with a mean value for soil carbon stock up to 1 m depth of 268.5 Mg C ha^{-1}). The vertical carbon distribution in the soil profile decreased with depth and shows differences between seasons. Our results pointed carbon concentration in dry biomass (CDB) and hydraulic conductivity (K0) as positively related to soil carbon in shallower layers and soil temperature (T60) and coefficient

of variation of the diameter at breast height in forest plots (CV DBH) positively related to soil carbon in deeper layers.

We reinforce the forest soil's potential to store carbon and, therefore, its crucial role in climate change mitigation. Forest conservation and management strategies should take forest soil carbon stock into account.

References

ABNT – Associação Brasileira de Normas Técnicas. Solo - Análise granulométrica. 2016. Rio de Janeiro.

Anderegg, W.R.L., Trugman, A.T., Badgley, G., Konings, A.G., Shaw, J., 2020. Divergent forest sensitivity to repeated extreme droughts. Nat. Clim. Chang. 10, 1091–1095. https://doi.org/10.1038/s41558-020-00919-1

Anderson-Teixeira, K.J., Belair, E.P., 2022. Effective forest-based climate change mitigation requires our best science. Glob. Chang. Biol. 28, 1200–1203. https://doi.org/10.1111/gcb.16008

Angst, G., Mueller, K.E., Eissenstat, D.M., Trumbore, S., Freeman, K.H., Hobbie, S.E., Chorover, J., Oleksyn, J., Reich, P.B., Mueller, C.W., 2019. Soil organic carbon stability in forests: Distinct effects of tree species identity and traits. Glob. Chang. Biol. 25, 1529–1546. https://doi.org/10.1111/gcb.14548

Aubrey, D. P. Relevance of Precipitation Partitioning to the Tree Water and Nutrient Balance. In: Van Stan, II, J. T.; Gutmann, E.; Friesen, J. (org.). Precipitation Partitioning by Vegetation. Cham, Switzerland: Springer International Publishing, 2020.

Brando, P.M., Paolucci, L., Ummenhofer, C.C., Ordway, E.M., Hartmann, H., Cattau, M.E., Rattis, L., Medjibe, V., Coe, M.T., Balch, J., 2019. Droughts, Wildfires, and Forest Carbon Cycling: A Pantropical Synthesis. Annu. Rev. Earth Planet. Sci. 47, 555–581. https://doi.org/10.1146/annurev-earth-082517-010235

Brazil MCTI, 2020 Fourth National communication of Brazil to the United Nations framework convention on climate change.

Costa, S. do V., Pesquero, M.A., Junqueira, M.H.M., 2019. Litterfall deposition and decomposition in an Atlantic Forest in Southern Goiás. Floresta e Ambient. 26, 1–9. https://doi.org/10.1590/2179-8087.074417

Cotrufo, M.F., Soong, J.L., Horton, A.J., Campbell, E.E., Haddix, M.L., Wall, D.H., Parton, W.J., 2015. Formation of soil organic matter via biochemical and physical pathways of litter mass loss. Nat. Geosci. 8, 776–779. https://doi.org/10.1038/ngeo2520

de Queiroz, M.G., da Silva, T.G.F., Zolnier, S., de Souza, C.A.A., de Souza, L.S.B., Neto, S., de Araújo, G.G.L., Ferreira, W.P.M., 2019. Seasonal patterns of deposition litterfall in a seasonal dry tropical forest. Agric. For. Meteorol. 279, 107712. https://doi.org/10.1016/j.agrformet.2019.107712

de Lima, R.A.F., Oliveira, A.A., Pitta, G.R., de Gasper, A.L., Vibrans, A.C., Chave, J., ter Steege, H., Prado, P.I., 2020. The erosion of biodiversity and biomass in the Atlantic Forest biodiversity hotspot. Nat. Commun. 11, 1–16. https://doi.org/10.1038/s41467-020-20217-w

De Vos, B., Cools, N., Ilvesniemi, H., Vesterdal, L., Vanguelova, E., Carnicelli, S., 2015. Benchmark values for forest soil carbon stocks in Europe: Results from a large scale forest soil survey. Geoderma 251–252, 33–46. https://doi.org/10.1016/j.geoderma.2015.03.008

Doetterl, S., Stevens, A., Six, J., Merckx, R., Van Oost, K., Casanova Pinto, M., Casanova-Katny, A., Muñoz, C., Boudin, M., Zagal Venegas, E., Boeckx, P., 2015. Soil carbon storage controlled by interactions between geochemistry and climate. Nat. Geosci. 8, 780–783. https://doi.org/10.1038/ngeo2516

Embrapa – Empresa Brasileira de Pesquisa Agropecuária. Manual de Métodos de Análise de Solo. 2ª edição. Centro Nacional de Pesquisa de Solos. Rio de Janeiro. 1997.

Fernandes, R.B.A., Junior, I.A. de C., Junior, E.S.R., de Sá Mendonça, E., 2015. Comparison of different methods for the determination of total organic carbon and humic substances in Brazilian soils. Rev. Ceres 62, 496–501. https://doi.org/10.1590/0034-737X201562050011

Fontaine, S., Barot, S., Barré, P., Bdioui, N., Mary, B., Rumpel, C., 2007. Stability of organic carbon in deep soil layers controlled by fresh carbon supply. Nature 450, 277–280. https://doi.org/10.1038/nature06275

Gomes, L.C., Faria, R.M., de Souza, E., Veloso, G.V., Schaefer, C.E.G.R., Filho, E.I.F., 2019. Modelling and mapping soil organic carbon stocks in Brazil. Geoderma 340, 337–350. https://doi.org/10.1016/j.geoderma.2019.01.007

Guillaume, T., Damris, M., Kuzyakov, Y., 2015. Losses of soil carbon by converting tropical forest to plantations: Erosion and decomposition estimated by δ13C. Glob. Chang. Biol. 21, 3548–3560. https://doi.org/10.1111/gcb.12907

Haghverdi, K., Kooch, Y., 2019. Effects of diversity of tree species on nutrient cycling and soil-related processes. Catena 178, 335–344. https://doi.org/10.1016/j.catena.2019.03.041

Hubau, W., Lewis, S.L., Phillips, O.L., Affum-Baffoe, K., Beeckman, H., Cuní-Sanchez, A., Daniels, A.K., Ewango, C.E.N., Fauset, S., Mukinzi, J.M., Sheil, D., Sonké, B., Sullivan, M.J.P., Sunderland, T.C.H., Taedoumg, H., Thomas, S.C., White, L.J.T., Abernethy, K.A., Adu-Bredu, S., Amani, C.A., Baker, T.R., Banin, L.F., Baya, F., Begne, S.K., Bennett, A.C., Benedet, F., Bitariho, R., Bocko, Y.E., Boeckx, P., Boundja, P., Brienen, R.J.W., Brncic, T., Chezeaux, E., Chuyong, G.B., Clark, C.J., Collins, M., Comiskey, J.A., Coomes, D.A., Dargie, G.C., de Haulleville, T., Kamdem, M.N.D., Doucet, J.L., Esquivel-Muelbert, A., Feldpausch, T.R., Fofanah, A., Foli, E.G., Gilpin, M., Gloor, E., Gonmadje, C., Gourlet-Fleury, S., Hall, J.S., Hamilton, A.C., Harris, D.J., Hart, T.B., Hockemba, M.B.N., Hladik, A., Ifo, S.A., Jeffery, K.J., Jucker, T., Yakusu, E.K., Kearsley, E., Kenfack, D., Koch, A., Leal, M.E., Levesley, A., Lindsell, J.A., Lisingo, J., Lopez-Gonzalez, G., Lovett, J.C., Makana, J.R., Malhi, Y., Marshall, A.R., Martin, J., Martin, E.H., Mbayu, F.M., Medjibe, V.P., Mihindou, V., Mitchard, E.T.A., Moore, S., Munishi, P.K.T., Bengone, N.N., Ojo, L., Ondo, F.E., Peh, K.S.H., Pickavance, G.C., Poulsen, A.D., Poulsen, J.R., Qie, L., Reitsma, J., Rovero, F., Swaine, M.D., Talbot, J., Taplin, J., Taylor, D.M., Thomas, D.W., Toirambe, B., Mukendi, J.T., Tuagben, D., Umunay, P.M., van der Heijden, G.M.F., Verbeeck, H., Vleminckx, J., Willcock, S., Wöll, H., Woods, J.T., Zemagho, L., 2020. Asynchronous carbon sink saturation in African and Amazonian tropical forests. Nature 579, 80–87. https://doi.org/10.1038/s41586-020-2035-0

IBGE - Instituto Brasileiro de Geografia e Estatística. Manual Técnico da Vegetação Brasileira. Rio de Janeiro, 2012.

Jandl, R., Lindner, M., Vesterdal, L., Bauwens, B., Baritz, R., Hagedorn, F., Johnson, D.W., Minkkinen, K., Byrne, K.A., 2007. How strongly can forest management influence soil carbon sequestration? Geoderma 137, 253–268. https://doi.org/10.1016/j.geoderma.2006.09.003

Jobbágy, E.G., Jackson, R.B., 2000. The vertical distribution of soil organic carbon and its relation to climate and vegetation. Ecol. Appl. 10, 423–436. https://doi.org/10.1890/1051-0761(2000)010[0423:TVDOSO]2.0.CO;2

Johnson, D.W., 1992. Effects of Forest Management on Soil Carbon Storage, in: Natural Sinks of CO2. Springer Netherlands, Dordrecht, pp. 83–120. https://doi.org/10.1007/978-94-011-2793-6_6

Junqueira, J.A., Mello, C.R., Owens, P.R., Mello, J.M., Curi, N., Alves, G.J., 2017. Time-stability of soil water content (SWC) in an Atlantic Forest - Latosol site. Geoderma 288, 64–78. https://doi.org/10.1016/j.geoderma.2016.10.034

Junqueira Junior, J.A., de Mello, C.R., de Mello, J.M., Scolforo, H.F., Beskow, S., McCarter, J., 2019. Rainfall partitioning measurement and rainfall interception modelling in a tropical semi-deciduous Atlantic forest remnant. Agric. For. Meteorol. 275, 170–183. https://doi.org/10.1016/j.agrformet.2019.05.016

INMET - Instituto Nacional de Meteorologia, 2018. Normais climatológicas do Brasil 1981-2010. Available: https://portal.inmet.gov.br/normais Access in August 2018

Legendre, P., Oksanen, J. and ter Braak, C.J.F. (2011), Testing the significance of canonical axes in redundancy analysis. Methods in Ecology and Evolution, 2: 269- 277. https://doi.org/10.1111/j.2041-210X.2010.00078.x

Macinnis-Ng, C., Schwendenmann, L., 2014. Litterfall, carbon and nitrogen cycling in a southern hemisphere conifer forest dominated by kauri (Agathis australis) during drought. Plant Ecol. 216, 247–262. https://doi.org/10.1007/s11258-014-0432-x

Mantovani, V.A., Terra, M. de C.N.S., de Mello, C.R., Rodrigues, A.F., de Oliveira, V.A., Pinto, L.O.R., 2022. Spatial and Temporal Patterns in Carbon and Nitrogen Inputs by Net

Precipitation in Atlantic Forest, Brazil. For. Sci. 68, 113–124. https://doi.org/10.1093/forsci/fxab056

Marques, J.D. de O., Luizão, F.J., Teixeira, W.G., Vitel, C.M., Marques, E.M. de A., 2016. SOIL ORGANIC CARBON, CARBON STOCK AND THEIR RELATIONSHIPS TO PHYSICAL ATTRIBUTES UNDER FOREST SOILS IN CENTRAL AMAZONIA. Rev. Árvore 40, 197–208. https://doi.org/10.1590/0100-67622016000200002

Moomaw, W.R., Law, B.E., Goetz, S.J., 2020. Focus on the role of forests and soils in meeting climate change mitigation goals: Summary. Environ. Res. Lett. 15. https://doi.org/10.1088/1748-9326/ab6b38

Morais, V. a., Scolforo, J.R.S., Silva, C. a., Mello, J.M. De, Gomide, L.R., Oliveira, a. D., 2013. Carbon and biomass stocks in a fragment of cerradao in Minas Gerais state, Brazil. Cern. Lavras 19, 237–245. https://doi.org/10.1590/S0104-77602013000200007

Morais, V.A., Ferreira, G.W.D., de Mello, J.M., Silva, C.A., de Mello, C.R., Araújo, E.J.G., David, H.C., da Silva, A.C., Scolforo, J.R.S., 2020. Spatial distribution of soil carbon stocks in the Cerrado biome of Minas Gerais, Brazil. CATENA 185, 104285. https://doi.org/10.1016/j.catena.2019.104285

Morellato, L.P.C., Haddad, C.F.B., 2000. Introduction: The Brazilian atlantic forest. Biotropica 32, 786–792. https://doi.org/10.1111/j.1744-7429.2000.tb00618.x

Myers, N., Mittermeier, R.A., Mittermeier, C.G., da Fonseca, G.A.B., Kent, J., 2000. Biodiversity hotspots for conservation priorities. Nature 403, 853–858. https://doi.org/10.1038/35002501

Oksanen, J., F. Guillaume, Blanchet, M. F., Roeland Kindt, Pierre Legendre, Dan McGlinn, Peter R. Minchin, R. B. O'Hara, Gavin L. Simpson, Peter Solymos, M. Henry H. Stevens, Eduard Szoecs and Helene Wagner (2020). vegan: Community Ecology Package. R package version 2.5-7. https://CRAN.R-project.org/package=vegan.

Paz, C.P., Goosem, M., Bird, M., Preece, N., Goosem, S., Fensham, R., Laurance, S., 2016. Soil types influence predictions of soil carbon stock recovery in tropical secondary forests. For. Ecol. Manage. 376, 74–83. https://doi.org/10.1016/j.foreco.2016.06.007

Pimentel, D., HEPPERLY, P., HANSON, J., DOUDS, D., SEIDEL, R., 2005. An Environmental, Energetic and Economic Comparison of Organic and Conventional Farming Systems. Bioscience 55, 573-. https://doi.org/10.1007/978-94-007-7796-5_6

Qualls, R. G. Role of Precipitation Partitioning in Litter Biogeochemistry. In: Van Stan, II, J. T.; Gutmann, E.; Friese, J. (org.). Precipitation Partitioning by Vegetation. Cham, Switzerland: Springer International Publishing, 2020.

R Core Team, 2019. R: A Language and Environment for Statistical Computing.

Ribeiro, M.C., Metzger, J.P., Martensen, A.C., Ponzoni, F.J., Hirota, M.M., 2009. The Brazilian Atlantic Forest: How much is left, and how is the remaining forest distributed? Implications for conservation. Biol. Conserv. 142, 1141–1153. https://doi.org/10.1016/j.biocon.2009.02.021

Sayer, E.J., Lopez-Sangil, L., Crawford, J.A., Bréchet, L.M., Birkett, A.J., Baxendale, C., Castro, B., Rodtassana, C., Garnett, M.H., Weiss, L., Schmidt, M.W.I., 2019. Tropical forest soil carbon stocks do not increase despite 15 years of doubled litter inputs. Sci. Rep. 9, 1–9. https://doi.org/10.1038/s41598-019-54487-2

Souza, C.R., Maia, V.A., Aguiar-Campos, N. de, Santos, A.B.M., Rodrigues, A.F., Farrapo, C.L., Gianasi, F.M., Paula, G.G.P. de, Fagundes, N.C.A., Silva, W.B., Santos, R.M., 2021. Long-term ecological trends of small secondary forests of the atlantic forest hotspot: A 30-year study case. For. Ecol. Manage. 489, 119043. https://doi.org/10.1016/j.foreco.2021.119043

Tabarelli, M., Peres, C.A., Melo, F.P.L., 2012. The “few winners and many losers” paradigm revisited: Emerging prospects for tropical forest biodiversity. Biol. Conserv. 155, 136–140. https://doi.org/10.1016/j.biocon.2012.06.020

Ter Braak, C.J.F., Looman, C.W.M., 1994. Biplots in Reduced-Rank Regression. Biometrical J. 36, 983–1003. Powell J. Multivariate Statistics Western Sidney University, Hawkesbury Institute for the Environment, Sidney (2018)

Terra, M. de C.N.S., Santos, R.M. Dos, Prado Júnior, J.A. Do, de Mello, J.M., Scolforo, J.R.S., Fontes, M.A.L., Schiavini, I., dos Reis, A.A., Bueno, I.T., Magnago, L.F.S., ter Steege, H., 2018. Water availability drives gradients of tree diversity, structure and functional traits in

the Atlantic–Cerrado–Caatinga transition, Brazil. J. Plant Ecol. 11, 803–814. https://doi.org/10.1093/jpe/rty017

Tian, H., Lu, C., Yang, J., Banger, K., Huntzinger, D.N., Schwalm, C.R., Michalak, A.M., Cook, R., Ciais, P., Hayes, D., Huang, M., Ito, A., Jain, A.K., Lei, H., Mao, J., Pan, S., Post, W.M., Peng, S., Poulter, B., Ren, W., Ricciuto, D., Schaefer, K., Shi, X., Tao, B., Wang, W., Wei, Y., Yang, Q., Zhang, B., Zeng, N., 2015. Global patterns and controls of soil organic carbon dynamics as simulated by multiple terrestrial biosphere models: Current status and future directions. Global Biogeochem. Cycles 29, 775–792. https://doi.org/10.1002/2014GB005021

Tobón, C., Sevink, J., Verstraten, J.M., 2004. Solute fluxes in throughfall and stemflow in four forest ecosystems in northwest Amazonia. Biogeochemistry 70, 1–25. https://doi.org/10.1023/B:BIOG.0000049334.10381.f8

Todd-Brown, K.E.O., Randerson, J.T., Post, W.M., Hoffman, F.M., Tarnocai, C., Schuur, E.A.G., Allison, S.D., 2013. Causes of variation in soil carbon simulations from CMIP5 Earth system models and comparison with observations. Biogeosciences 10, 1717–1736. https://doi.org/10.5194/bg-10-1717-2013

USDA – US Department of Agriculture. Soil Survey Staff, 1999. Soil Taxonomy: A Basic System of Soil Classification for Making and Interpreting Soil Surveys. 2nd Edition. Natural Resources Conservation Service.

Vitória, A.P., Alves, L.F., Santiago, L.S., 2019. Atlantic forest and leaf traits: an overview. Trees - Struct. Funct. 33, 1535–1547. https://doi.org/10.1007/s00468-019-01864-z

Walker, X.J., Baltzer, J.L., Cumming, S.G., Day, N.J., Ebert, C., Goetz, S., Johnstone, J.F., Potter, S., Rogers, B.M., Schuur, E.A.G., Turetsky, M.R., Mack, M.C., 2019. Increasing wildfires threaten historic carbon sink of boreal forest soils. Nature 572, 520–523. https://doi.org/10.1038/s41586-019-1474-y

Supplementary Material

Table 1: Descriptive statistics of the spatial distribution of soil carbon concentration (%) to 1-m depth (n=10 for each soil layer), in 4 months of analyzes (May and August 2018 representing the dry season, and December 2018, and April 2019 the wet season)

			May-18			
Soil layer	Mean	Median	Min	Max	SD	CV
0-5	10.0	8.5	5.7	27.1	6.4	63%
05-10	6.2	5.5	3.4	13.8	3.0	48%
10-20	3.2	3.3	2.0	4.1	0.7	22%
20-30	3.3	3.5	1.8	4.1	0.7	21%
30-40	3.0	2.9	2.1	3.7	0.5	18%
40-60	2.4	2.4	2.0	2.9	0.3	11%
60-100	2.0	1.9	1.7	2.5	0.2	12%
			Aug-18			
Soil layer	Mean	Median	Min	Max	SD	CV
0-5	9.8	7.5	5.8	22.1	5.8	59%
05-10	5.6	4.6	3.4	11.8	2.6	46%
10-20	3.3	3.3	1.7	4.4	0.8	26%
20-30	2.9	2.7	1.7	5.4	1.1	37%
30-40	2.2	2.1	1.6	3.2	0.5	24%
40-60	1.9	1.8	1.3	2.5	0.4	20%
60-100	1.7	1.6	1.1	2.4	0.4	23%
			Dec-18			
Soil layer	Mean	Median	Min	Max	SD	CV
0-5	14.8	14.2	8.8	28.8	6.1	41%
05-10	7.9	6.2	3.9	24.3	5.9	75%
10-20	3.2	3.1	2.4	3.9	0.5	14%
20-30	3.0	2.9	2.2	4.8	0.8	27%
30-40	2.4	2.4	1.7	3.5	0.6	23%
40-60	2.1	2.1	1.4	2.8	0.4	21%
60-100	1.8	1.8	1.2	2.5	0.4	21%
			Apr-19			
Soil layer	Mean	Median	Min	Max	SD	CV
0-5	10.7	7.7	3.6	30.4	8.3	78%
05-10	7.2	6.2	3.3	14.4	3.6	50%
10-20	3.2	3.3	2.1	3.9	0.5	16%
20-30	2.9	3.0	1.8	3.4	0.6	19%
30-40	2.4	2.4	1.7	3.0	0.4	18%
40-60	2.1	2.1	1.5	2.7	0.4	18%
60-100	1.6	1.6	1.0	2.0	0.3	17%

Table 2: Descriptive statistics of the temporal distribution of soil carbon concentration (%) to 1-m depth (n=4 for each ID location and each soil layer)

		Soil Carbon Concentration (%)					
ID	Soil layer	Mean	Median	Min	Max	SD	CV
1	(0-5 cm)	27.1	27.9	22.1	30.4	3.6	12%
2		6.9	6.3	6.0	8.8	1.3	15%
3		7.7	7.6	6.3	9.4	1.5	16%
4		7.2	7.1	3.6	11.3	3.3	29%
5		9.8	8.3	7.1	15.4	3.8	25%
6		9.2	9.2	7.2	11.2	1.7	16%
7		17.3	18.9	10.9	20.6	4.3	21%
8		11.1	12.1	5.8	14.3	4.0	28%
9		9.2	8.1	4.8	15.8	4.7	30%
10		7.9	6.0	5.3	14.1	4.2	30%
1	(5-10 cm)	16.1	14.1	11.8	24.3	5.6	23%
2		3.9	3.8	3.4	4.5	0.6	12%
3		5.1	5.3	3.4	6.5	1.4	21%
4		5.0	5.1	3.3	6.6	1.5	22%
5		4.9	4.8	3.9	6.0	1.0	17%
6		5.7	5.9	4.7	6.3	0.7	11%
7		8.9	8.5	7.9	10.8	1.3	12%
8		7.1	6.7	4.3	10.5	2.6	24%
9		5.3	5.3	4.5	6.1	0.7	12%
10		5.1	5.0	4.4	6.2	0.8	13%
1	(10-20 cm)	3.5	3.5	3.1	3.9	0.5	12%
2		2.2	2.0	1.7	3.0	0.6	19%
3		3.0	3.1	2.6	3.2	0.2	8%
4		3.3	3.3	3.0	3.5	0.3	7%
5		2.9	2.9	2.3	3.5	0.6	18%
6		3.7	3.7	3.5	4.1	0.2	5%
7		3.8	3.6	3.4	4.4	0.5	11%
8		3.6	3.6	3.1	3.9	0.4	10%
9		3.5	3.4	2.9	4.4	0.6	14%
10		2.7	2.7	2.6	2.9	0.1	4%
1	(20-30 cm)	3.6	3.5	2.5	4.8	1.0	20%
2		1.8	1.8	1.7	2.2	0.2	10%
3		2.7	2.8	2.0	3.3	0.5	16%
4		3.3	3.3	2.8	3.7	0.4	11%
5		2.7	2.7	2.3	2.9	0.3	9%
6		3.2	3.1	2.9	3.8	0.4	12%
7		4.1	3.8	3.3	5.4	0.9	17%
8		3.3	3.3	2.3	4.1	0.7	18%

		Soil Carbon Concentration (%)					
ID	Soil layer	Mean	Median	Min	Max	SD	CV
9		3.1	3.2	2.4	3.4	0.5	14%
10		2.4	2.3	2.2	2.9	0.3	11%
1		2.5	2.5	1.9	2.9	0.4	14%
2		1.9	2.0	1.7	2.1	0.2	9%
3		2.0	1.9	1.6	2.8	0.5	19%
4		2.7	2.6	2.4	3.1	0.3	10%
5	(30-40 cm)	2.6	2.6	2.2	3.0	0.3	11%
6		2.7	2.5	2.3	3.5	0.5	16%
7		3.2	3.3	2.6	3.6	0.5	13%
8		2.9	2.9	2.0	3.7	0.7	18%
9		2.3	2.1	2.0	3.1	0.5	16%
10		2.0	1.8	1.6	2.6	0.5	18%
1		2.3	2.2	1.8	2.9	0.4	15%
2		1.8	1.8	1.7	2.0	0.1	6%
3		1.6	1.5	1.3	2.0	0.3	14%
4		2.2	2.2	2.1	2.4	0.1	5%
5	(40-60 cm)	2.6	2.6	2.5	2.7	0.1	3%
6		2.2	2.2	2.0	2.6	0.2	8%
7		2.4	2.4	2.2	2.8	0.2	7%
8		2.2	2.4	1.8	2.5	0.3	11%
9		1.9	1.9	1.6	2.3	0.3	11%
10		1.8	1.6	1.5	2.4	0.4	15%
1		1.6	1.7	1.3	1.9	0.3	14%
2		1.6	1.7	1.6	1.7	0.1	3%
3		1.3	1.2	1.0	1.9	0.4	22%
4		1.8	1.9	1.6	2.0	0.2	8%
5	(60-100 cm)	2.2	2.3	1.9	2.5	0.3	12%
6		1.9	2.0	1.6	2.1	0.2	10%
7		2.2	2.2	2.0	2.4	0.2	8%
8		1.8	1.7	1.6	2.0	0.1	7%
9		1.6	1.6	1.5	1.8	0.1	6%
10		1.6	1.5	1.4	1.9	0.3	13%

Figure 1 - Vertical distribution of the average soil carbon concentration (%), with standard deviation, considering the analysis of the 4 months in each location - 1 (a), 2 (b), 3 (c), 4 (d), 5 (e), 6 (f), 7 (g), 8 (h), 9 (i), 10 (j).

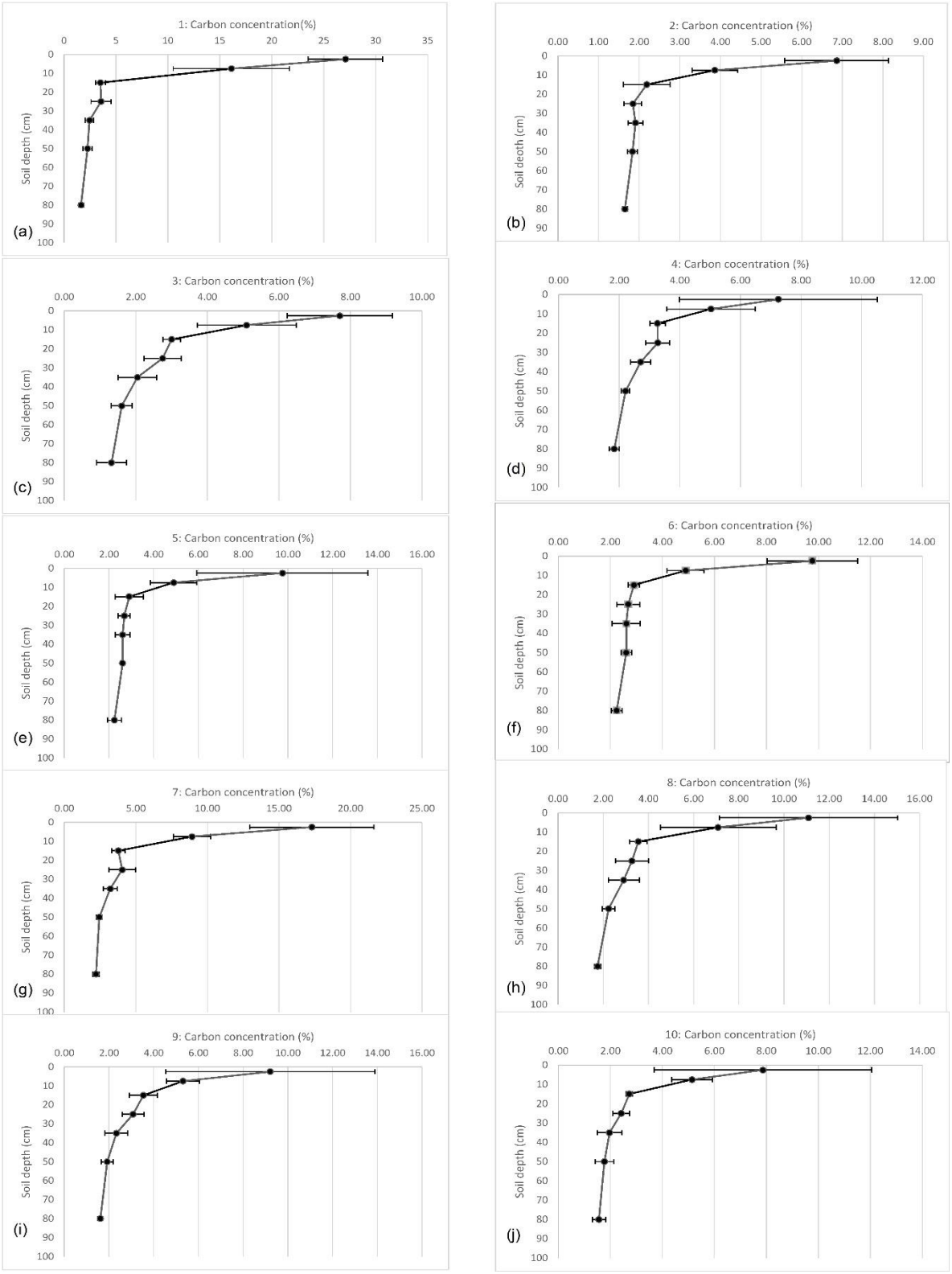

Table 3: Dry biomass (g m^{-2}) sampled in the study period (from May 2018 to April 2019), and the descriptive statistics.

ID	May-18	Jun-18	Jul-18	Aug-18	Sep-18	Oct-18	Nov-18	Dec-18	Jan-19	Feb-19	Mar-19	Apr-19	Total
1	55.3	84.7	32.2	54.5	77.0	61.8	72.9	183.9	136.3	126.0	92.3	98.4	1075.4
2	40.6	161.3	89.0	133.3	268.9	158.5	183.3	138.6	175.2	136.1	82.4	108.2	1675.5
3	50.2	75.2	60.7	81.5	116.0	106.2	209.5	196.1	107.9	353.0	121.6	97.5	1575.4
4	53.5	78.3	128.4	70.6	97.4	201.3	66.3	69.6	89.5	47.9	57.8	82.4	1043.1
5	67.9	131.6	53.9	58.7	127.8	80.9	101.4	77.2	136.0	156.5	103.5	330.3	1425.6
6	34.3	90.9	34.2	50.9	125.6	98.4	74.5	64.3	267.5	110.0	68.4	84.0	1103.1
7	21.3	84.4	43.2	65.0	104.4	100.4	52.1	92.0	111.0	81.9	41.3	57.1	854.3
8	32.9	94.8	84.5	103.1	320.3	176.3	84.3	80.9	290.5	149.2	68.5	83.0	1568.3
9	39.6	64.9	25.5	30.2	52.1	47.3	40.1	60.1	155.8	113.3	67.2	98.3	794.4
10	99.0	123.3	534.8	103.6	163.3	146.8	137.6	74.0	187.5	92.0	155.7	86.6	1904.3
Mean	49.5	98.9	108.7	75.1	145.3	117.8	102.2	103.7	165.7	136.6	85.9	112.6	1301.9
Maximum	99.0	161.3	534.8	133.3	320.3	201.3	209.5	196.1	290.5	353.0	155.7	330.3	1904.3
Minimum	21.3	64.9	25.5	30.2	52.1	47.3	40.1	60.1	89.5	47.9	41.3	57.1	794.4
SD	21.9	30.2	153.1	30.6	85.1	50.8	56.7	50.6	67.1	82.7	33.7	77.7	377.0
CV (%)	44%	30%	141%	41%	59%	43%	55%	49%	40%	61%	39%	69%	29%

Table 4: Dry biomass carbon concentration (%) in the selected months of analysis (May, August and December 2018, and April 2019) and the descriptive statistics.

ID	May 2018	August 2018	December 2018	April 2019	Mean	SD	CV (%)
1	51.2	51.0	51.0	49.7	50.7	0.7	1%
2	42.4	48.2	48.2	45.1	46.0	2.8	6%
3	48.3	48.5	48.5	43.3	47.2	2.6	5%
4	51.0	48.6	48.6	47.4	48.9	1.5	3%
5	50.8	47.4	47.4	45.0	47.7	2.4	5%
6	49.0	48.6	48.6	44.2	47.6	2.3	5%
7	48.9	48.6	48.6	48.0	48.5	0.4	1%
8	51.0	47.7	47.7	48.1	48.6	1.6	3%
9	48.7	47.6	47.6	46.0	47.5	1.1	2%
10	46.7	48.1	48.1	46.0	47.2	1.1	2%
Mean	48.8	48.4	48.4	46.3			
Maximum	51.2	51.0	51.0	49.7			
Minimum	42.4	47,4	47.4	43.3			
SD	2.7	1.0	1.0	2.0			
CV (%)	6%	2%	2%	4%			

3. CONSIDERAÇÕES FINAIS

Os achados do presente estudo contribuem para o melhor entendimento do papel das florestas nos ciclos biogeoquímicos, justificando a conservação de remanescentes florestais e fornecendo informações para o manejo mais adequado desses ecossistemas.

Assim, os resultados obtidos para o carbono e o nitrogênio na precipitação que atinge a floresta e na precipitação que atravessa o dossel, e atinge o solo, foram fundamentais para o entendimento do comportamento temporal e espacial desses nutrientes. Os resultados obtidos indicam a importância da sazonalidade, considerando que 75% do carbono e nitrogênio atingiram o solo via precipitação efetiva na estação chuvosa. Neste sentido, alterações nos padrões da precipitação podem modificar a dinâmica das entradas dos nutrientes nas florestas, proporcionando consequências ainda pouco conhecidas.

Também foi constatado que o escoamento pelo tronco é uma via importante de entrada de água e nutrientes no solo da floresta. O enriquecimento do carbono no escoamento pelo tronco foi afetado por características estruturais das árvores e pelas condições meteorológicas. As árvores com casca muito rugosa e copas pequenas foram mais eficazes no transporte do carbono, assim como os eventos de precipitação com maiores intensidades máximas. Os resultados obtidos reforçam a importância do escoamento pelo tronco como um caminho relevante de entrada de água e carbono no solo das florestas.

Por fim, foi observado que o estoques de carbono do solo até 1 metro na área de estudo variaram de 201,0 Mg C ha^{-1} a 396 Mg C ha^{-1}, como valor médio de 268,5 Mg C ha^{-1}. A concentração de carbono na biomassa seca e a condutividade hidráulica apresentaram uma relação positiva com o armazenamento do carbono no solo nas camadas superiores e a temperatura do solo e o coeficiente de variação do diâmetro das árvores apresentaram uma relação positiva com o armazenamento do carbono no solo nas camadas mais profundas. Esses resultados obtidos foram fundamentais para avançar no entendimento do papel do solo das florestas tropicais na mitigação das mudanças climáticas.